Characterization of the role of fibroblast growth factor 10 (Fgf10) and its receptor Fgfr2b on multipotent epithelial progenitor cells during early lung development

Inaugural Dissertation

submitted to the

Faculty of Medicine

in partial fulfillment of the requirements

for the PhD-Degree

of the Faculties of Veterinary Medicine and Medicine

of the Justus Liebig University Giessen

by

Salma Dilai

of

Fez, Morocco

Giessen 2020

From the Department of Internal Medicine II and
Excellence Cluster cardio-Pulmonary System (ECCPS)
of the Faculty of Medicine of the Justus Liebig University Giessen
Director / Chairman: Prof. Dr. Werner Seeger

First Supervisor: Prof.Dr. Saverio Bellusci
Second Supervisor: Dr. Denise Al Alam

Declaration

"I declare that I have completed this dissertation single-handedly without the unauthorized help of a second party and only with the assistance acknowledged therein. I have appropriately acknowledged and referenced all text passages that are derived literally from or are based on the content of published or unpublished work of others, and all information that relates to verbal communications. I have abided by the principles of good scientific conduct laid down in the charter of the Justus Liebig University of Giessen in carrying out the investigations described in the dissertation."

Salma Dilai

Table of Contents

Declaration 3
Table of Contents 4
List of figures 7
List of tables 9
Abbreviations and acronyms 10
1. Introduction 13
1.1 Lung morphogenesis 13
1.1.1 Embryonic lung: Formation, phases of development and signaling pathways 13
1.1.2 Cell types in the adult mouse lung 15
1.1.3 Difference between mouse and human lung 16
1.2 Fibroblast growth factors 18
1.3 Fibroblast growth factors receptors 19
1.4 Fgf10/ Fgfr2b signaling 21
1.5 Human diseases related to FGF10/FGFR2b deficiency 25
1.6 Fgf signaling downstream targets: *Etv4 / Etv5* 26
1.6.1 Characterization of a *Tg*(*Etv4-GFP*) reporter line 27
2. Objectives 28
3. Material and methods 29
3.1 Study approval 29
3.2 Generation and genotyping of mice 29
3.2.1 Generation of the double transgenic mice: *Rosa26* $^{rtTA/rtTA}$*; Tg(Tet(O)sFgfr2b)/+* and *Rosa26* $^{rtTA/rtTA}$; *Tg(Tet(O)Fgf10)/+*. 29
3.2.2 Genotyping of Rosa26 $^{rtTA/rtTA}$; Tet(O)sFgfr2b)/+ and Rosa26 $^{rtTA/rtTA}$;Tet(O)Fgf10)/+ mice. 29
3.3 RNA extraction 30
3.4 cDNA synthesis and quantitative PCR 30
3.5 Lung culture, time lapse microscopy and quantification 31
3.6 Tissue processing and Immunostaining 31
3.6.1 Sox2 Immunostaining 31
3.6.2 Sox9 Immunostaining 32
3.7 Microarray experiments 33

4. Results 34

4.1 Use of the reporter mouse line *Tg(Etv4-GFP)* to visualize the dynamics of Fgf signaling during lung development. 34

4.1.1. Dynamic GFP Expression Reports FGF10 Signaling 35

4.2 Loss of function (LoF): The use of the double transgenic (DTG) approach *Rosa26$^{rtTA/rtTA}$; tet(O)sFgfr2b/+* to attenuate the activity of the FGFR2b ligands during early lung development 39

4.2.1 Expression of the main FGFR2b ligands during early lung development, and validation of the double transgenic approach.....39

4.2.2 Impact of Fgf10 inhibition on branching morphogenesis 41

4.3 Identification of FGF10 downstream target genes by gene array approach.....43

4.3.1 Early versus Late clusters.....45

4.3.2 The genes differentially expressed between the epithelium and mesenchyme and regulation of gene expression upon Fgf10 signal inhibition .45

4.3.3 Identification of the transcription factors controlled by FGF10 50

4.3.4 Validation of the array: Fgf10, Fgfr2b, Etv4/5, Shh connection.....52

4.3.5 The FGF10 transcriptomic signature is active throughout alveolar lineage formation during lung development 54

4.3.6 Role of Fgf10 signaling in the differentiation of multipotent epithelial progenitors. 56

4.4 Gain of function (GoF): The use of the double transgenic approach *Rosa26$^{rtTA/rtTA}$;tg(tet(O)Fgf10)/+* to over express *Fgf10*. Validation of the system, impact on branching morphogenesis and gene array approach. 59

4.5 Comparison between LoF and GoF experiments 9 hours after Dox IP.....61

5. Discussion.....66

5.1. Visualization of the FGF signaling domains of action. 66

5.2 Validation of the double transgenic approach: *Rosa26$^{rtTA/rtTA}$;Tg(tet(O)sFgfr2b)/+* in other developmental models: limbs, mammary glands rodent incisors and lung. 67

5.3 Validation and limitations of *in vivo* inhibition of Fgf10 signaling 68

5.4 LoF: Discussion on the genes, their biological activities and KEGG analysis 68

5.4.1 Identification of lung-specific transcription factors controlled by FGF10 69

5.4.2 FGF10's regulation of tip cell differentiation and morphology.....70

5.5 GoF: Validation and limitation.....70

5.6 LoF vs. GoF: Discussion on the genes, their biological activities and KEGG analysis 71

6. Summary....72
7. Supplementary Data....74
7.1 Loss of function part....75
7.1.1 List 1: Definition of genes in Early4 group....83
7.1.2 List 2: Definition of genes in Late 4 group....85
7.2 Gain of function part....90
7.2.1 List 3: Definition of genes in the cluster 1....93
7.2.2 List 4: Definition of genes in the cluster 2....96
7.2.3 List 5: Definition of genes in the cluster 3....100
7.2.4 List 6: Definition of genes in the cluster 4....101
8. References....106
9. Acknowledgments....118

List of figures

Figure 1: Structure of the mouse lung at E12.5.

Figure 2: Major cell types along the proximo-distal axis of the adult mouse lung.

Figure 3: Difference between mouse and human lung architecture.

Figure 4: Fgfs Subfamilies.

Figure 5: Schematic diagram of FgfR structure

Figure 6: Diagram showing relative activity of Fgfs subfamilies on Fgfr isoforms.

Figure 7: Mechanism of action of Fgf10.

Figure 8: Schematic representation of the generation of *Tg*(*Etv4-EGF)* mice.

Figure 9: Determination of the expression pattern in different organs responding to Fgf signaling.

Figure 10: Etv4-GFP is dynamically expressed in regions of active FGF10 signaling during early lung development.

Figure 11: The effect of adding exogenous recombinant human FGF7 and FGF10 on *Tg(Etv4-GFP)* lungs.

Figure 12: Expression of the main Fgfr2b ligands during early lung development and validation of the double transgenic (DTG) approach: $Rosa26^{rtTA/rtTA}$*;Tg(tet(O)sFgfr2b)/*+.

Figure 13: The impact of inhibiting Fgf10 on branching morphogenesis.

Figure 14: Identification of early Fgf10 target genes by gene array approach.

Figure 15: The genes differentially expressed between the epithelium and mesenchyme of E12.5 wild type lungs and regulation of gene expression upon Fgf10 inhibition.

Figure 16: Detail analysis of the genes found in Late 4.

Figure 17: Identification of the transcription factors controlled by Fgf10 signaling. Figure 18: Validation of the array: The Fgf10, FgfR2b, Etv4/5, Shh connection.

Figure 18: Validation of the array: *The Fgf10, FgfR2b, Etv4/5, Shh* connection.

Figure 19: Role of Fgf10 signaling in the differentiation of multipotent epithelial progenitors.

Figure 20: The Fgf10 transcriptomic signature is active throughout alveolar lineage formation during lung development.

Figure 21: Gain of function using the double transgenic approach *Rosa26$^{rtTA/rtTA}$;Tg(tet(O)Fgf10)/+* .

Figure 22: Comparison between LoF and GoF experiments 9 hours after Dox IP.

Figure S1: The effect of adding exogenous recombinant human FGF7 and FGF10 on Tg(*Etv4-GFP)* lungs.

Figure S2-S5: Gene expression level and gene expression pattern in Early1 - Early4 (LoF).

Figure S6-S9: Gene expression level and gene expression pattern in Late1 - Late4 (LoF).

Figure S10-S14: Gene expression level in the Cluster 1-5 (GoF).

List of tables

Table 1: Stages of lung development in Human and Mouse.

Table 2: Subfamilies of E26 Transformation-Specific (Ets).

Table 3: Primer sequences used in the genotyping of Rosa26 rtTA/+; Tg(tet(o)sFgfr2b)/+ .

Table 4: Primer sequences for *Fgf1*, *Fgf7*, *Fgf10* and *Hprt* (reference gene) used for qPCR.

Table 5: The list of primary and secondary antibodies used for Sox2 and Sox9 Immunostaining.

Table 6: KEGG analysis for *Rosa26 rtTA/rtTA; Tg(tet(o)sFgfr2b* transgenic lungs versus control lungs at E12.5 harvested 6 hours and 9 hours post Dox IP.

Table 7: KEGG analysis for the loss and gain of function at E12.5 lungs harvested 9 hours post Dox IP.

Abbreviations and acronyms

α –SMA	α -Smooth Muscle Actin
Alv	Alveolus
Ab	Acid box
AB	Antibody
AECI	Alveolar epithelial cell type I
AECII	Alveolar epithelial cell type II
ALSG	Aplasia of lacrimal and salivary glands
ASMC	Airway smooth muscle cells
BADJ	Broncho-alveolar duct junction
BASC	Bronchoalveolar stem cell
BMP 4	Bone morphogenetic protein 4
BP	Bipotential progenitor
BPD	Bronchopulmonary dysplasia
Br	Bronchi
Brl	Bronchiole
BSA	Bovine serum albumin
COPD	Chronic obstructive pulmonary disease
DMEM	Dulbecco's Modified Eagle Medium
DOX	doxycycline
E	Epithelium
E	Embryonic stage
ECM	Extracellular matrix
EMT	epithelial-mesenchymal transition
ETV	ETS translocation variant
FACS	Fluorescence-activated cell sorting
FGF	Fibroblast growth factor
FGFR	Fibroblast growth factor receptor
GFP	Green fluorescent protein
GoF	gain of function
GLI1	Glioma-Associated Oncogene 1
HBS	Heparin binding site
hFGF	Hormone-like Fgf

HPRT	Hypoxanthine-guanine phosphoribosyltransferase
HS	Heparan sulfate
HSPG	Heparan sulfate proteoglycans
ID2	Inhibitor of differentiation 2
iFGF	Intracrine Fgf
IP	Intraperitoneal
IPF	Idiopathic pulmonary fibrosis
LADD	Lacrimo-auriculo-dento-digital syndrome
LIF	Lipofibroblast
LM	Limb mesenchyme
MAPK	Mitogen-activated protein kinases
Mes.	Mesenchyme
MHJ	Midbrain/hindbrain junction
MMP	Mandilary/maxillary processes
MYF	Myofibroblast
NE	Neuroendocrine cell
NEB	Neuroepithelial body
NP	Nasal placode
P	Postnatal
PBS	Phosphate-buffered saline
PBST	Phosphate Buffered Saline Tween 20
PBSMC	parabronchial smooth muscle cell
PCR	polymerase chain reaction
PDGF	Platelet derived growth factor
PDPN	Podoplanin
PECAM	Platelet endothelial cell adhesion molecule
PFA	Paraformaldehyde
PI3K	phosphatidylinositide 3-kinases
PKC	Protein kinase C
PLCγ	Phosphoinositide phospholipase C
qPCR	quantitative polymerase chain reaction
rtTA	reverse tetracycline transactivator
SEM	Subepithelial mesenchyme

SFTPC/Spc	Surfactant protein C
SFTPB	Surfactant protein B
SHH	Sonic hedgehog
SMM	Submesothelial mesenchyme
SOX	SRY (sex determining region Y)-box
SPRY 2	Sprouty 2
TB	Tail bud
TBS	TRIS-buffered saline
TBS-T	TRIS-buffered saline with + 0.1% Tween 20
TBX	T-box transcription factor
tet(O)	tetracycline binding site
TGF-β	Transforming growth factor β
Tr	Trachea
VEGF	Vascular endothelial growth factor
VEGFR	Vascular endothelial growth factor receptor
VSMC	Vascular smooth muscle cell
WNT	Wingless and int
Wt	Wild-type

1. Introduction

The main function of the lung is to allow efficient gas exchange between the external environment and the bloodstream and thus, to maintain body homeostasis. Every cell in the body needs to be oxygenated, therefore, a complex organ 'the lung' allows the air we breathe to reach the bloodstream allowing to oxygenate each cell in the body. The respiratory system allows also to get rid of the waste gas carbon dioxide. An efficient gas exchange is only performed with a well-structured and branched lung; the branching process is controlled by growth factors. Fibroblast growth factor 10 (Fgf10) is one of the key growth factors controlling the branching process of many organs including the lung, mammary gland, kidney (Carlton M. Bates, 2007), and prostate (Schwertfeger KL, 2009). In the developing lung, Fgf10 is expressed in the mesenchyme adjacent to nascent epithelial buds (Bellusci et al., 1997). It is acting via the Fgf receptor 2b (Fgfr2b) mostly expressed in the epithelium. Any defect in the function of the growth factors can cause severe pulmonary diseases such as chronic obstructive pulmonary disease (COPD) and broncho-pulmonary dysplasia (BPD); it was also showed that the inactivation of *Fgf10* in mice leads to lung agenesis (Sekine et al., 1999). Almost 20 years after the discovery of Fgf10 by Itoh and colleagues (Emoto et al., 1997) the role of Fgf10 on the lung epithelium is still elusive.

1.1 Lung morphogenesis

1.1.1 Embryonic lung: Formation, phases of development and signaling pathways

Lung development can histologically be divided into four stages: pseudoglandular, canalicular, saccular and alveolar (Table1). In humans, lung development starts around the 4th week of gestation, and continues for many years after birth. In mouse, the lung begins to develop at embryonic day E9.5 and ends 30 days after birth. In both species, the lung buds originate as an outgrowth from the ventral wall of the primitive foregut endoderm into the surrounding mesoderm; then, a repeated mechanism of branching occurs to form first the conducting airways and then the alveolar ducts. During alveologenesis, the distal surface area expands to generate an efficient air-blood barrier for gas exchange in the alveoli. During the different developmental stages, precursor cells located in the epithelium and mesenchyme progressively differentiate into various cell types lining the proximal and distal airways. This differentiation process is associated with the formation of alveoli and a mature vascular system (Warburton et al., 2000). During branching morphogenesis, cell-cell communication

between the mesenchyme and the lung epithelium is required for lung development and lung homeostasis, both depend on precise molecular signaling involving different fibroblast growth factors (Fgf), sonic hedgehog (Shh), bone morphogenic protein (Bmp), transforming growth factor b (Tgf β), retinoic acid (RA), the wingless (Wnt) related family of proteins, and various transcription factors (Cardoso et al., 2006; Chen et al., 2010).

Stage	Human	Mouse	Features
Pseudoglandular	5-17 wk	E9.5-E16.5	• Branching morphogenesis
Canalicular	24-26 wk	E16.5-E17.5	• Formation of capillaries • Beginning of alveolar epithelium development
Saccular	26-36 wk	E17.5-birth	• Formation of terminal sacs • Differentiation of AEC into type I and type II cells • Surfactant production
Alveolar	36 wk-3years	birth-P20	• Secondary septation • Formation of the majority of the gas exchange surface

Table 1: Stages of lung development in Human and Mouse; wk: week of gestation, E: embryonic day, P: postnatal, AECs: alveolar epithelial cells.

In human, the lung is divided into two asymmetrical sides: the right lung has three lobes and the left lung has two; whereas the right lung in mouse has four lobes: cranial, medial, caudal lobes, plus the accessory lobe, and one lobe in the left (Figure1). As in many vertebrates, the air enters through the nose (or mouth) by the inhalation travels to the larynx, and continues to the trachea which splits into two bronchial tubes that enter the lungs; then, the air enters progressively the ramified network of bronchi and bronchioles, until it reaches the functional unit of the lung called alveoli where the gas exchange occurs: the oxygen is then released into the bloodstream, and the carbon dioxide is released from the bloodstream into the alveoli, and then exhaled.

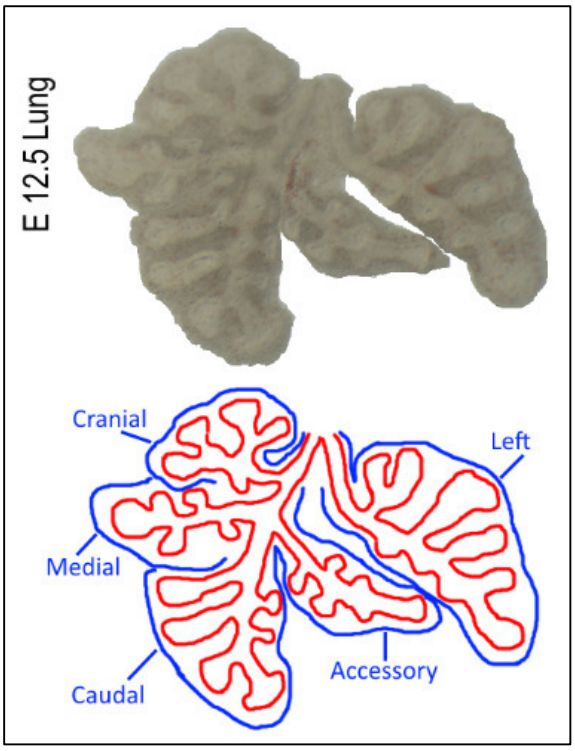

Figure 1: Structure of the mouse lung at E12.5. The lung has one lobe on the left side and four lobes on the right: Cranial, Medial, Caudal and Accessory lobe.

1.1.2 Cell types in the adult mouse lung

About 50 cell types were recognized in the adult mouse lung, these cells can be classified into epithelial and mesenchymal cells. Epithelial cells populate the airways and start to emerge during the pseudoglandular stage: basal, ciliated, neuroendocrine and secretory cells; whereas the mesenchymal cells populate the surrounding extracellular matrix: airway smooth muscle cells (ASMCs), vascular smooth muscle cells (VSMCs), endothelial cells, nerve cells, cartilage and lymphatics. The type I and type II alveolar epithelial cells (AECI, AECII) start to appear during the canalicular stage (E16.5). The proximal region of the mouse lung includes the trachea, which is a ringed-cartilaginous tube, and the main bronchi (which also display cartilage in their most proximal part). This region is populated by basal, goblet, ciliated, clara and neuroendocrine cells. The distal region lack cartilage and mucin producing cells and comprises bronchioles which end into alveolar sacs; it contains few goblet, ciliated, secretory, and alveolar epithelial cells which differentiate between E16.5 and E18.5 into AECI and AECII. AECI are squamous epithelial cells that occupy 95% of alveolar space and responsible for gas exchange. AECII are cuboidal epithelial cells responsible for surfactant production that prevent the alveoli from collapsing (Rawlins and Hogan, 2006; Rock et al., 2010; Rock and Hogan, 2011; McQualter and Bertoncello, 2012) (Figure 2). It has been proposed that AECI and AECII lineages emerge from a common alveolar bipotential progenitor (BP) cells (Treutlein et al. 2014; Desai et al., 2014).

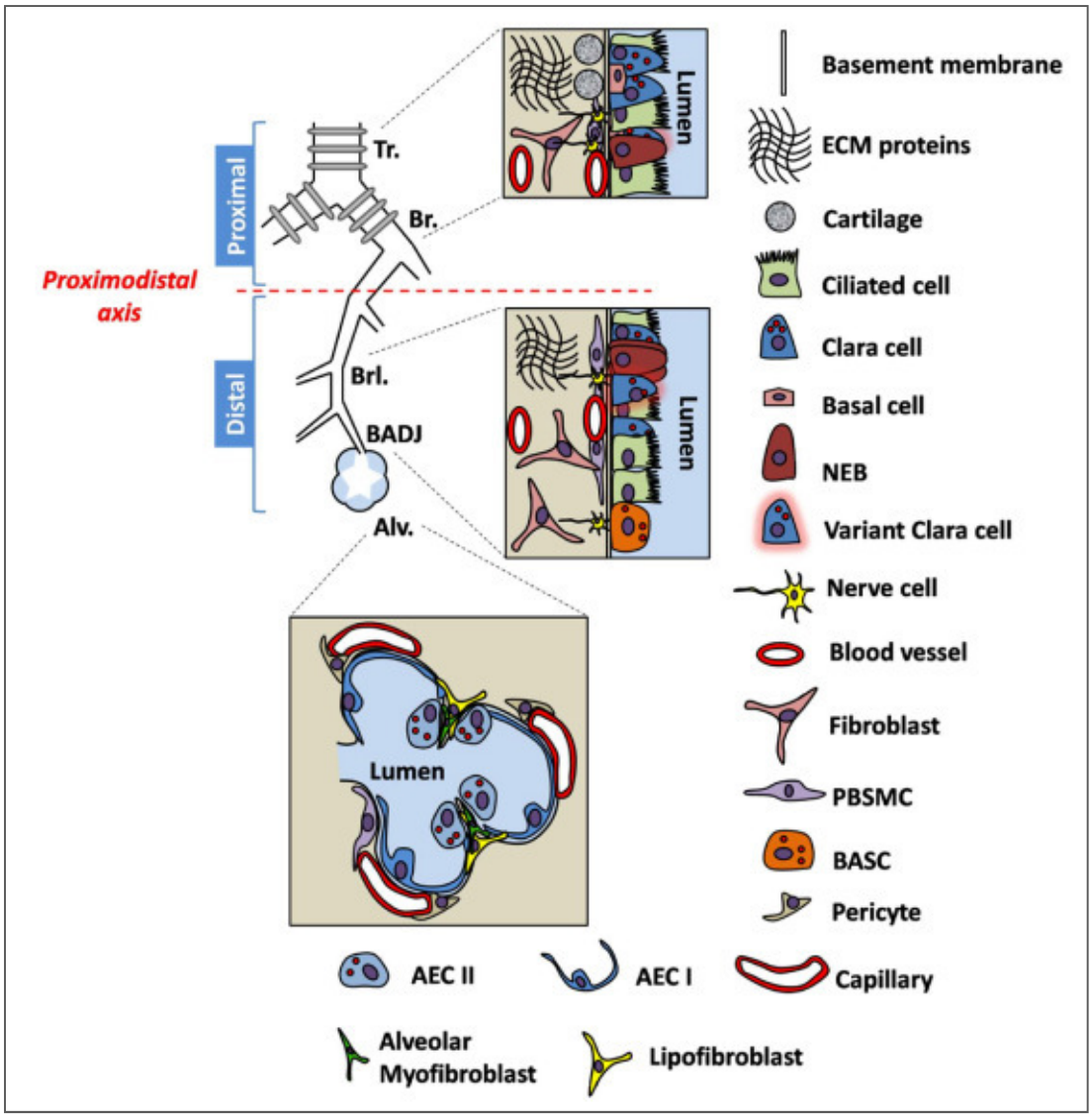

Figure 2: Major cell types along the proximodistal axis of the adult mouse lung. The lung is composed of the conducting (proximal) and respiratory airways (distal) which are composed of special cell types. The conducting airways are composed of basal, ciliated, Clara, and goblet cells. The respiratory airways are mainly composed of AEC1, AEC2, lipofibroblast, myofibroblasts, and alveolar macrophages (not shown in the figure). (Figure adapted from El Agha, Scientifica 2014).

1.1.3 Difference between mouse and human lung

In human, the cartilage extends along the conducting airway which consists of pseudostratified epithelium with basal, multiciliated and secretory cells surrounded by smooth muscle, fibroblasts, vasculature and neurons, and reaches the respiratory airways. Whereas in the mouse, only the conducting airway which is composed of pseudostratified epithelium of the trachea (Tr) and bronchi are surrounded by cartilage. In human, The bronchi (Br) is lined

with an epithelium composed predominantly of mucus-secreting goblet cells, neuroendocrine cells and neuroendocrine bodies (NEBs), whereas the bronchiolar epithelium (Brl) is lined by club cells and an increased number of neuroendocrine cells and NEBs. In the distal alveolar region (Alv), both in human and mouse, the epithelium is highly vascularised and composed of flat alveolar type 1 cells (AEC1), flanked by cuboidal alveolar type 2 cells (AEC2) (Figure 3), which form a thin barrier and provide an extensive surface area for gas diffusion (Gkatzis K et al., 2018). At the tip of each bud reside multipotent epithelial progenitor cells, which are positive for the transcription factors SOX9 and ID2. These cells either self-renew, if they remain distally, or give rise to bronchial progenitors when they exit the tip domain, subsequently acquiring SOX2 expression (Rawlins, 2008)

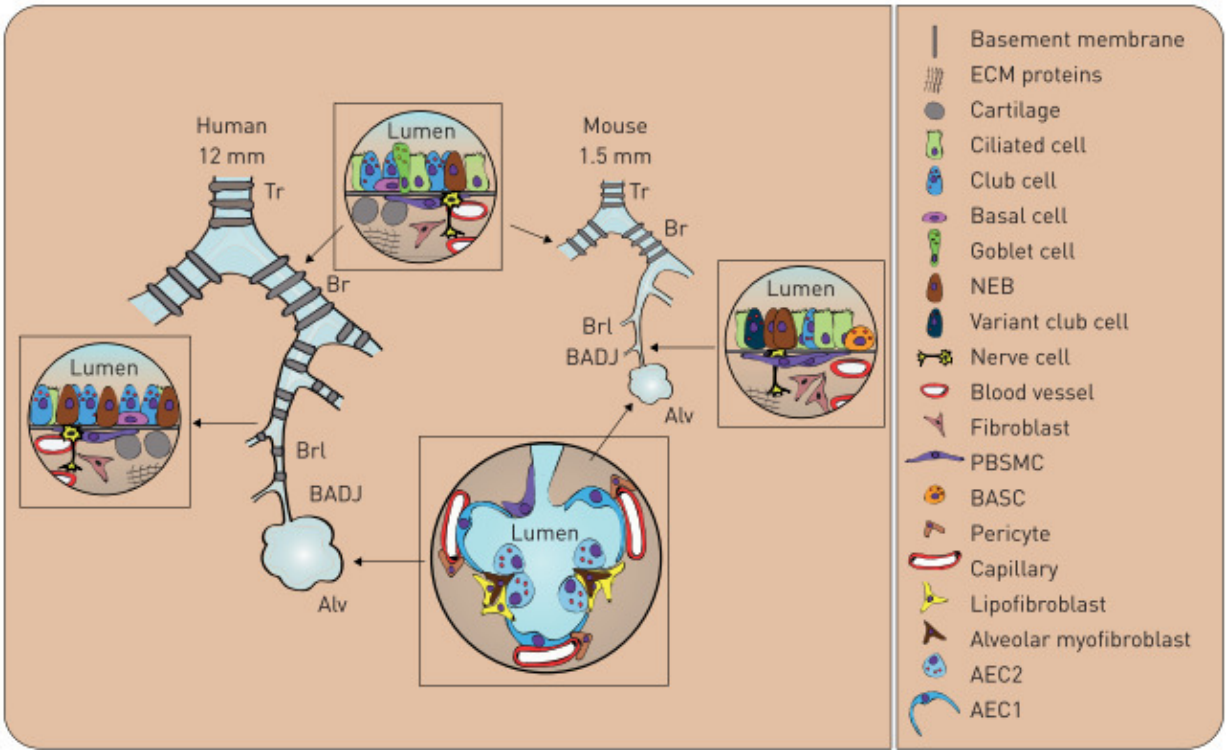

Figure 3: Difference between mouse and human lung architecture. In human, the conducting airways (proximal) consist of ciliated, Basal Goblet and club cells surrounded by smooth muscle, fibroblasts, cartilage, vasculature and neurons. The bronchiolar epithelium (Brl) is lined by club cells and an increased number of neuroendocrine cells and NEBs. The respiratory airways are mainly composed of AEC1, AEC2, lipofibroblasts and myofibroblasts. The cartilage in human extends along the conducting airways and reaches the respiratory airways; while in mouse only the conducting airway is surrounded by cartilage. BADJ: bronchoalveolar duct junction; ECM: extracellular matrix; PBSMC: parabronchial smooth muscle cell. (Figure adapted from Gkatzis K et al., 2018).

1.2 Fibroblast growth factors

Fibroblast growth factors (Fgfs) are a family of growth factors involved in multiple biological processes such as cell division, wound healing, angiogenesis, and they regulate the repair of many organs. Fgfs are also essential for embryonic development in regulating cell proliferation, migration and differentiation. Postnatally, they also act as homeostatic factors (Ornitz and Itoh 2001). The discovery of Fgfs was in 1970, when Armelin reported in his paper that pituitary extracts stimulate the growth of an established line of mouse fibroblast (Armelin, 1973). The first Fgfs (Fgf1, Fgf2) were isolated from the bovine brain and pituitary gland as growth factors for fibroblasts (Gospodarowicz, 1975; Gospodarowicz et al., 1978). Therefore the name 'fibroblast growth factor' was given to Fgfs, because they could induce the proliferation of fibroblasts. Several Fgfs have since been isolated as growth factors for cultured cells. The Fgf family comprises 22 members (Fgf1-23, Fgf15 has not been identified in humans whereas FGF19 has not been identified in mouse, Fgf15 is likely the mouse ortholog of human FGF19), many of which have been implicated in multiple aspects of vertebrate development (Ornitz et al., 2001). The Fgf family can be classified into three groups according to their function: paracrine, endocrine and intracrine. Paracrine and endocrine Fgfs act via cell-surface Fgf receptors (FgfRs); while intracrine Fgfs act independent of FgfRs (Itoh and Ornitz, 2011).

- Paracrine Fgfs comprise members of Fgf/1/2/5, Fgf3/4/6, Fgf7/10/22, Fgf8/17/18 and Fgf9/16/20 subfamilies; they mediate biological responses as extracellular proteins by binding to FgfRs with heparin/heparan sulphate as a cofactor, these Fgfs are involved in multiple organogenetic programs such as heart, lung, kidney and brain.

- Endocrine Fgfs, a hormone-like Fgfs (hFgfs), comprise Fgf 15|19, 21 and 23, can act as a classic endocrine hormone to regulate bile acid homeostasis as well as glucose and lipid metabolism, they require the Klotho gene family of transmembrane proteins as a cofactor to activate Fgf receptors (Makoto Kuro-o, 2008).

- Intracrine Fgfs (iFgfs), Fgf11/12/13/14 are not secreted extracellularly. They act as intracellular molecules in an FgfR-independent manner (Itoh and Ornitz, 2011); they regulate the function of voltage gated sodium channels (Goldfarb et al. 2007).

According to Phylogenetic and gene location analysis, Fgfs can be further divided into seven subfamilies. Fgf1 (1,2), Fgf4 (4,5,6), Fgf7 (3,7,10,22), Fgf8 (8,17,18), Fgf9 (9,16,20), iFgfs (11,12,13,14), and hFgfs (15, 21, 23) (Itoh and Ornitz, 2008) (Figure 4).

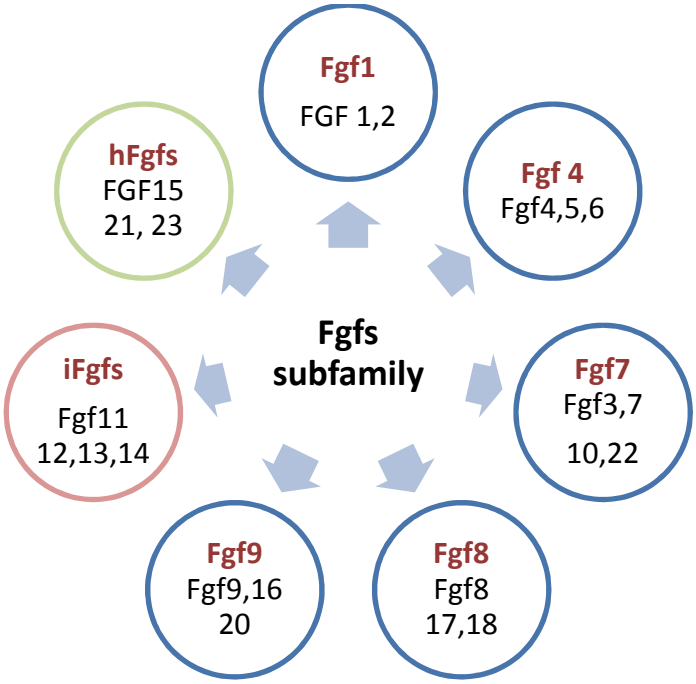

Figure 4: Fgfs Subfamilies. Phylogenetic analysis suggests that the Fgfs can be divided into seven subfamilies containing two to four members each (Itoh and Ornitz, 2008), which can be grouped in three families: paracrine (Blue circle), endocrine (green circle) and intracrine (Red circle).

1.3 Fibroblast growth factors receptors

Fgfs bind with high affinity four ligand-dependent Fgf receptor tyrosine kinase molecules (FgfR1–4). FgfRs are composed of an extracellular domain, which contains three immunoglobulin-like (Ig) subdomains (D1, D2 and D3), a single transmembrane helix segment, and a tyrosine kinase domain in the cytoplasm (Figure 5) (Szebenyi G, 1999). Fgf ligands stably bind FgfR in D2 and D3 domains, in the presence of either heparin, heparan sulfate (HS) or other glycosaminoglycan chains, FgfR get activated (Ornitz et al. 1992, Taylor et al. 2005), leading to the formation of Fgf-FgfR-HS dimers, which enables the cytoplasmic kinase domains to transphosphorylate one another and activates different intracellular signaling pathways, allowing the transmission of biological responses (Mohammadi et al. 2005). Ligand and tissue specificity is an essential mechanism for regulating Fgf activity; it is achieved by alternative splicing in D3 domain. In FgfR (1-3), two alternative exons (IIIb and IIIc) code for the second half of D3 and are spliced to the common exon IIIa (encoding the first half of D3) (Mohammadi et al. 2005). “III” in the isoforms (IIIb and IIIc) refers to the third IgG domain D3, “b” isoform is restricted to epithelial lineages and “c” is restricted to mesenchymal lineages (Alarid et al. 1994, Yan et al. 1993), thereby increasing the number of

principal FgfRs to seven: FgfR1-3(IIIb, IIIc) and FgfR4, each bind a specific repertoire of Fgf ligands (Figure 6) (Ornitz et al., 1996, Zhang et al. 2006). It was proposed by Mohammadi et al. that D1 and D1-D2 linker play a role as FgfR autoinhibitor by repressing Fgf and heparin binding. The acidic region (acidic box (AB)) in D1-D2 linker engages electrostatic interactions with the basic heparin binding site (HBS) of D2, which occlude heparin binding. These interactions likely position D1 to interact with D2-D3 region, which would prevent Fgf binding. The reason why FgfR needs to be subjected to an autoinhibition is that the components of Fgf signaling are often colocalized. Thus, the probability of Fgf or heparin independent dimerization is high, which require tight autoinhibitory control. To overcome the receptor autoinhibition, it is necessary that Fgf and heparin both bind to the receptor. The importance of receptor autoinhibition lies in the fact that when FgfR isoforms are lacking D1 and the acidic box (AB) a progression of pancreatic cancers towards a more malignant state was observed. This finding strongly supports the idea that these regions have an essential negative regulatory role in receptor function (Mohammadi et al. 2005).

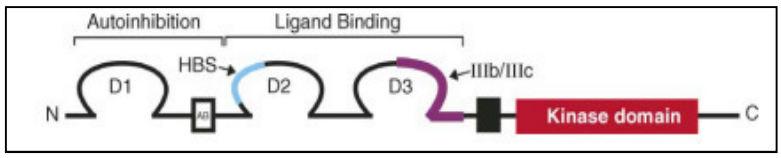

Figure 5: Schematic diagram of FgfR structure. FgfR is composed of an extracellular region containing three immunoglobulin (Ig)-like domains (D1, D2 and D3), 'AB' stands for acid box, a single transmembrane helix (black box), and a cytoplasmic domain with protein tyrosine kinase activity (red box). The heparin binding site (HBS) is colored in blue. The alternatively spliced second half of D3 is colored in purple. FgfR portions involved in receptor autoinhibition and Fgf ligand binding are indicated. Figure adapted from (Mohammadi et al. 2005).

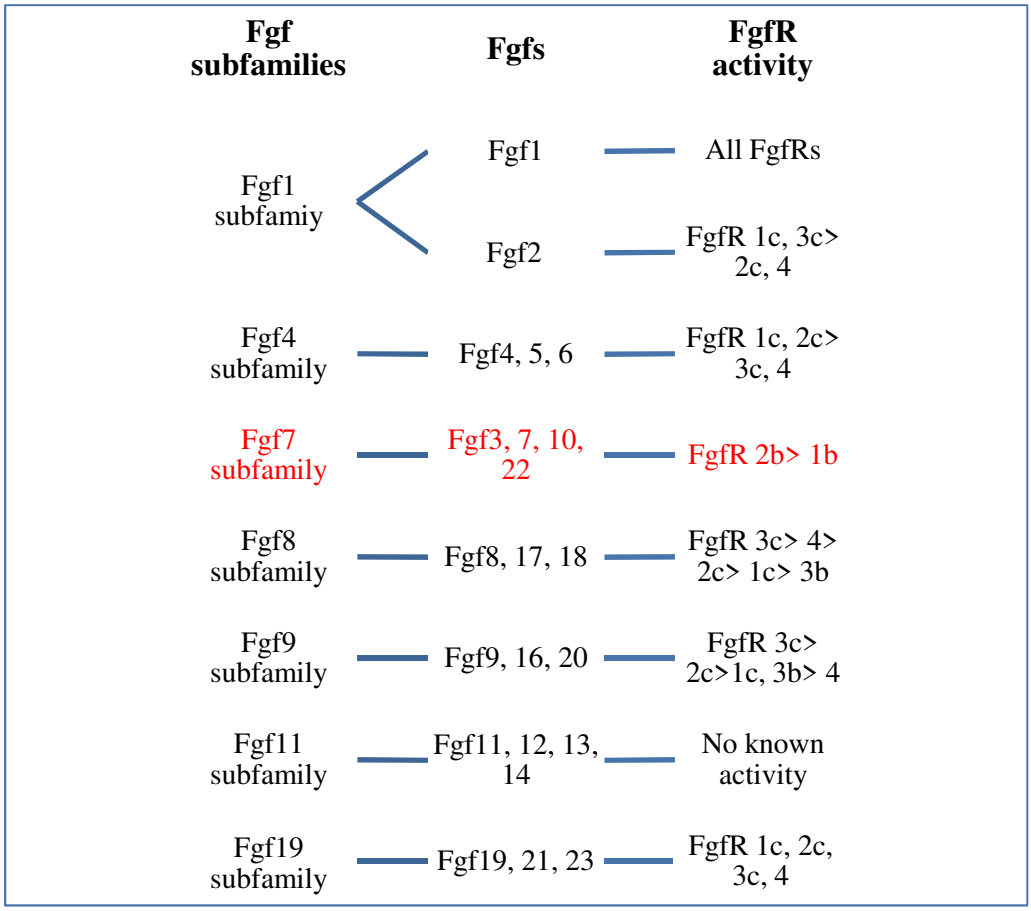

Figure 6: Diagram showing relative activity of Fgfs subfamilies on FgfR isoforms. Data adapted from Zhang et al. using BaF3 cells *in vitro*, showing that Fgf10 binds with high affinity to FgfR2b, but have also some affinity to FgfR1b. (Zhang et al. 2006).

1.4 Fgf10/ Fgfr2b signaling

Fgf10 is a mesenchymal molecule which signals through the receptor Fgfr2b that is expressed mainly in the epithelium (Miki et al. 1991, Igarashi et al. 1998). Fgf10 is expressed in the distal mesenchyme at sites where prospective epithelial buds will appear; it induces budding and outgrowth of early lung endoderm (Bellusci et al., 1997) and exerts a powerful chemoattractant effect on the distal but not on proximal lung epithelium (Park et al. 1998). Fgfr2b binds four known ligands Fgf1, Fgf3, Fgf7 and Fgf10 (Figure 6). Fgf10 is the primary ligand for Fgfr2b during embryonic development as demonstrated by the phenotypic similarities exhibited by embryos where these genes have been inactivated (De Moerlooze et al. 2000, Ohuchi et al. 2000, Mailleux et al. 2002). Fgf10 activates Fgfr2b in a paracrine manner, and the signaling mediated is required for the development of many branched organs including lungs, thyroid, pituitary, lacrimal, and salivary glands (Bellusci et al., 1997;

Makarenkova et al., 2000; Ohuchi et al., 2000). Fgf10 binds Fgfr2b in Ig(II) and Ig(III)domains. In the presence of heparan sulfate proteoglycans (HSPG), Fgfr2b get activated which enables the cytoplasmic kinase domains to transphosphorylate one another and activates different intracellular signaling pathways including: Ras/MAPK, PI3K/Akt, and PLCγ/PKC, these pathways control a variety of cellular behaviors involved in development and repair such as proliferation, differentiation, migration or survival (Figure 7). Mice lacking *Fgf10* or *Fgfr2b* die shortly after birth, due to lung agenesis as well as a complete truncation of the fore-and hind limbs (kato et al. 1999, Sekine et al. 1999). Abnormalities in *Fgf10* or *Fgfr2b* cause agenesis of the anterior pituitary gland, lung, thyroid, salivary gland, and limb, and dysgenesis of inner ear, teeth, skin, pancreas, kidney, palate, and hair follicles (Sekine et al., 1999, Arman et al., 1999; De Moerlooze et al., 2000; Ohuchi et al., 2000). Inhibition of *Fgf10* activity with a soluble dominant negative receptor during the pseudoglandular-canalicular period of development cause decreased lung morphogenesis and severe emphysema at maturity; the inhibition of *Fgf10* activity after birth did not alter alveolarization (Hokuto et al., 2003). In addition, *Fgf10* hypomorphic lungs, which exhibit around a 20% normal *Fgf10* mRNA level, display severe lung hypoplasia, as well as vascular defects with a decreased expression of vascular markers Pecam and Laminin. Smooth muscle cells are also affected with a decrease in α -SMA expression in the respiratory airway (Ramasamy et al., 2007). These results indicate that *Fgf10* plays an important role for the formation and maintenance of multiple mesenchymal and epithelial cell progenitor populations as well as coordinating alveolar smooth muscle cell formation and vascular development. *Fgf10* is also critical for epithelial–mesenchymal interactions necessary for the development of epithelial components of multiple organs (Min et al. 1998). In epithelial-mesenchymal interactions, signals from the mesenchyme direct the epithelial components to generate specific structures through budding or branching morphogenesis and reciprocal interactions between the two tissues must be maintained during further development (Ohuchi et al., 2000). *Fgf10* is also important in the epithelial-mesenchymal transition (EMT), which is a process where epithelial cells change their identity to become mesenchymal cells. EMT plays an essential role in wound healing, organ fibrosis and carcinoma progression. EMT has been categorized into three types: type I in gastrulation, type II in wound healing and type III in metastasis (Thiery et al. 2009, Abolhassani et al. 2014). It has been shown that *Fgf10* plays a role in type I EMT during gastrulation (Gross et al. 2014) and type III EMT on cancer cells and the initiation of metastasis (Abolhassani et al. 2014). During lung development, *Fgf10* is negatively regulated by sonic hedgehog (*Shh*) (Bellusci et al., 1997a), *Tgfβ* (Lebeche et al.,

1999) as well as *Bmp4* (Weaver et al. 2000). *Shh* is a secreted growth factor, which is expressed in the distal epithelium and signals in a paracrine manner via the mesenchymal receptor patched (*Ptc*) and serves to limit the action of FGF10/FGFR2b signaling (Bellusci et al., 1997a). *Fgf10* and *Shh* form a feedback loop where *Fgf10* up-regulate *Shh* expression, *Shh* in turn inhibits *Fgf10* expression. It has been shown that *Shh* induce mesenchymal cell proliferation and differentiation (El Agha and Bellusci, 2014; Minowada et al., 1999). In addition, *Fgf10* plays an important role in inducing and maintaining the expression of *Sprouty2* in the epithelium, which acts as a negative modulator of embryonic lung morphogenesis and growth (Mailleux et al., 2001). *Fgf10* is positively regulated by *Fgf9* likely via *Tbx4/5* (De Langhe et al., 2006; del Moral et al., 2006) as well as *Wnt2* (Goss et al., 2011). Fgf10 acts on the distal lung epithelium via its receptor Fgfr2b activating β-catenin signaling which acts as a regulator of branching morphogenesis and functions to prevents the distal epithelial progenitor cells from differentiating into airway epithelial cells by inhibiting Sox2 expression (Park et al., 1998; Que et al., 2007; Ramasamy et al., 2007; Nyeng et al., 2008; Hashimoto et al., 2012). It has been shown that β-Catenin is a downstream transcriptional target of epithelial Fgf10 signaling (Lü et al., 2005); which upon activation, participates in the induction of Fgfr2b expression to increase Fgf10 signaling further (Shu et al., 2005). Localized Fgf10 expression is not required for lung branching morphogenesis, Volckaert and co-workers showed that lung agenesis in Fgf10 −/− mice can be rescued by ubiquitous over-expression of Fgf10, suggesting that epithelial branching morphogenesis is not dependent on exact Fgf10 localization. They also showed that Fgf10 gain-of-function experiments prevent the differentiation of the multipotent epithelial stem cells towards the bronchial progenitor lineage (Volckaert et al., 2013).

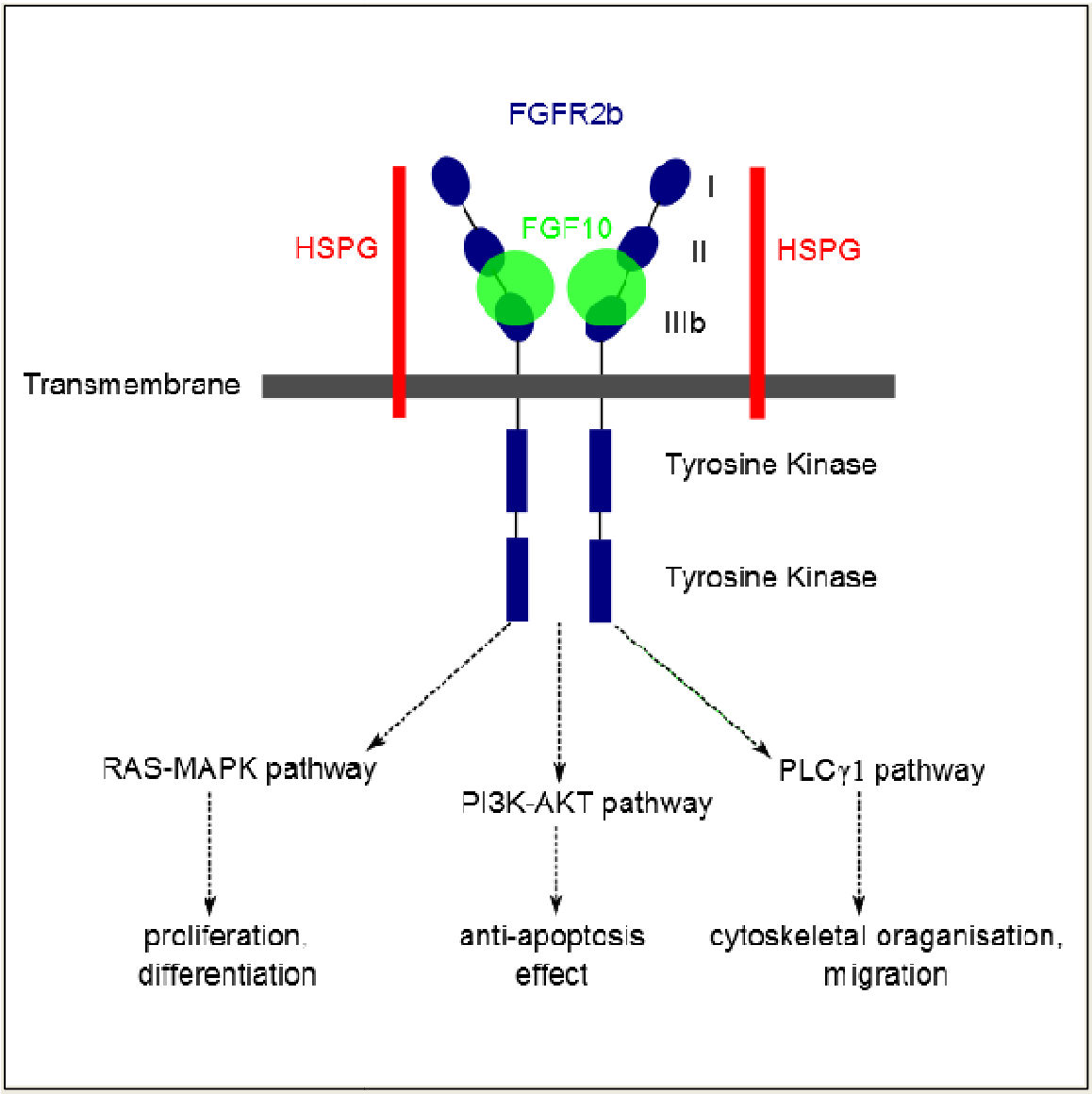

Figure 7: Mechanism of action of Fgf10. In the presence of Heparan sulfate proteoglycan (HSPG), Fgf10 binds FgfR2b with high affinity. The activation of FgfR2b induces activation of the Ras-Mapk, PI3k-Akt, and Plcγ1 pathways. These pathways allow the transmission of biological responses involved in development and repair (Review Itoh 2016).

1.5 Human diseases related to FGF10/FGFR2b deficiency

In humans, deficiency in FGF10 – FGFR2b signaling pathway result in inherited diseases including Lacrimo-auriculo-dento-digital (LADD) syndrome, which is characterized by abnormalities in tear-producing lacrimal and salivary glands, cup-shaped ears, hearing loss and dental and digital abnormalities (Milunsky et al., 2006). FGF10 is also involved in aplasia of lacrimal and salivary gland syndrome (ALSG) which is characterized by aplasia, atresia, or hypoplasia of the lacrimal and salivary systems *(*Entesarian et al., 2007). FGF10 deficiency has been also associated with chronic obstructive pulmonary disease (COPD) which is a complex disease and one of the leading causes of death in developed countries. The most important risk factor for the development of COPD is cigarette smoking, but only a minority of smokers will develop the disease, suggesting contributions of genetic factors (Molfino 2004); Klar and co-workers have shown that haploinsufficiency for FGF10 is associated with reduced pulmonary function consistent with COPD, and their results support the idea that genetic variants affecting the FGF10 signaling pathway are important determinants of lung function that may ultimately contribute to COPD (Klar et al., 2011). FGF10 is also involved in the oncogenesis of pancreatic (Nomura et al., 2008) and breast cancers (Theodorou et al., 2004). In addition, FGF10 deficiency has been associated with bronchopulmonary dysplasia (BPD) which is a chronic lung disease of prematurely born infants characterized by arrested alveolar development (Chao et al., 2017). Single nucleotide polymorphisms in FGF10 are also potential risk factors for limb deficiencies (Browne et al., 2012) cleft lip and palate (Riley et al., 2007), and extreme myopia (Hsi et al., 2013).

1.6 Fgf signaling downstream targets: Etv4 / Etv5

Ets Translocation Variant (Etv) is a part of E26 Transformation-Specific (Ets) family, which is one of the largest families of transcription factors. The Ets family is divided into 12 subfamilies (Table 2). Etv1, Etv4 and Etv5 are members of the Pea3 subfamily which has been implicated in various cellular processes, including proliferation, differentiation, and tumorigenesis (Bartel et al., 2000; Maroulakou and Bowe, 2000; Sharrocks, 2001).Evidence from multiple studies has demonstrated that ETV4 and ETV5 are primary mediators of fibroblast growth factor (FGF) signaling via fibroblast growth factor receptor 2b (FGFR2b), and play overlapping roles in the patterning, morphogenesis, differentiation, and homeostasis of multiple organs and structures (Jones et al., 2019 b) . Etv4 and Etv5 are expressed predominantly in the lung bud epithelium at E10.5. At later developmental stages (E11-E15) Etv5 becomes restricted to the distal growing epithelium of the branching ducts, and Etv4 is expressed in the epithelial and mesenchymal compartment (Chotteau-Le-lievre et al., 1997). It has been shown that Etv4 is a specific downstream transcriptional target for Fgf signaling (Mao et al., 2009).

Subfamily	Mammalian family members
Elf	Elf1, Elf2 (Nerf), Elf4 (Mef)
Elg	Gabpα
Erg	Erg, Fli1, Fev
Erf	Erf (Pe2),Etv3 (Pe1)
Ese	Elf3 (Ese1/Esx), Elf5 (Ese2), Ese3 (Ehf)
Ets	Ets1, Ets2
Pdef	Spdef (Pdef/Pse)
Pea3	Etv4 (PEA3/E1AF), Etv5 (ERM), Etv1 (ER81)
Er71	Etv2 (Er71)
Spi	Spi1 (Pu.1), Spib, Spic
Tcf	Elk1,Elk4 (Sap1), Elk3 (Net/Sap2)
Tel	Etv6 (Tel), Etv7 (Tel2)

Table 2: Subfamilies of E26 Transformation-Specific (Ets). The Ets family is divided into 12 subfamilies. Etv4 and Etv5 belong to Pea3 subfamily.

1.6.1 Characterization of a *Tg*(*Etv4-GFP*) reporter line

Tg(Etv4-GFP) is a recently reported transgenic mouse, generated using a bacterial artificial chromosome containing the *Etv4* gene with a knock in of *GFP* in frame with exon 9, allowing monitoring the activation of the Fgf signaling through the detection of the reporter gene for the expression of *Etv4*. In the process, exons 10–13 of the Etv4 construct were deleted. Thus, the randomly inserted Tg(Etv4-GFP) transgene is non-functional, and does not interfere with endogenous Etv4 activity (Lamballe et al. 2011) (Figure 8). The *Tg*(*Etv4-GFP)* reporter line has been quite useful to follow up the activation domain of Fgf10 in the embryonic lung epithelium during the process of branching morphogenesis.

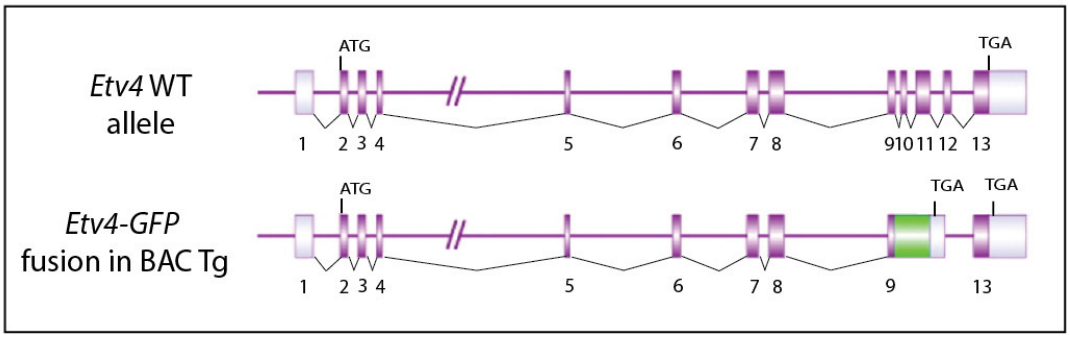

Figure 8: Schematic representation of the generation of *Tg(Etv4-GFP)* mice. The *Etv4* locus is located on mouse chromosome 11. *GFP* cassette is inserted in frame with exon 9 of *Etv4*. After fusion to the *GFP* cassette (green), the resulting *Tg(Etv4*-GFP) fragment has been introduced into the BAC RP24–79P16. The strategy also included the deletion of exons 10–13 of *Etv4* in the BAC, such that the *Etv4* locus is knocked out and does not lead to expression of functional Etv4 protein. (Figure adapted from Lamballe et al. 2011).

2. Objectives

The work presented in this dissertation is intended to explore the role of Fgf10/FgfR2b signaling during early lung development, in the first part of the Results section, we visualized the dynamics of Fgf signaling during lung development using a reporter mouse line Tg(*Etv4-GFP).* In the second part, we studied the loss of function by using the double transgenic (DTG) approach *Rosa26*$^{rtTA/rtTA}$*; Tg(tet(O)sFgfr2b)/+* to attenuate the activity of the Fgfr2b ligands during early lung development. Then, we used time-lapse fluorescence imaging on the left lobe of embryonic lungs to study the impact of *Fgf10* inhibition on branching morphogenesis. We identified the *Fgf10* downstream target genes using gene array approach where we identified the transcription factors controlled by *Fgf10*, and its role in the differentiation of multipotent epithelial progenitors. In the third part, we studied the gain of function by using of the double transgenic approach *Rosa26*$^{rtTA/rtTA}$; Tg(tet(O)Fgf10)/+ to over express Fgf10, we validated the transgenic system, we studied the impact on branching morphogenesis and finally we performed a gene array approach to identify the genes that are up or down-regulated upon Fgf10 over expression. In the last part, we compared the loss and gain of function experiments at 9 hours post dox IP. The aims of this work are summarized as the following:

1. Validation and visualization of the *Etv4*-GFP reporter mouse line to follow Fgf signaling.
2. Loss of function: Validation of the dominant negative approach *Rosa26*$^{rtTA/rtTA}$*; Tg(tet(O)sFgfr2b)/+ in vitro/in vivo* (protocol in USA for *in vivo*).
3. Impact of Fgf10 inhibition on branching morphogenesis.
4. Identification of genes induced or repressed by FgfR2b signaling using gene array approach.
5. Role of Fgf10 signaling in the differentiation of multipotent epithelial progenitors.
6. Gain of function: Validation of the double transgenic approach *Rosa26*$^{rtTA/rtTA}$; Tg(tet(O)Fgf10)/+ .
7. Impact of over-expressing Fgf10 on branching morphogenesis.
8. Identification of genes induced or repressed upon Fgf10 over expression using gene array approach.
9. Comparison between LoF and GoF experiments 9 hours after Dox IP.

3. Material and methods

3.1 Study approval

Animal experiments were performed at Children's Hospital Los Angeles under the research protocols 31-08 and 31-11, approved by the Animal Research Committee and in strict accordance with the recommendations in the Guide for the Care and Use of Laboratory Animals of the National Institutes of Health. The approval identification for Children's Hospital Los Angeles is AAALAC A3276-01. Harvesting organs and tissues from wild type and mutant mice following euthanasia using CO2 was approved at Justus Liebig University Giessen by the federal authorities for animal research of the Regierungspräsidium Giessen, Hessen, Germany (Approved Protocol No. 452_M).

3.2 Generation and genotyping of mice

3.2.1 Generation of the double transgenic mice: *Rosa26* $^{rtTA/rtTA}$; *Tg(Tet(O)sFgfr2b)/+* and *Rosa26* $^{rtTA/rtTA}$; *Tg(Tet(O)Fgf10)/+*.

The inducible mouse model (*Rosa26*$^{rtTA/rtTA}$*;Tg(Tet(O)sFgfr2b /+* and (*Rosa26*$^{rtTA/rtTA}$*; Tg(Tet(O)Fgf10 /+)* were generated by first crossing *CMV-Cre* mice [*c-Tg(CMV-cre)1Cgn/J*; Jackson Laboratories] with *Rosa26-rtTAflox* mice (Belteki et al. 2005). The resulting *Rosa26rtTA/+* mice were then crossed with *Tet(O)sFgfr2b* mice (Hokuto et al., 2003) and *Tet(O)Fgf10 (*Clark et al., 2001) respectively for several generations on a mixed background. Different allelic combinations for the *Rosa26rtTA* and the *Tet(O)sFgfr2b (Tg)* or the *Tet(O)Fgf10* (Tg) transgene ([*Rosa26rtTA/+ ;Tg/+],* [*Rosa26rtTA/+ ;Tg/Tg*] and [*Rosa26rtTA/rtTA;Tg/Tg*]) were generated to allow the expression of different levels of soluble *Fgfr2b* or *Fgf10* following doxycycline (Dox) treatment. All mice were generated on a CD1 mixed background and allowed the expression of soluble *Fgfr2b* and *Fgf10* respectively by administration of doxycycline-containing food (625 mg doxycycline/kg) or via a single intraperitoneal (IP) injection of doxycycline (0.0015 mg per gram body weight) injected to pregnant females.

3.2.2 Genotyping of Rosa26 $^{rtTA/rtTA}$; Tet(O)sFgfr2b)/+ and Rosa26 $^{rtTA/rtTA}$;Tet(O)Fgf10)/+ mice.

The genotype of *Rosa26* $^{rtTA/rtTA}$*; Tet(O)sFgfr2b)/+ and Rosa26* $^{rtTA/rtTA}$ *;Tet(O)Fgf10)/+* was performed by digesting tissues from the tip of the tails in 200µl Viagen including 1µl proteinase K in 55°C on a shaker overnight, then the temperature was raised to 85°C for 30

min to stop the reaction. Genotyping were done by PCR. For primer sequences please see Table 3.

Mouse line	Primer sequence
Rosa26 rtTA/rtTA	1. GAG TTC TCT GCT GCC TCC TG 2. CGA GGC GGA TAC AAG CAA TA 3. AAG ACC GCG AAG AGT TTG TC
Tet(O)sFgfr2b/+	1. GAA GGA GAT CAC GGC TTC C 2. AGA CAG ATG ATA CTT CTG GGA CTG T
Tet(O)Fgf10/+	1. GAC GCC ATC CAC GCT GTT TTG ACC 2. ATT TGC CTG CCA TTG TGC TGC CAG

Table 3: Primer sequences used in the genotyping of *Rosa26* $^{rtTA/rtTA}$; *Tg(Tet(O)sFgfr2b)/+* and *Rosa26* $^{rtTA/rtTA}$ *;Tg(Tet(O)Fgf10)/+.*

3.3 RNA extraction

The left lobe was removed for histology; the right lobe was removed and placed in QIAzol lysis reagent (Qiagen GmbH, Hilden, Germany). Tissue was homogenized in GentleMACs for 1 min and tubes were spun down at 1200 rpm for 5 min in room temperature. Supernatant was collected and frozen in liquid nitrogen and stored at -80°C until RNA extraction could be performed. RNA was purified using RNeasy or miRNeasy kit (Qiagen, Hilden, Germany) following the kit instructions. The samples were quantified using Nanodrop for RNA concentration and purity; then stored at -80°C until reverse transcription was performed.

3.4 cDNA synthesis and quantitative PCR

After RNA isolation, cDNA is synthesized using QuantiTect Reverse Transcription Kit (Qiagen, Hilden, Germany). Primers were designed using Roche Applied Sciences online Assay Design Tool. Syber Green Master Mix (invitrogen, Germany) was used for Real Time-PCR with a Roche LightCycler 480 machine. Samples were run in triplicates using *Hprt* as a reference gene and the ΔΔCT method was used for relative quantification.
Delta Ct (ΔCT) and deltadelta Ct (ΔΔCT) values were calculated according to the following formulas:

$\Delta Ct = Ct_{Reference} - Ct_{gene\ of\ interest}$

$\Delta\Delta Ct = MeanΔCt_{Experimental} - MeanΔCt_{Control}$

The mouse primers are listed in the table below:

Gene	Forward sequence (5'-3')	Reverse sequence (5'-3')
Hprt	CCTAAGATGAGCGCAAGTTGAA	CCACAGGACTAGAACACCTGCTAA
Fgf1	CCGAAGGGCTTTTATACGG	TCTTGGAGGTGTAAGTGTTATAATGG
Fgf7	ACTATCTGCTTATAAAATGGCTG CT	GTGGGGCTTGATCATCTGAC
Fgf10	CGGGACCAAGAATGAAGACT	GCAACAACTCCGATTTCCAC

Table 4: Primer sequences for *Fgf1*, *Fgf7*, *Fgf10* and *Hprt* (reference gene) used for qPCR.

3.5 Lung culture, time lapse microscopy and quantification

Embryonic lungs were harvested and grown *in vitro* on Nucleopore membrane filters placed in 500 µl Dulbecco's Modified Eagle's Medium (DMEM) with 10% Fetal Bovine Serum (FBS) and 1% Penicillin/Streptomycin. Culture dishes were then placed into the culture chamber (37°C; 5%CO2) of Leica DMI6000 B live imaging microscope time-lapse imaging was performed. The intensity of GFP signal was measured using Metamorph software from Leica version 1.5.0. The quantification of the lungs (number of buds, distance between epithelium-mesothelium and the length of branches) were measured using Image J software (NIH, Bethesda, MD, USA).

3.6 Tissue processing and Immunostaining

3.6.1 Sox2 Immunostaining

Lungs were fixed in 4% PFA/PBS according to standard procedures. After embedding tissues in paraffin and sectioned at 5 µm thickness, slides were deparaffinized. The slides were washed for 5 min in MilliQ, then in TBS for 5min and blocked with 3% BSA and 0.4% Triton-X (in TBS) at RT for 1 hour. Then, they were incubated with primary antibodies

(1:100 diluted) at 4°C overnight and washed three times in TBS for 5 min. Slides were then incubated with secondary antibodies (1:500 diluted) at RT for 1 hour and mounted with Prolong® Gold Anti-fade Reagent with DAPI (Invitrogen) (The antibodies used are listed in Table 5). Fluorescent images were acquired using Leica DM5500 B fluorescence microscope and Leica DFC360 FX camera.

3.6.2 Sox9 Immunostaining

After the fixation of lungs with 4% PFA, tissues were embedded in paraffin and sectioned at 5 µm thickness. After that, slides were deparaffinized and washed for 5 min in MilliQ. For antigen retrieval, sections were immersed in citrate buffer for 20 min, then in ice for 30 min. The slides were then washed in PBST (Phosphate Buffered Saline Tween-20) for 5min and blocked with 3% BSA and 0.4% Triton-X (in TBS) at RT for 60 min. Then, they were incubated with primary antibodies (AB) (1:200 diluted) at 4°C overnight. Then, slides were washed three times in PBST for 5 min. And then incubated with secondary antibodies (1:500 diluted) at RT for 1h. Slides were mounted with Prolong® Gold Anti-fade Reagent with DAPI (Invitrogen) (The antibodies used are listed in Table 5). Fluorescent images were acquired using Leica DM5500 B fluorescence microscope and Leica DFC360 FX camera.

	Antibodies	**Host**	**Supplier**
Primary AB. used for Sox2 and Sox9	SOX 2 Polyclonal.Ab rabbit	Rabbit	Acris
	SOX9 rabbit anti-human pAb 50UG	Rabbit	Biozol
Secondary AB. used for Sox2 and Sox9	Alexa Fluor®-555 anti-rabbit	Goat	Invitrogen
	Alexa Fluor®-594 anti-rabbit	Donkey	Life technologies

Table 5: The list of primary and secondary antibodies used for Sox2 and Sox9 Immunostaining.

3.7 Microarray experiments

After the purification of the RNA using RNeasy Mini Kit (Qiagen, Hilden, Germany) following the kit instructions, RNA samples were given to Dr. Jochen Wilhelm and microarray experiments were performed in his laboratory according to the following steps: Purified total RNA was amplified and Cy3-labeled using the LIRAK kit (Agilent) following the kit instructions. 200ng of total RNA was used per reaction. The Cy3-labeled aRNA was hybridized overnight to 8x60K 60mer oligonucleotide spotted microarray slides (Agilent Technologies, design ID 028005). Hybridization and subsequent washing and drying of the slides were performed following the Agilent hybridization protocol. The dried slides were scanned at 2 µm/pixel resolution using the InnoScan is900 (Innopsys, Carbonne, France). Image analysis was performed with Mapix 6.5.0 software, and calculated values for all spots were saved as GenePix results files. Stored data were evaluated using the R software (R Development Core Team 2007) and the limma package (Ritchie et al. 2015) from BioConductor (Gentleman et al. 2004). Mean spot signals were background corrected with an offset of 1 using the NormExp procedure on the negative control spots. The logarithms of the background-corrected values were quantile-normalized (Ritchie et al. 2015, Silver et al. 2009). The normalized values were then averaged for replicate spots per array. Different probes addressing the same NCBI gene ID were tested, the probe showing the maximum average signal intensity over the samples was used in subsequent analyses. Genes were ranked for differential expression using a moderated t-statistic (Ritchie et al. 2015). Pathway analyses were done using gene set tests on the ranks of the t-values (Ritchie et al. 2015).

4. Results

4.1 Use of the reporter mouse line *Tg(Etv4-GFP)* to visualize the dynamics of Fgf signaling during lung development.

To characterize *Tg(Etv4-GFP)* expression in various organs during development, embryos were generated at different stages (E9.5, E11.5, E12.5, and E13.5).We visualized mouse embryos using fluorescence microscopy, the expression of *GFP* (Green signal) was detected in the organs responding to Fgf signaling: head, tail, limb, and lung (Figure 9). At E9.5, GFP was detected in the nasal placode, the mandibullary and maxillary processes, and at the mid-brain/hindbrain junction (Figure 9c), the anterior limb bud and the mammary line (Figure 9e), the otic placode (Figure 9d), and the tail bud (Figure 9f). Similar expression sites were found at E11.5 (Figures 9h–l). Close examination of the lung indicated that GFP was expressed specifically at the tips in the epithelium and mesenchyme (Figure 9m). At E12.5, GFP was enriched in the posterior (glandular) stomach (Figure 9o), the developing kidneys (Figure 9q), the epithelium of the cecum (Figure 9s), and the lung epithelium and mesenchyme (Figure 9t). At E13.5, GFP was found in similar places (Figure 9w, y, z). In addition, GFP was located at the tip of the forming digits (Figure 9x) (Jones et al., 2019b).

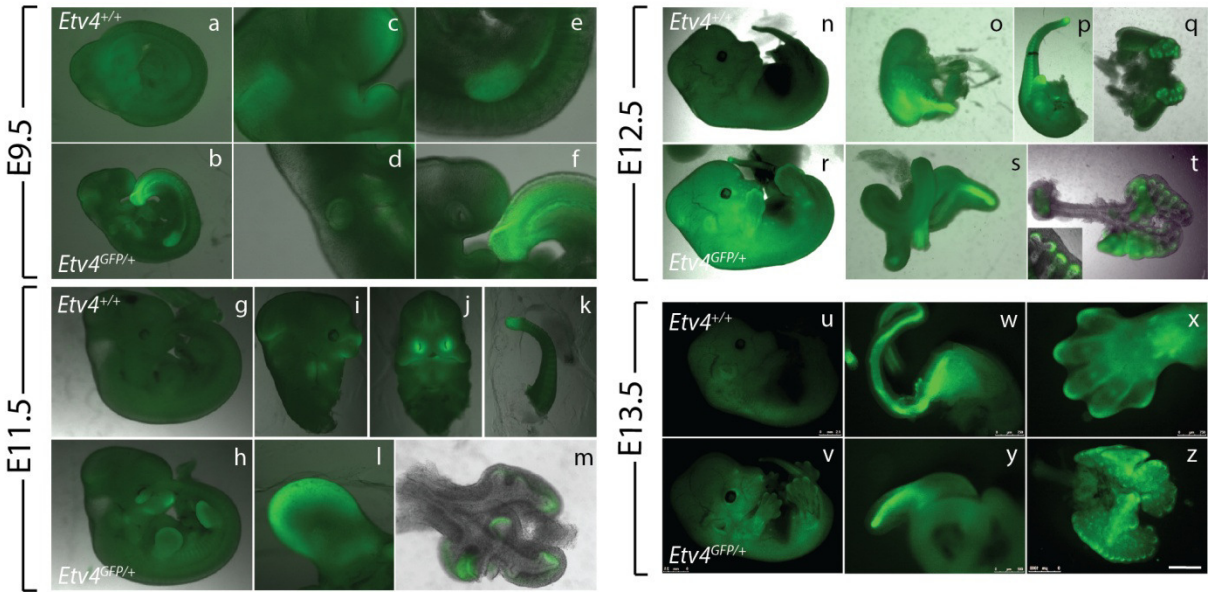

Figure 9: Determination of the expression pattern in different organs responding to FGF signaling. Expression of *Tg*(*Etv4*-GFP) at E9.5, E11.5, E12.5 and E13.5 in the mouse embryo visualized by fluorescence microscopy. (a, g, n and u) wild type embryos. (B) *Tg*(*Etv4*-GFP) embryo. Expression of *GFP* in areas of known Fgf signaling including the head (i, j), tail (f,k), limb (l, x) and Lung (m, t and z).

4.1.1. Dynamic GFP Expression Reports FGF10 Signaling

To monitor the expression of *Tg(Etv4-GFP)* in the epithelial buds of pseudoglandular stage lungs in the context of FGF10 signaling, E12.5 *Tg(Etv4-GFP)* lungs were cultured and live imaged for 24 h, then FGF10 signaling was blocked using an anti-FGF10 antibody for an additional 24 h (Figure 10A). During the first 24 h, Etv4-GFP was dynamically expressed, showing greater expression at the distal tips of growing buds, in likely regions of active FGF10 signaling (Figures 10Ba–c). During the Fgf10 signal inhibition, Etv4-GFP expression was greatly reduced. Still images from multiple time points during the live imaging from three independent lungs were used to quantify these global changes in fluorescence intensity (Figure 10C). As the expression of Etv4-GFP in E12.5 transgenic lungs was maintained in culture for at least 38 h (Figure 11A), we confirmed that the loss of GFP expression of the E12.5 lungs after 24h in culture was neither due to bleaching, nor to a normal decrease in Etv4-GFP expression. Furthermore, still images of individual buds were used to quantify the dynamic expression of Etv4-GFP in three regions of the bud during a branching event (Figure 10D, E). Intensity was measured during new branch formation at the tip (regions 4 and 6), stalk (regions 1–3; 7– 9) and cleft (region 5). Tip Etv4-GFP fluorescence intensity initially increased before stabilizing (Figure 10Ea), whereas stalk and cleft fluorescence intensity increased before decreasing to initial levels (Figures 10Eb, c). The expression patterns of the stalk and cleft reflected the initial single bud branching into two buds. These results suggest that the *Tg(Etv4-GFP)* mouse line can be used as a valid tool to report FGF10 signaling in the distal tips of lungs during pseudoglandular development. This conclusion is supported by the previously described dynamic expression pattern of Sprouty2 during the branching process (Mailleux et al., 2001). Sprouty2 is a well-accepted target of FGF10 signaling in the lung, and displays a remarkably similar expression pattern to what we found for *Tg(Etv4-GFP) (*Jones et al., 2019b).

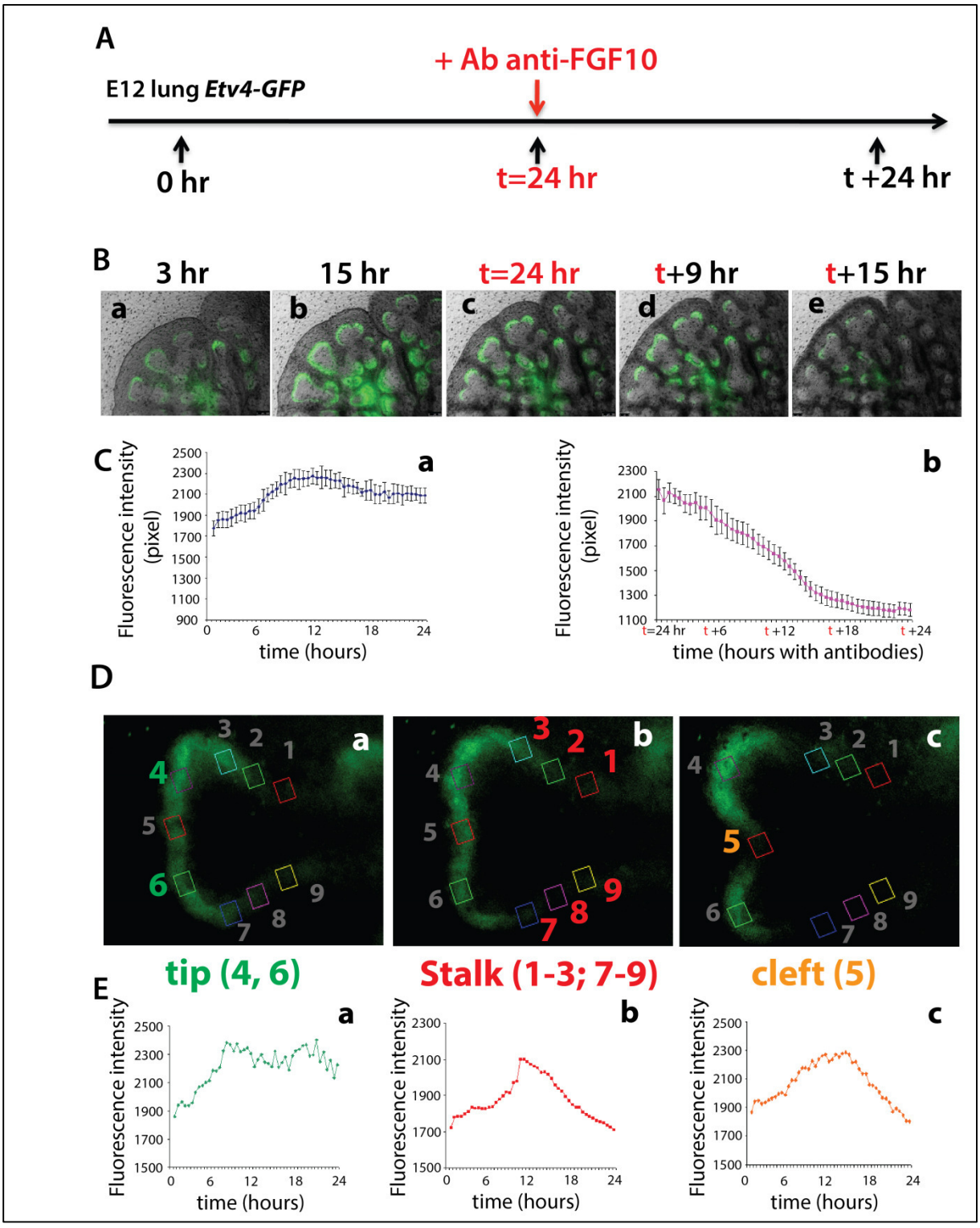

Figure 10: Etv4-GFP is dynamically expressed in regions of active FGF10 signaling during early lung development. (A) Experimental design: E12.5 *Tg(Etv4-GFP)* lungs were isolated, cultured and live imaged for 48 h. After 24 h anti-FGF10 antibody was added to inhibit Fgf10 activity. (B) Still images from different time points during the live imaging experiment. Note how Etv4-GFP expression increases before leveling off within the first 24 h (a–c), and once the antibody is added, the expression decreases to almost zero by the end of

the experiment (c–e). Scale bar: 125 µm. (C) Global Etv4-GFP fluorescence intensity measured at various time points before (a) and after (b) adding the FGF10 blocking antibody. (n = 3; data are presented as average fluorescence intensity in arbitrary units (a.u.) ± standard deviation). (D) Example images of a branching tip at three successive time points (a–c), highlighting three regions of dynamic Etv4-GFP expression: the tip (4 and 6), the stalk (1–3, and 7–9), and the cleft (5). Scale bar: 30 µm. (E) Representative plot of ETV4-GFP expression in three independent regions [(a) tip, (b) stalk and (c) cleft] of a single bud over a period of 24 h (n = 1; a.u. = arbitrary units).

Then, we tested the effect of adding exogenous FGF7 and FGF10 on embryonic Tg(*Etv4-GFP)* lungs. E12.5 lungs were grown *in vitro* and incubated with human recombinant protein FGF7 (25 ng/ml) or FGF10 (250 ng/ml) for 40 hours (Figure 11A). The quantification shows that exogenous FGF7 increases the width of the branches while FGF10 increases the number of buds (Figure 11Am-o), and both of them amplify Sox9 positive distal epithelial progenitors (Figure 11B). FGF7 as well as FGF10 both amplify Sox9 positive distal epithelial progenitors but not Sox2 proximal epithelial progenitors (Figure S1), this amplification shows that over-expression of FGF10 at E12.5 prevent some distal epithelial progenitors to differentiate into Sox2-expressing airway epithelial cells, which correlate with what was published by Volckaert group where they show that over-expression of FGF10 from E12.5 onwards was able to prevent the differentiation of some distal Sox9-expressing epithelial progenitors into Sox2-expressing airway epithelial cells (Volckaert et al. 2013).

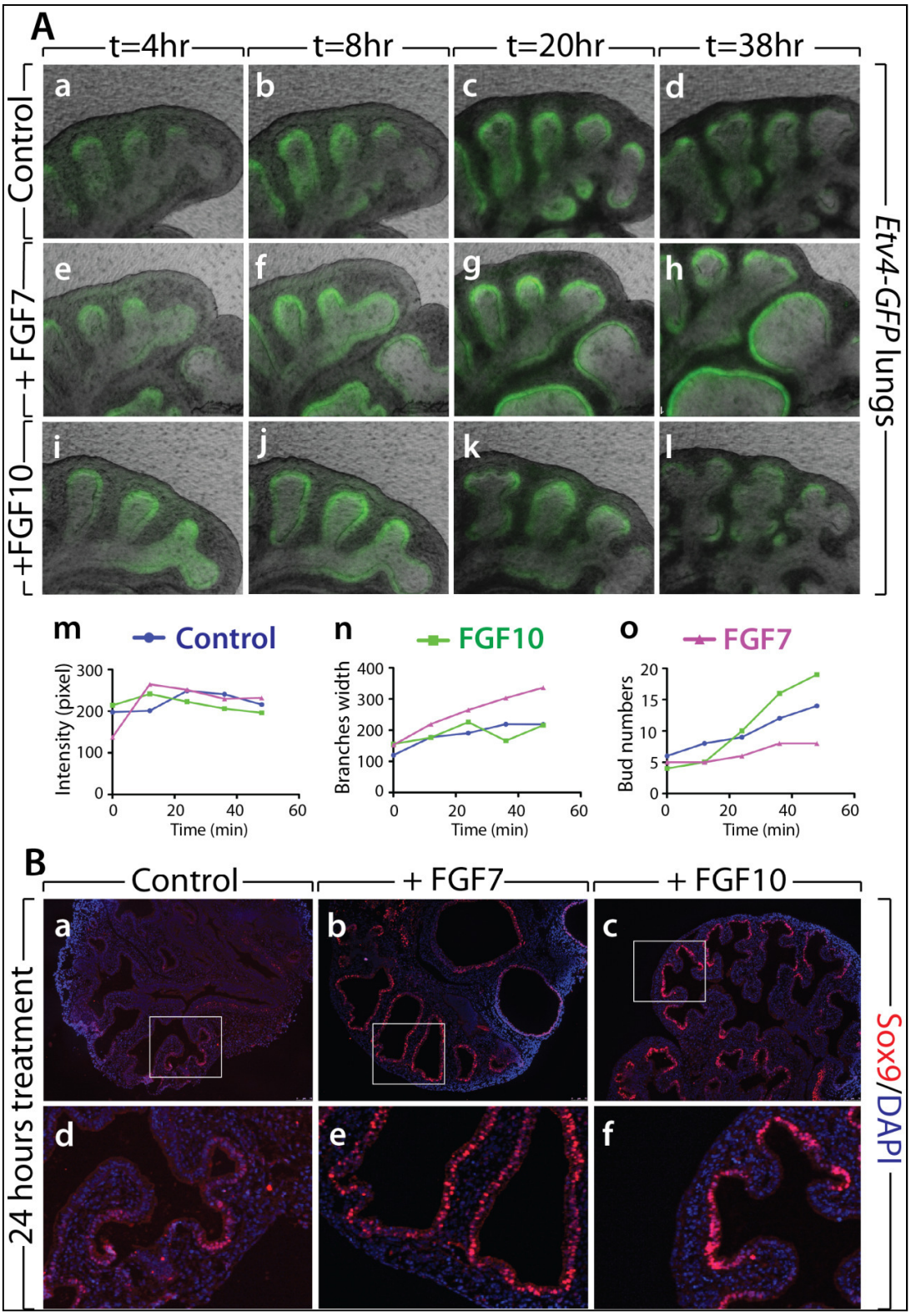

Figure 11: The effect of adding exogenous FGF7 and FGF10 on *Etv4-GFP* lungs. (A) E12.5 *Tg*(*Etv4-GFP)* lung grown and incubated with FGF7 (25 ng/ml) and FGF10 (250 ng/ml) *in vitro* for 40 hours. (B) SOX9 Immunostaining on *Tg*(*Etv4*-GFP) lungs incubated with FGF7 and FGF10.

4.2 Loss of function (LoF): The use of the double transgenic (DTG) approach *Rosa26$^{rtTA/rtTA}$; tet(O)sFgfr2b/+* to attenuate the activity of the FGFR2b ligands during early lung development

4.2.1 Expression of the main FGFR2b ligands during early lung development, and validation of the double transgenic approach

To determine which FGFR2b ligands are mainly expressed during early lung development, a qPCR was performed for *Fgf1, 3, 7, 10* and *22*. Only *Fgf1*, *7* and *10* were detected, and *Fgf10* was the only ligand predominantly expressed at E12.5 (Figure 12A). The expression of *Fgf1* starts only at E13.5 while *Fgf7* starts later (Bellusci et al., 1997). To determine the role of these ligands during early lung development, we have used a double transgenic system, Rosa26$^{rtTA/rtTA}$; tet(O)sFgfr2b, which allows to attenuate the ligands activity. Upon exposure to Doxycycline (dox) via food or intraperitoneal (IP) injection, the transactivator rtTA is activated and the soluble FGFR2b is expressed. This fusion protein binds to FGFR2b ligands preventing them to interact with their endogenous receptor (Figure 12B). To validate the use of our double transgenic mice *in vivo*, pregnant females were placed on dox food starting at different time point: E10.5-E14.5; then the lungs were harvested at E18.5 (Figure 12C). The results show a severe defect in the branching of the lung, with elongated and simplified epithelial tubes; we can notice that the earlier the treatment is given the more severe phenotype occurs. The same results were observed in the limbs development when FGFR2b ligands were blocked (Danopoulos et al. 2013). To validate the inactivation of FGFR2b ligands *in vitro*, DTG *Rosa26$^{rtTA/rtTA}$; Tg(tet(o)sFgfr2b)/+* (experimental) and single transgenic (STG) *Rosa26$^{rtTA/rtTA}$; +/+* (control) lungs were harvested at E12.5, and cultured in the presence of (1µg/ml) doxycycline for 72 hours (Figure 12D), we observed a simplification in DTG lungs shape, elongation of the epithelium tubes and reduced number of buds, comparing to STG lungs. To summarize, *Fgf10* is the main ligand predominantly expressed at E12.5 (the other FGFR2b ligands are expressed at much lower levels). In addition, the knockout (KO) of *Fgf10* and *Fgfr2b* lead to the same lung agenesis phenotype demonstrating that FGF10 is the main ligand for FGFR2b during early lung development. For this reason, we have chosen to perform our next experiments at that time point, as inhibiting FGFR2b ligands at this stage is equivalent to block FGF10 activity specifically. It was also demonstrated that the genetic inactivation of the genes encoding the other FGFR2b ligands (*Fgf1* and *Fgf7*) lead to completely viable mice (Miller et al. ,2000; Guo et al., 1996).

We have also validated an inducible transgenic system allowing the blockade of Fgfr2b ligands *in vivo* and *in vitro*.

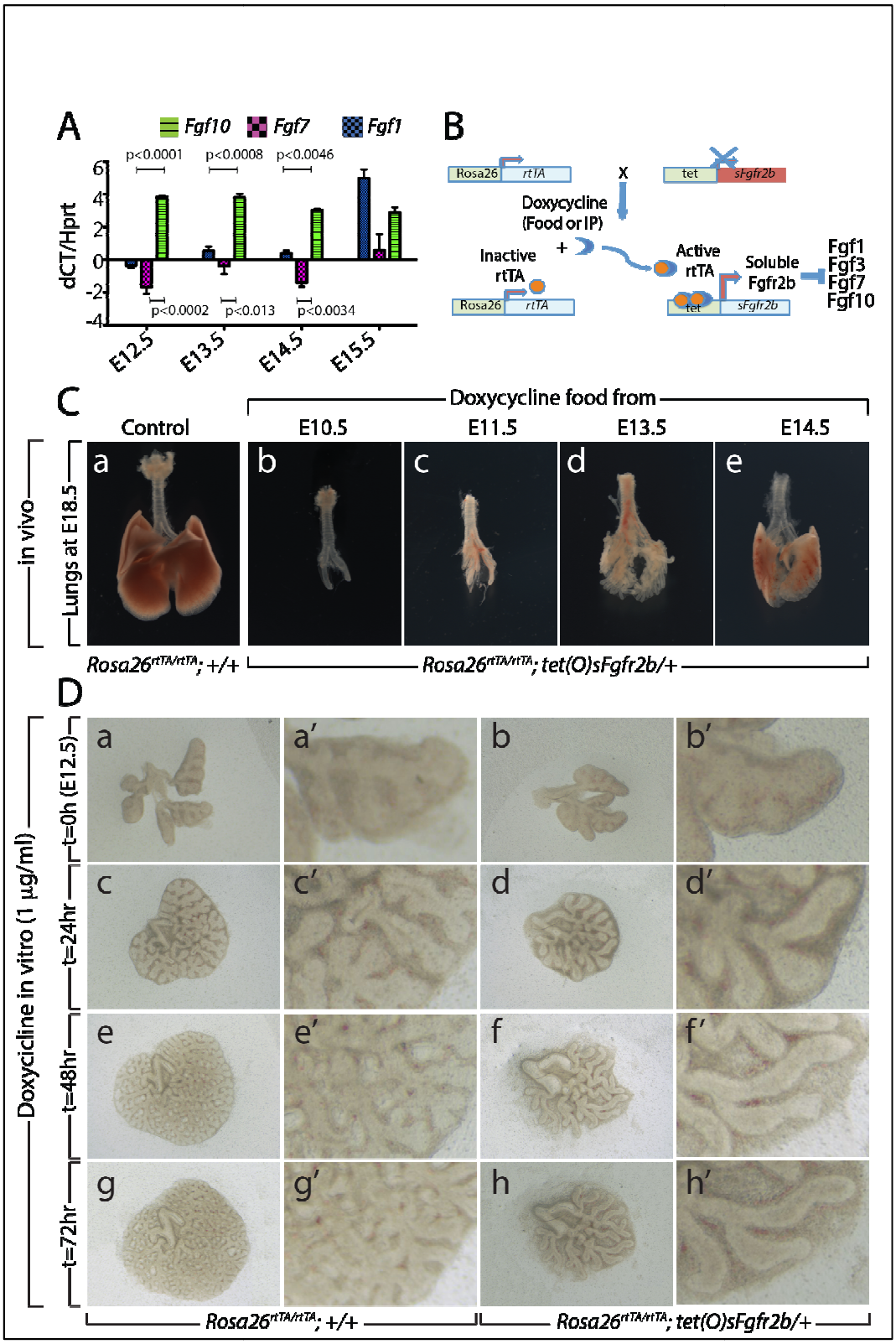

Figure 12: Expression of the main FGFR2b ligands during early lung development and validation of DTG approach*: Rosa26$^{rtTA/rtTA}$;Tg(tet(O)sFgfr2b)/+*. (A) qPCR for Fgf1, 7

and 10 in mouse embryonic lungs at different time point. Fgf10 is the main ligand expressed at E12.5. (B) DTG system *Rosa26$^{rtTA/rtTA}$; Tg(tet(O)sFgfr2b)/+* allowing upon dox exposure to induce the expression of a soluble form of FGFR2b, which attenuate the FGFR2b ligands activity by preventing them to interact with their endogenous receptor. (C) *In vivo* validation of the DTG system. Pregnant females are exposed to dox food starting from (b) E10.5, (c) E11.5, (d) E13.5 and (e) E14.5; then sacrificed at E18.5. (a) The corresponding control and (b-e) experimental lungs are examined. Note the severe growth arrest in the experimental lungs with a more severe phenotype when dox is delivered at earlier developmental stages. (D) *In vitro* validation of FGFR2b ligands inactivation. E12.5 STG (a, a') and DTG (b, b') lungs exposed to dox (1µg/ml) in the culture medium for 24 hours (C, c', d, d'), 48 hours (e, e', f, f') and 72 hours (g,g', h, h'). Note: data shown in Figure 9C were obtained at Children Hospital Los Angeles.

4.2.2 Impact of Fgf10 inhibition on branching morphogenesis

To determine the effect of blocking Fgf10 on branching morphogenesis, we performed live imaging for the left lobe of DTG and STG lungs (n=3) at E12.5 grown *in vitro* under (1µg/ml) doxycycline for 24 hours (Figure 13A-J), it allows us to visualize the changes occurring in the branching morphogenesis while blocking Fgf10. The number of buds in DTG lungs doesn´t increase overtime while it increases in STG lungs (from 12 buds to 17 buds at 24h) (Figure 13K). The epithelium surface decreases in DTG lungs (-12% at 3h, -15% at 6h, -16,6% at 9h and -9.8% at 24h) comparing to STG lungs which increases (+4% at 3h, +13% at 6h, +12,7% at 9h and + 24% at 24h) (Figure 13L). The distance between the tip of the epithelium and the mesothelium increases in DTG lungs (+18% at 3h, +24% at 6h,+29.5% at 9 h and +31% at 24h) comparing to the control lungs (-8.7% at 3h, -10.5% at 6h, -16% at 9h and -36.6% at 24h) (Figure 13M). Using the nomenclature already described in Metzger paper (Metzeger et al., 2008b), we quantified the length of the epithelial branches (Figure 13N-S). The control lung seems to be more developed comparing to the experimental lung, also L1 and L2 were already ramified in STG lung, while in DTG lung only L1 was ramified, this difference in size and branching can often occur between lungs within the same litter. Our results show that there is no difference between STG and DTG lungs when a branch is already ramified (Figure 13N). We noticed also that when a branch gets newly ramified, the elongation is arrested in control lungs, compared to the one in DTG lungs (which did not ramify) continue to grow (Figure 13O). L3, L4, D1 and D2 were not ramified in both lungs, but the elongation of branches is decreased in DTG lungs comparing to STG lungs over time (Figure 13P-S).

In conclusion, we have shown that the impact of blocking FGF10 is already seen after only 3 hours of adding Doxycycline, with a simplification of the epithelium, reduced number of buds and dilatation of the mesenchyme: augmentation of the distance between the epithelium and mesothelium.

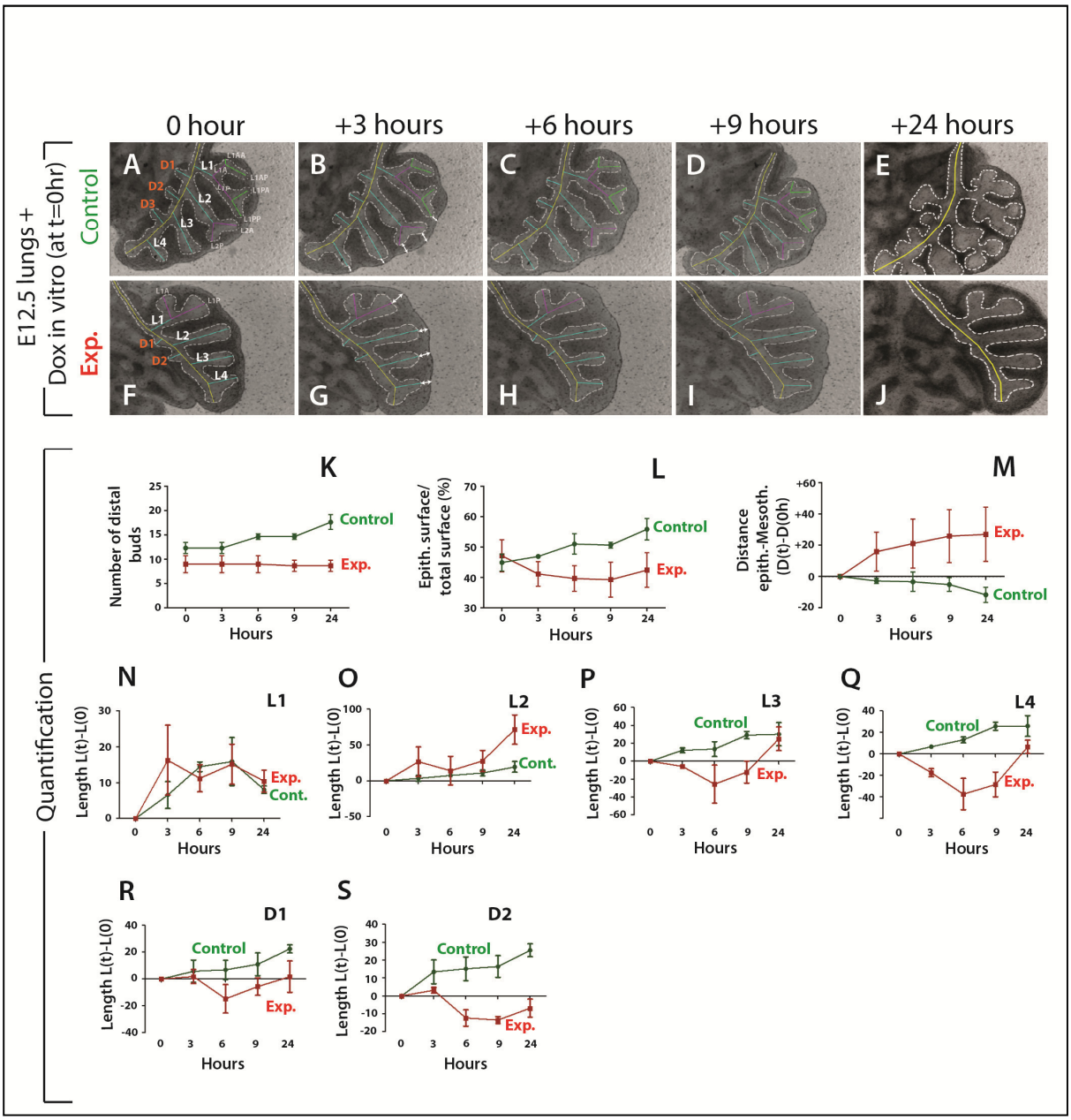

Figure 13: The impact of inhibiting Fgf10 on branching morphogenesis. (A-J) Attenuation of Fgfr2b ligands (*Rosa26*$^{rtTA/rtTA}$; *Tg(tet(O)sFgfr2b)*/+ mice) using doxycycline *in vitro* (1µg/ml) for 24 hours. (K-M) Quantifications using Metamorph software for the number of buds, epithelial surface and the distance between the epithelium and the mesothelium. (N-S) Quantifications of the length of the branches.

4.3 Identification of FGF10 downstream target genes by gene array approach

To determine the FGF10 downstream target genes during early lung development, we used an *in vivo* approach to block FGFR2b ligands by the administration of a single Dox IP to a pregnant female at E12.5, after 6 hours and 9 hours, the lungs were harvested (Figure 14A), and a gene array approach was performed. After 6 hours of dox IP, some branching abnormalities start to be seen but not very obvious, while after 9 hours, clear branching defects with a simplification of the epithelium and increased epithelial-mesothelial distance were observed (Figure 14B). The gene array analysis revealed that the genes are either up or down-regulated after 6 or 9 hours of Dox IP comparing to the control, with a slightly more significance at 9h dox-IP, the results are plotted in a Volcano Plot (Figure 14C). To analyze the gene array, we created a heatmap for the first 100 genes based on their significance (p-values), with 6 hours as reference time point (Figure 14D); then 9 hours as reference time point (Figure 14F). For each time point three biological replicates were used. We divided the data into two main classes of genes based on their expression pattern, Early (identified by the comparison between dox-IP+6 hours and control conditions), and Late (identified by the comparison between dox-IP+9 hours and control conditions) which in turn are divided into four subgroups: Early 1- 4 (Figure 14E), and Late 1- 4 (Figure 14G).

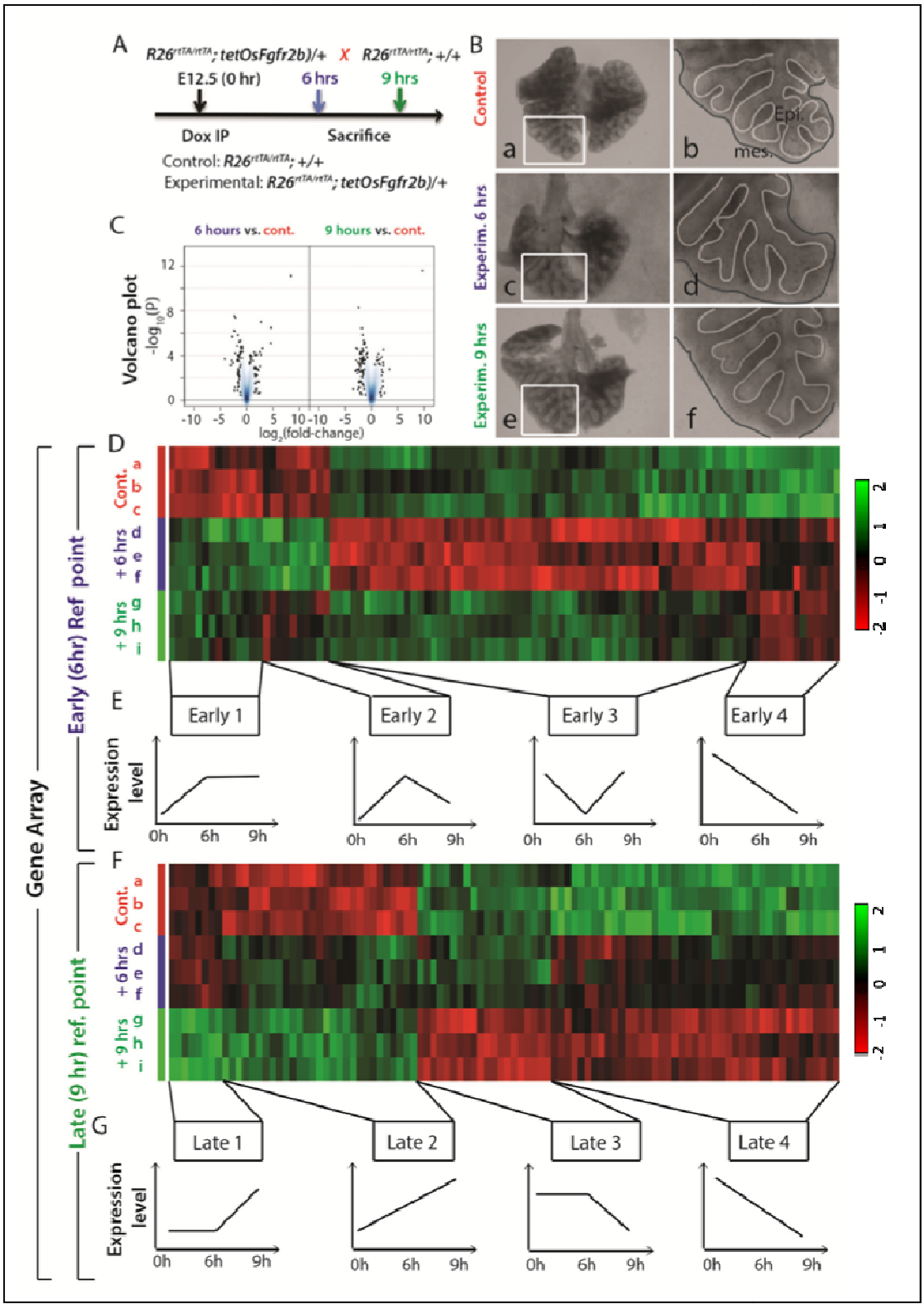

Figure 14: Identification of early FGF10 target genes by gene array approach. (A) Littermate control STG and experimental DTG lungs are collected 6 hours and 9 hours after a single Dox-IP injection to pregnant females carrying STG and DTG embryos at E12.5. (B) FGFR2b signaling attenuation leads to visible branching defects at dox-IP+9 hours (increased mesothelial-epithelial distance, branching inhibition). Note that dox IP+6 hrs lungs do not

show obvious abnormalities. (C) Volcano plots showing genes which are either down or up-regulated at 6 hrs dox-IP or 9 hrs dox-IP compared to the time matched STG control lungs. (D) Heatmap of the first 100 genes between experimental and control lungs at 6 hrs (based on p-values). (E) Fours classes of genes, based on their expression pattern were found (Early 1-4), these genes are identified on the basis of the comparison between dox-IP+6 hours and control conditions. (F) Heatmap of the first 100 genes between experimental and control lungs at 9 hrs (based on p-values). (G) Fours classes of genes, based on their expression pattern were found (Late 1-4), these genes are identified on the basis of the comparison between dox-IP+9 hours and control conditions.

4.3.1 Early versus Late clusters

In the cluster Early 1 the genes are up-regulated, while in Early 2 the genes are first up-regulated then down-regulated after 9h. In Early 3, the genes are down-regulated at 6h and again up-regulated after 9h. In Early 4, the genes are down-regulated. In the cluster Late 1 the expression increases after 9h. In Late 2 cluster, the genes are up-regulated. In Late 3, the genes are down-regulated after 9h. In the last subgroup Late 4, the genes are down-regulated. Interestingly, the genes in the clusters Early 4 and Late 4 might be the one directly controlled by FGF10, as they are down-regulated upon FGF10 attenuation, these two clusters will be next called 'FGF10 signature'. To show the expression pattern of the genes in the mouse lung (expressed in the epithelium, the mesenchyme or both), we used a database of gene expression patterns in the mouse embryo at E14.5 called "gene paint" (www.genepaint.org). The heat maps with the full list of genes contained in the clusters as well as their expression pattern is shown in supplementary data (Figure S1-S7).

4.3.2 The genes differentially expressed between the epithelium and mesenchyme and regulation of gene expression upon Fgf10 signal inhibition

For a better understanding of the genes identified, we isolated only the tip of the epithelium and the tip of the mesenchyme of a wild type lung at E12.5 to reduce other factors that can influence the results (Figure 15A), then we performed a gene array. We calculated the fold change of the genes in the epithelium versus (vs.) mesenchyme. The results show that there is no difference in the expression of 89% of the genes; however, 2.4% of the genes are expressed in the epithelium (with a fold change more than 1) and 2.3% of the genes are expressed in the mesenchyme (with a fold change more than 1). We plugged these new results

into the genes belonging to the four groups: Early 4, Late 4 (FGF10 signature) and Late 1, Late 3. The figure 15C shows that all the genes contained in the group Early 4 are expressed in the epithelium, some of them are highly expressed (LogFc more than 2) (*Id2, Sftpc, Tspan8, Lin7a, Sp5, Sema4f, Arrdc1, Gprc5a, Slco2a1*). We also included the fold change obtained from the gene array control vs. experimental (6 hours post dox IP) described previously in the figure 14, to show the value of genes regulation upon FGF10 inhibition. We found that some of these genes are highly regulated upon FGF10 inhibition (LogFc between -1 and -2) (*Id2, Sftpc, Tspan8, Lin7a, Sp5, Sema4f, Gprc5a, Etv5, Slco2a1).* Early 4 contains genes linked to multipotent epithelial cell differentiation, such as *Sftpc* and *Id2*. The transcription factor *Etv5*, a target of FGF signaling, was also among the first genes to be down-regulated. The Early 4 cluster also contains genes linked to cell adhesion (e.g. *Tspan8* and *Lin7a*), signaling and transcriptional regulation (e.g. *Gprc5a* and *Sp5*), neuronal processes (e.g. *Gprin3, Enc1,* and *Sema4f*), apoptosis and cell cycle (e.g. *Bid* and *Rai14),* and transport (e.g. *Arrdc1* and *Slco2a1*). We deduce from these results, that the genes that are highly expressed in the epithelium and which are highly regulated upon FGF10 signal inhibition might be important in FGF10 activity (*Id2s*, *Sftpc*, *Tspan8*, *Lin7a*, *Sp5*, *Sema4f*, *Gprc5a*, and *Slco2a1*). In the group Late 1 (Figure 15F), out of 8 genes, 2 genes are expressed in the epithelium, 4 genes are expressed in the mesenchyme, and 2 other genes are not available in the array. *Elmo3* is highly expressed in the epithelium (LogFc =2), and following FGF10 inactivation, *Rgs11* is highly regulated (LogFc more than 1). In this cluster belong *Fgf10* which is slightly up-regulated upon FGF10 signal inactivation (LogFc more than 0.5). In the Late 3 group (Fig. 15E), out of 20 genes, 8 genes are expressed in the epithelium, 5 genes are expressed in the mesenchyme, and 6 genes are not available in the array. Some of these genes are highly expressed in the epithelium (LogFc more than 2) (*Wnt7b, Pcsk6*). We classified the genes according to their regulation level following FGF10 inactivation some of them are highly regulated (LogFc between -1 and -2) (*Wnt7b, Pcsk6, Fgd3, Hmga2, Gli1, Hk2, Dusp9*). Interestingly, we can notice in this group that *Wnt7b* is highly up-regulated. It has been reported that FGF10/WNT7b loop allow the repair process in conducting airways following naphthalene injury (Volckaert et al., 2011). We noticed also in this group, that the genes expressed in the mesenchyme and that are involved in Hedgehog signaling (*Foxl1, Foxf1 and Gli1*) are down-regulated. Therefore, it appears that our array allows reconstituting one of the best known epithelial-mesenchymal interactions, the FGF10-SHH interaction (reviewed in (Warburton et al., 2008; Warburton et al., 2010)).

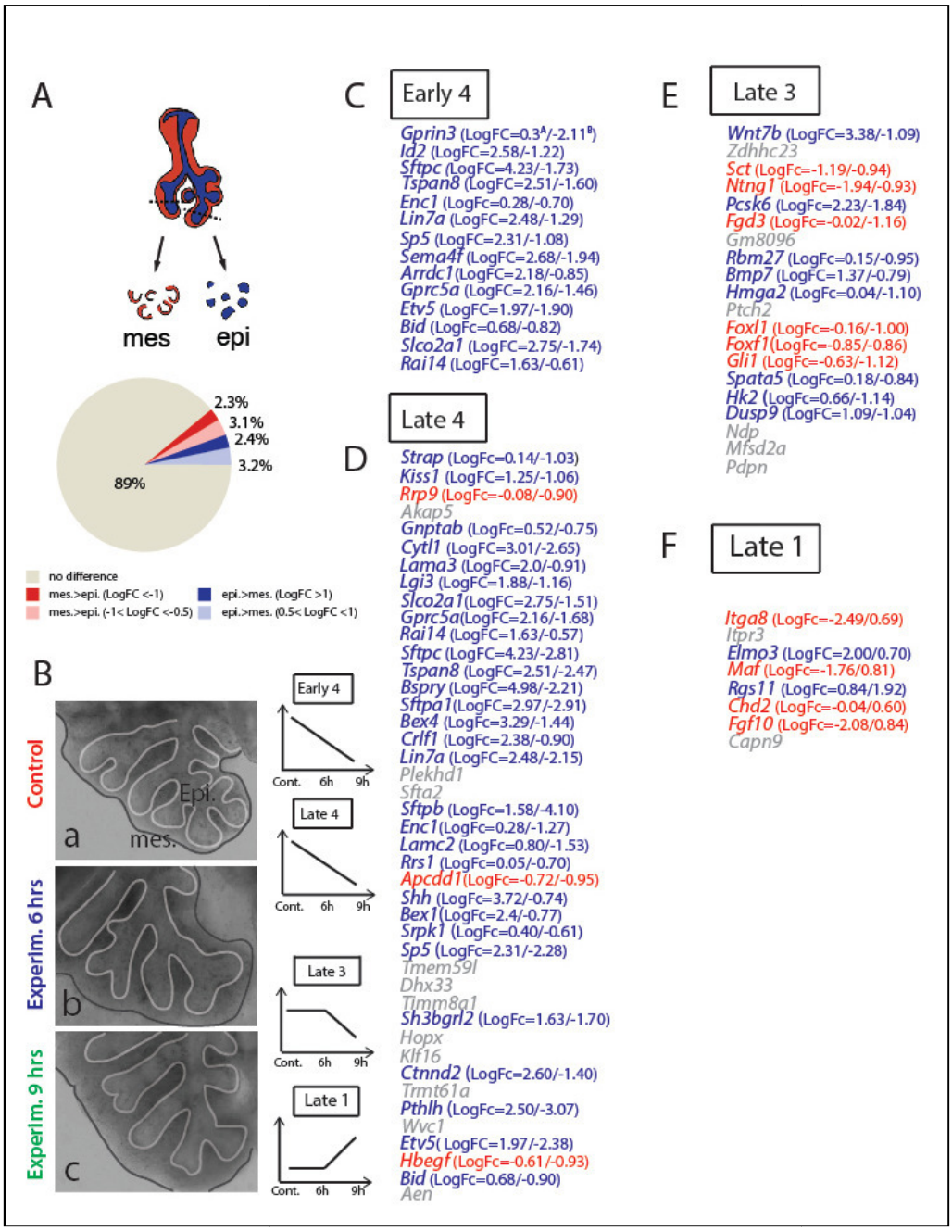

Figure 15: The genes differentially expressed between the epithelium and mesenchyme of E12.5 wild type (WT) lungs and regulation of gene expression upon Fgf10 inhibition. (A) Determination of genes differentially expressed in the distal epithelium versus mesenchyme of E12.5 wild type lungs by gene array. (B) Impact of Fgf10 inhibition on lung branching in vivo at 6 hours and 9 hours using our double transgenic system. (C) Analysis of the genes found in Early 4 cluster. The first LogFC (identified with "A" after the LogFc value represents the differential expression of this gene in the epithelium vs. mesenchyme of WT E12.5 lungs. The second LogFc identified with "B" after LogFc value represents the level of regulation upon Fgf10 inhibition. Blue indicates a gene enriched in the epithelium, red a gene enriched in the mesenchyme. Genes in gray were not found in our gene array. Note that all the

genes in Early 4 are enriched in the epithelium. (D) Analysis of the genes found in Late 4 cluster. Note again that most of the genes are blue confirming the enrichment in the Late 4 cluster for epithelial genes. (E) Analysis of the genes found in Late 3 cluster. Note the presence of genes belonging to the Hedgehog signaling pathway (F) Analysis of the genes found in Late 1 cluster. Note the presence of *Fgf10* in this cluster. Note: The dissection of the epithelium and mesenchyme was carried out by Dr. Gianni Carraro.

For the last group Late 4 (Figure 15D), we carried out the same analysis but more in detail (Figure 16) almost all the genes in Early 4 are found in Late 4. Out of 43 genes (10 of which overlap with the Early 4 genes), 2 genes are expressed in the mesenchyme, 11 genes are not available in genepaint, and 29 genes are expressed in the epithelium (67.5%), from the functional point of view the corresponding proteins act as transporter (*Slco2a1)*, transmembrane receptor *(Crlf1, Gprc5a*), growth factors *(Shh, Cytl1, Pthlh, Kiss1)*, signal transduction (*Tspna8, Strap, Enc1, Bid*), transcription factors (*Bex1, Bex4, Sp5 and Etv5*), differentiation markers (*Sftpc, Sftpb, Ftpa1* and *Hopx)* and cell adhesion (*Ctnnd2, Lamc2, Lama3*). Some of these genes are highly expressed (LogFc more than 2) (*Cytl1, Lama3, Slco2a1, Gprc5a, Sftpc, Tspan8, Bspry, Sftpa1, Bex4, Crlf1, Lin7a, Shh, Bex1, Sp5, Ctnnd2, Pthlh*). We also included the fold change obtained from the gene array experimental vs. control (9h post dox IP) described in the Figure 13. We found that some of these genes are highly regulated upon FGF10 signal inhibition (LogFc less than -2) (*Cytl1, Sftpc, Bspry, Sftpa1, Lin7a, Sftpb, Sp5, Pthlh, Etv5*). Then, we carried out a KEGG pathway analysis at 6 and 9 hours post Dox IP between control and experimental lungs (Table 6) highlighting the cellular and environmental information processes, the analysis reveal some changes in cellular processes: transport and catabolism (lysosome and peroxisome) and cellular community (focal adhesion) at both 6 and 9 hours. In the environmental information processes, we observed significant changes in cytokine-cytokine receptor interactions, calcium signaling, WNT signaling and Hedgehog signaling at 6 hours, in addition to these changes, we also observed significant alterations in the ECM-receptor interaction and cell adhesion molecules at 9 hours. These KEGG data support changes in the rearrangements of the epithelial changes linked to impaired cell- cell or cell-matrix interactions. In addition, the change in Hedgehog pathway is functionally supported by the increase in Fgf10 expression.

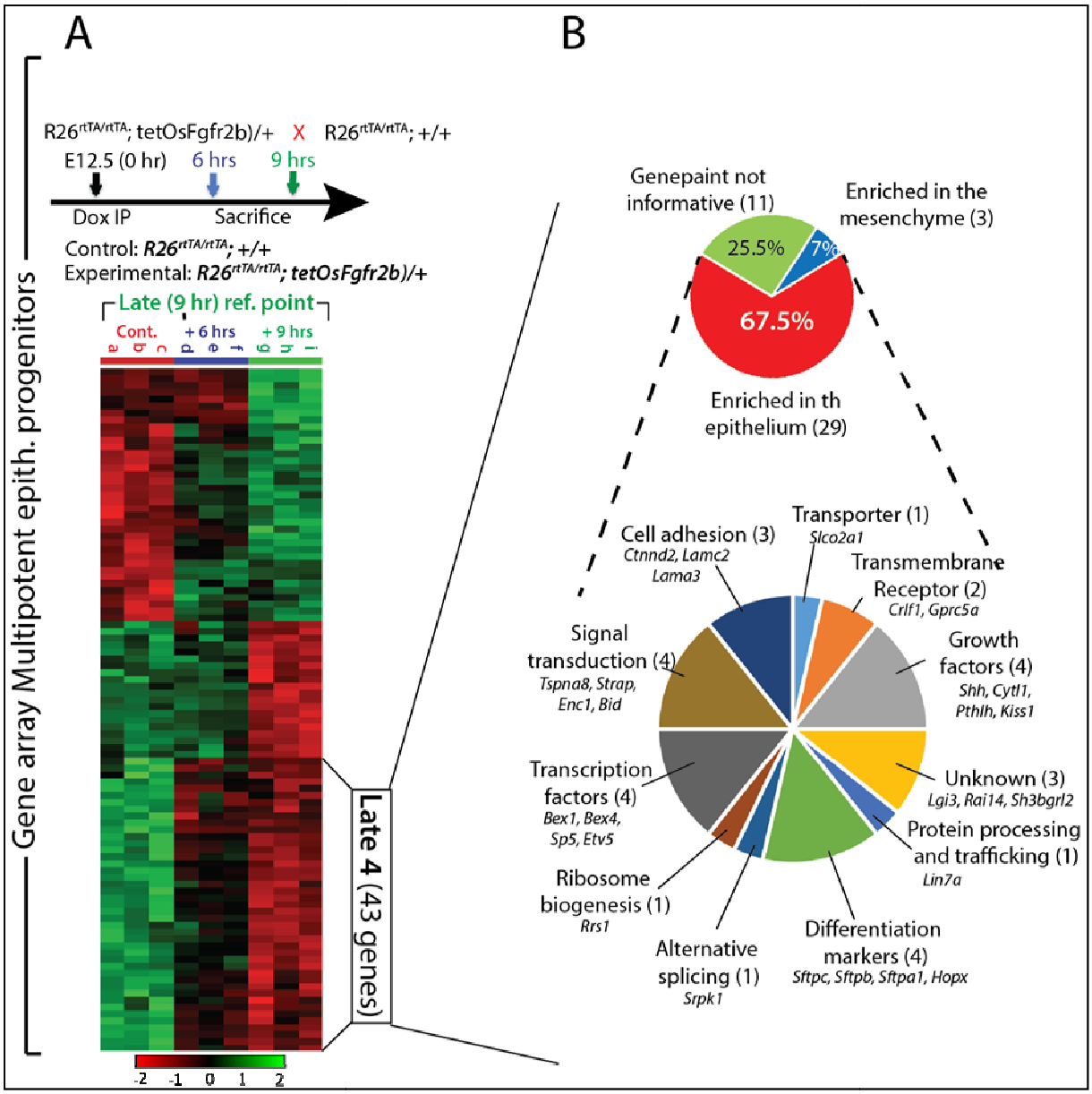

Figure 16: Detail analysis of the genes found in Late 4. (A) Littermate control STG and experimental DTG lungs are collected 6 hrs and 9 hrs after a single dox-IP injection to pregnant females carrying STG and DTG embryos at E12.5. Heatmap of the first 100 genes between experimental and control lungs at 9 hrs (based on p-values). The genes are identified on the basis of the comparison between dox-IP+9 hours and control conditions; Late 4 which contains 43 genes is indicated. **(B)** Classification of the genes from Late 4 according to their biological function: signal transduction, cell adhesion, transporter, transcription factor, growth factor…

KEGG analysis at E12.5 (DoxIP+6 hrs vs. control)

	KEGG name	n GenesInSet	n expr. genes	*p* value
Cellular processes	Peroxisome	80	62	0,00861
	Lysosome	123	106	0,02259
	Cell Cycle	124	110	0,03108
	P53 signaling pathway	68	55	0,03661
	Focal adhesion	201	154	0,05589
Environment. info. process.	Cytokine-cytokine receptor int.	179	88	0,00031
	Calcium signaling pathway	87	59	0,00787
	Wnt signaling pathway	146	71	0,00876
	Hedgehog signaling pathway	275	59	0,01179

KEGG analysis at E12.5 (DoxIP+9 hrs vs. control)

	KEGG name	n GenesInSet	n expr. genes	*p* value
Cellular processes	Focal adhesion	201	155	1.40E-05
	Lysosome	123	105	0,00028
	Endocytosis	217	169	0,00088
	Peroxisome	80	63	0,00105
	Cell cycle	124	110	0,02304
	Phagosome	170	101	0,02569
	Regulation of actin cytoskeleton	216	152	0,04386
Environment. info. process.	Calcium signaling pathway	179	88	1.17E-05
	ECM-receptor interaction	87	59	2.00E-05
	Cell adhesion molecules (CAMs)	146	71	5.61E-05
	Neuroactive ligand-receptor int.	275	59	0,00107
	ABC transporters	45	29	0,00450
	Cytokine-cytokine receptor int.	238	100	0,01277
	Hedgehog signaling pathway	55	38	0,02436
	MAPK signaling pathway	268	189	0,02677
	Wnt signaling pathway	153	121	0,04889

Table 6: KEGG analysis for *Rosa26* $^{rtTA/+}$*; Tg(tet(o)sFgfr2b/+* transgenic lungs vs. control lungs at E12.5 harvested 6 hours and 9 hours post Dox IP.

4.3.3 Identification of the transcription factors controlled by FGF10

During genes analysis, we identified transcription factors (TF) that are controlled by FGF10. The heatmap in the Figure 17A allows identifying the most regulated one by FGF10. Six classes of transcription factors TF1-6 could be identified based on their expression profile (Figure 17A). the TF 1-3 classes (*Lef1, Etv4/5, Snai1, Sox9, Foxf1, Grhl2, Nkx2-1* and *Id2*) are induced by FGF10 as they are down-regulated upon Fgf10 attenuation, while TF 4-6 (*Sox2, Nkx1-2, Pitx2, Hoxa1, Lmo1, Ets1, Elf5* and *Tcf21*) are repressed by FGF10 as they are up-regulated upon Fgf10 attenuation. To determine the expression pattern of these TFs in the lung, we used Genepaint database as shown in the figure (Figure 17B).

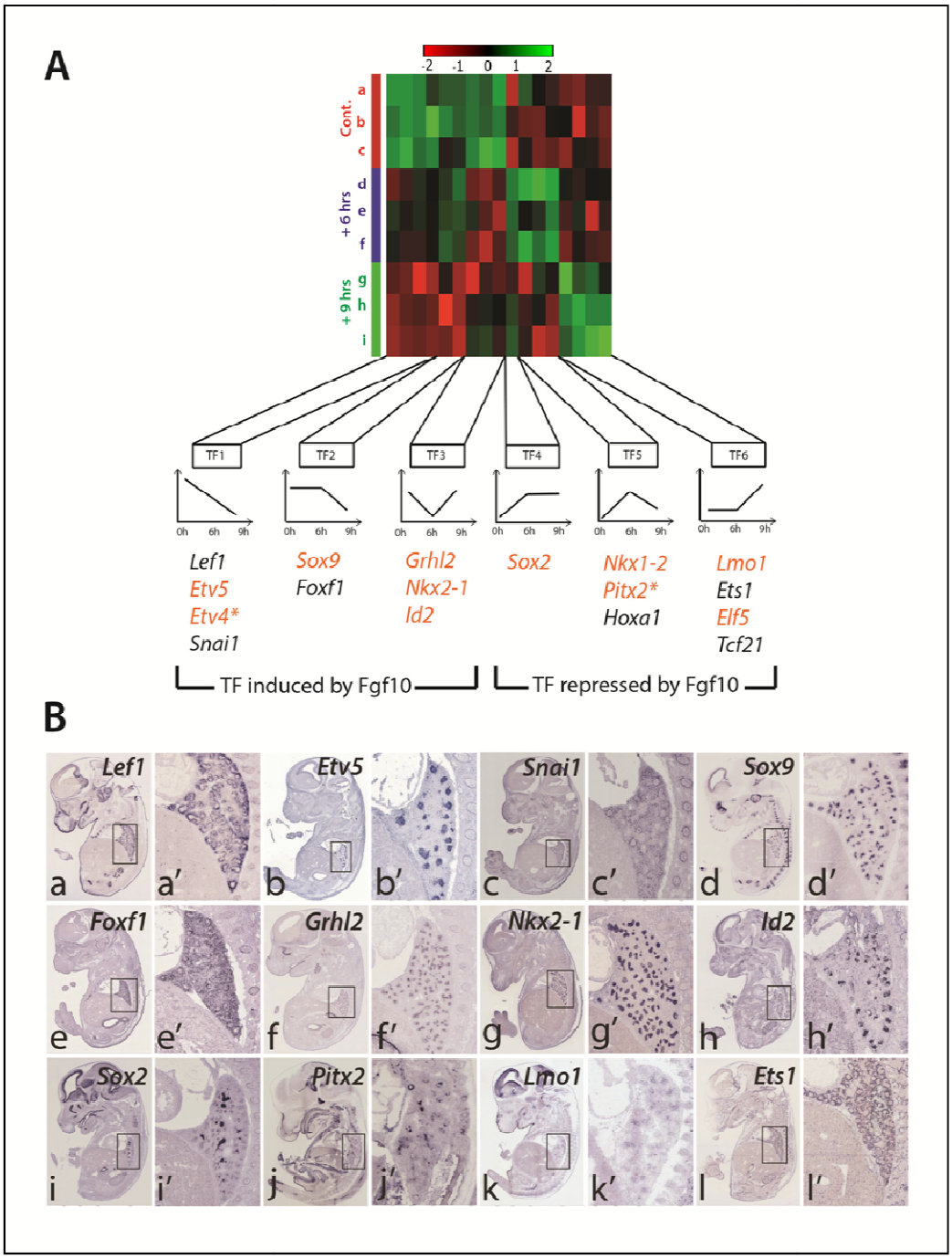

Figure 17: Identification of the transcription factors controlled by FGF10 signaling. (A) Heatmap for the most regulated transcription factor (TF) between control, dox-IP+6 hours and dox-IP+9 hours conditions. 6 classes of transcription factors (*TF1-6*) could be identified based on their expression profile between control, dox-IP+6 hours and dox-IP+9 hours conditions. TFs 1-3 classes induced by FGF10 while TFs 4-6 are repressed b FGF10. Genes in orange are expressed in the epithelium and genes in black are expressed in the mesenchyme. **(B)** In situ hybridization from *www.genepaint.com* for lungs at E14.5 for (a, a') *Lef1*, (b, b') *Etv5*, (c, c') *Snai1*, (d, d') *Sox9*, (e, e') *Foxf1*, (f, f') *Grhl2*, (g, g') *Nkx2*-1, (h, h') *Id2*, (i, i') *Sox2*, (j, j') *Pitx2*, (k, k') *Lmo1* and (l, l') *Ets1*.

4.3.4 Validation of the array: Fgf10, FgfR2b, Etv4/5, Shh connection.

Figure 18 displays the genes found in the groups Early 4, Late 4 as well as Late 1 and Late 3. The group Early 4 contains genes such as *Sftpc* and *Id2* which are related to epithelial cell differentiation. It contains also *Etv5* which has been shown to be positively regulated by FGF signaling. In the Late 1 group, *Fgf10* is up-regulated between 6 and 9 hours after dox-IP, which support the decrease in SHH signaling. In the Late 3 group, the presence of *Ptch2*, *Foxl1*, *Foxf1* and *Gli1*, suggesting decreased SHH signaling to the mesenchyme upon FGFR2b ligand inhibition between 9 hours and 6 hours after dox-IP. And finally, the group Late 4 contains genes that are linked to the epithelial differentiation such as *Sftpa1*, *Sftpb*, *Sftpc* as well as *Hopx*, it contains also sonic hedgehog (*Shh*) suggesting that *Fgf10* controls *Shh* expression positively. Through our analysis, we can deduce that our data supports the model published by Herriges et al. where they reported that Fgf10, acting via FgfR2b in the epithelium, promotes the expression of the transcription factors *Etv4* and *Etv5*, which in turn promote *Shh* expression. *Shh* is then secreted by the epithelium and binds to *Ptch2* to release the inhibition of Smoothened (Smo). *Smo* in turn activates *Gli1*, and this last one activates the expression of *Foxf1* and *Foxl*. Then, Shh signaling represses *Fgf10* expression (Herriges et al., 2015). Our data revealed that by the attenuation of FGF10 signaling, *Etv4/5*, *Shh*, *Ptch2*, *Gli1*, *Foxf1* and *Foxl1* are all reduced, while *Fgf10* is increased (Figure 18E). We propose that Fgf10 acts via FgfR2b, positively regulating the expression of Etv*4/Etv5*, which in turn regulates Shh expression, and therefore the downstream genes involved in the SHH pathway, validating the well-established FGF10-SHH regulatory feedback loop during lung development.

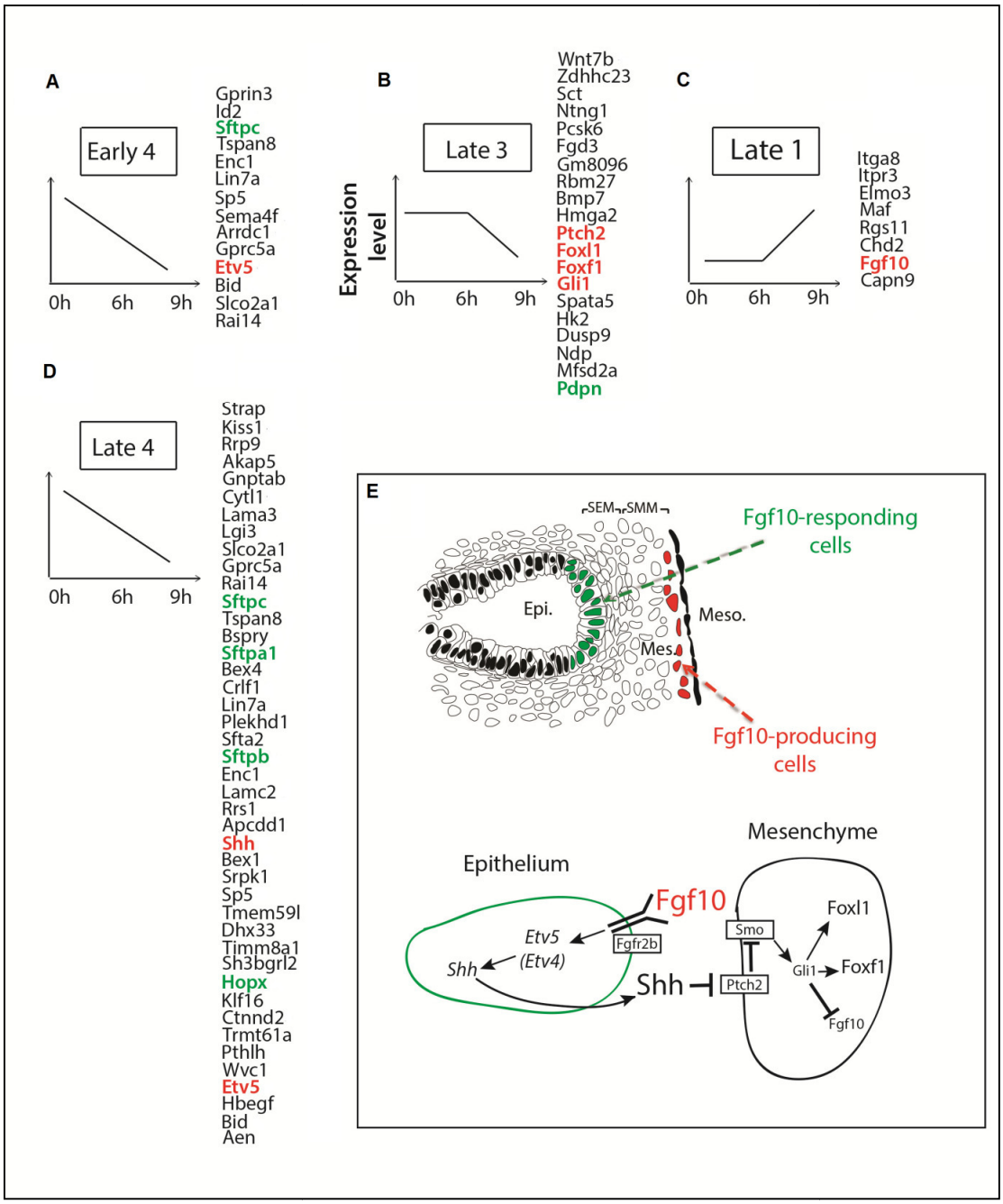

Figure 18: Validation of the array: The *Fgf10, FgfR2b, Etv4/5, Shh* connection. **(A)** Main genes in the Early 4 cluster (selected through their p-value) these genes are down regulated between dox-IP+6 hours and control and further down-regulated between dox-IP+6 hours and dox-IP+9 hours conditions. (B) Main genes in the Late 3 cluster (selected through their p-value), the expression of these genes are not changed between dox-IP+6 hours and control but down-regulated between dox-IP+6 hours and dox-IP+9 hours conditions. (C) Main genes in the Late 1 cluster (selected through their p-value). The expressions of these genes are not changed between dox-IP+6 hours and control but up-regulated between dox-IP+6 hours and dox-IP+9 hours conditions. (D) Main genes in the Late 4 cluster (selected through their p-value) these genes are down-regulated between dox-IP+6 hours and control and further down-

regulated between dox-IP+6 hours and dox-IP+9 hours conditions. (E) Schematic representation of a distal bud at E12.5. *Fgf10* producing cells are mostly located in the sub-mesothelial mesenchyme and acts on the distal epithelium (*Fgf10*-responding cells). *Fgf10*, acting via *FgfR2b*, promotes the expression of *Etv4* and *Etv5*, which in turn promote *Shh* expression. *Shh* then binds to *Ptch2* to release *Smo* which in turn activates *Gli1*, and this last one activates the expression of *Foxf1* and *Foxl*. Then, Shh signaling represses Fgf10 expression.

4.3.5 The FGF10 transcriptomic signature is active throughout alveolar lineage formation during lung development

Next, to determine if the FGF10 transcriptomic signature (FGF10 signature (early4 + late4 clusters) and the transcription factors regulated by FGF10) is active at E12.5 in different types of epithelial cells along the alveolar epithelial lineage, we used a data-mining approach based on the results of Treutlein et al. analyzing single cell transcriptome in the epithelium at E14.5 (before sacculation), E16.5 (early in sacculation) and E18.5 (late in sacculation) (Treutlein et al., 2014). The authors proposed a list of specific markers for alveolar epithelial cell type I (AECI) and type II (AECII) cells, and showed that a common progenitor cell, called a bipotent progenitor (BP), expressed markers of both cell types. At E18.5, single-cell suspensions of micro-dissected distal lung regions were purified by magnetic-activated cell sorting (MACS), and then the different types of alveolar epithelial cells were clustered according to their specific gene expression pattern. We assessed the AEC1 and AEC2 signatures from our gene array (experimental vs. control) at the 9 hours time point. Figure 19 displays the results of this approach, we examined the expression of AECI signature (Figure 19E), as well as AECII signature (Figure 19F); we used *Sftpc* (AECII marker) and *Pdpn* (AECI marker) as internal control (Figure 19D). The FGF10 transcriptomic signature (divided into FGF10 signature called ‘targets’ in the figure (Figure 19G) and ‘transcription factors’ (Figure 19H)) is active at E14.5 and E16.5 (even though in a quite heterogenous way), and becomes restricted in E18.5 BP cells which are proposed to give rise to both AECI and AECII. BP cells are expressing *Sftpc* and *Pdpn* as well as the AECI and AECII signatures; and are even further restricted in AECI (positive for the AECI signature) and AECII (positive for the AECII signature). AECI cells express more *Pdpn* than *Sftpc* as well as display an increased AECI signature. On the other hand, AECII cells express more Sftpc than Pdpn and are enriched in the AECII signature (compared to the AECI signature). Most of the transcription factors expressed in these isolated cells at E14.5, E16.5 and E18.5, are expressed

in the epithelium. And some of them are expressed in the mesenchyme such as Lef1 and Ets1. In few cells, TFs positively regulated by FGF10 (*Etv4/5, Sox9, Grhl2, Nkx2.1* and *Id2*) co-express with TFs negatively regulated by FGF10 (*Sox2, Lmo1*). At E18.5, FGF10 targets could be subdivided into two groups. The group1 contains *Ctnnd2, Bspry, Bex1, Bex4, Etv5, Sftpc, Sftpa1* and *Sftpb* and is enriched in AECII. Group2 contains *Hbegf, Akap5, Hopx, Gprc5a, Tspan8, Lamc2, Lama3, Sfta2* and *Shh* and is enriched in AECI. Both groups are expressed in BP. We also found that the transcription factors positively regulated by FGF10 (*Etv4/5, Sox9, Grhl2, Nkx2.1* and *Id2*) are enriched in BP. Again, this TF signature can be subdivided into two groups. Group A (*Etv4/5, Sox9, Grhl2* and *Id2*) is predominantly expressed in AECII while Group B (*Nkx2.1*) is expressed at higher level in AECI. Overall our data mining results allow us to conclude that the FGF10 transcriptomic signature initially identified at E12.5 is active in the alveolar epithelial lineage during lung development. We have also identified subsets of this signature which are enriched in either AECI or AECII.

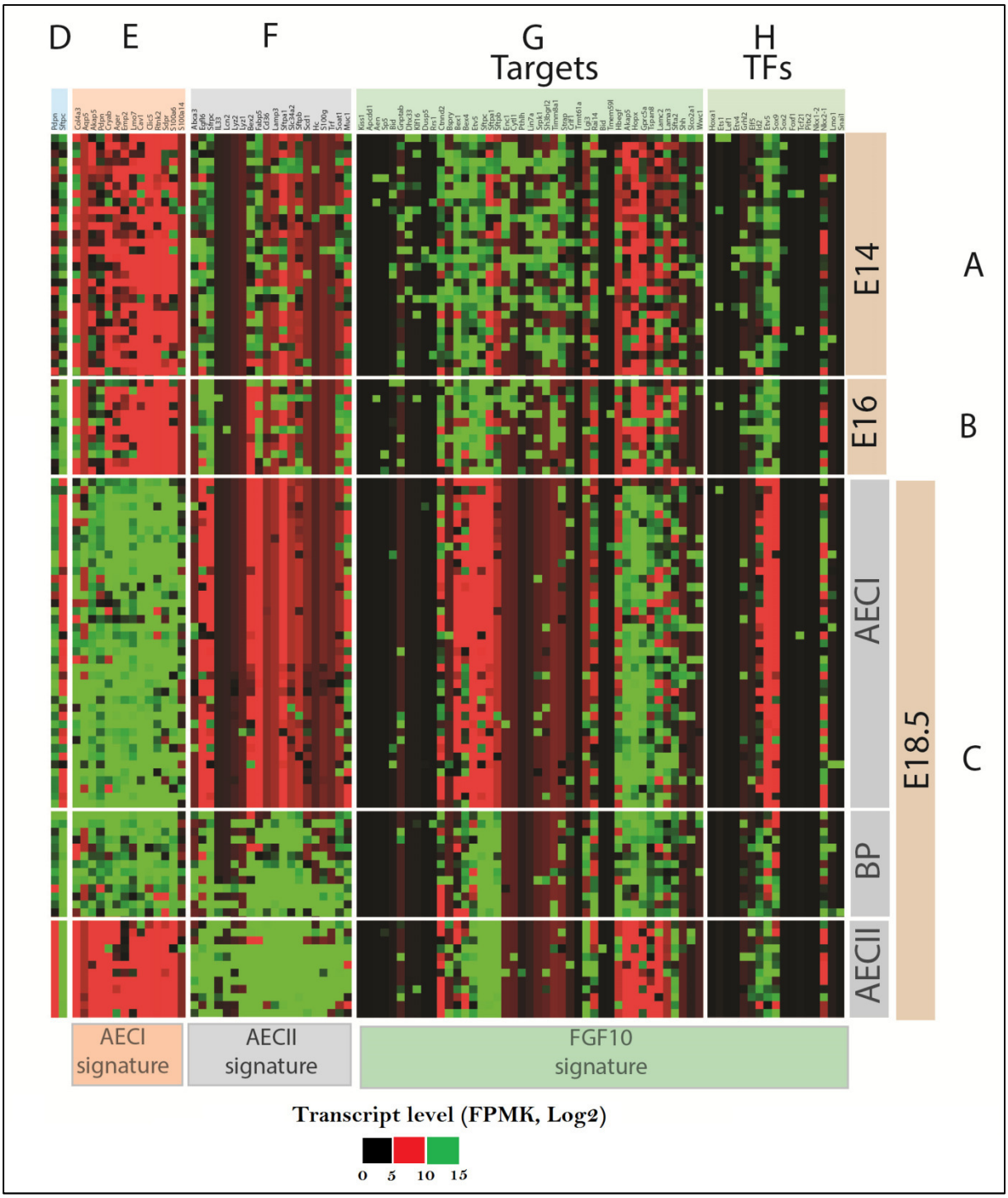

Figure 19: The FGF10 transcriptomic signature is active throughout alveolar lineage formation during lung development. Data mining based on the results of Treutlein paper (Treutlein et al. 2014) where they analyze cells from distal mouse lung epithelium of embryonic mice at (**A**) E14.5, (**B**) E16.5 and (**C**) E18.5. Note that single cells are shown in rows; genes are shown in columns. (**D**) *Sftpc* and *Pdpn* expression as internal control. (**E**) AECI, (**F**) AECII signature, (**G**) target genes controlled by FGF10 (Early4+Late4) (**H**) transcription factors regulated by FGF10.

4.3.6 Role of Fgf10 signaling in the differentiation of multipotent epithelial progenitors.

Next, we examined the impact of attenuated FGFR2b signaling on the differentiation of the multipotent epithelial progenitor cells, we used our double transgenic system, to attenuate the ligands activity upon the administration of Doxycycline IP, after 9 hours we harvested the lungs, then we performed Immunostaining for Sox9 (marker for distal airway progenitor cells) and Sox2 (marker for proximal airway progenitor cells). The result shows a reduction of Sox9 expression distally in experimental (Figure 20Ac, d) compared to control (Figure 20Aa, b) lungs. In control lungs, Sox2 is expressed in the proximal epithelium, and established a clear boundary between proximal and distal regions (Figure 20Ae, f). However, in experimental lungs, Sox2 is expressed in the proximal and expands more distally (Figure 20Ag, h) with an increased expression in the mesenchyme adjacent to the epithelium. To characterize the genetic signatures of lung distal epithelial cells, Treutlein et al. (2014), used single cell transcriptomic approaches at E14.5, E16.5 and E18.5, they proposed a list of specific markers for AECI and AECII. Our gene array data indicate that some of these markers of differentiation (Sftpc, Etv5, Sftpa1, Sftpb, Hopx, Pdpn) are actually regulated by *Fgf10* in multipotent epithelial progenitors. To examine the status of these differentiation markers in the epithelial tip cells, we assessed the AEC1 and AEC2 signatures from our gene array (experimental vs. control) at the 9 hours time point. Figure 20B shows a clear decrease of the AECII signature with almost no change in the AECI signature. From these results, we can conclude that the distal epithelium is enriched with differentiated genes encoding for AECII, and the expression of these genes is controlled by *Fgf10*.

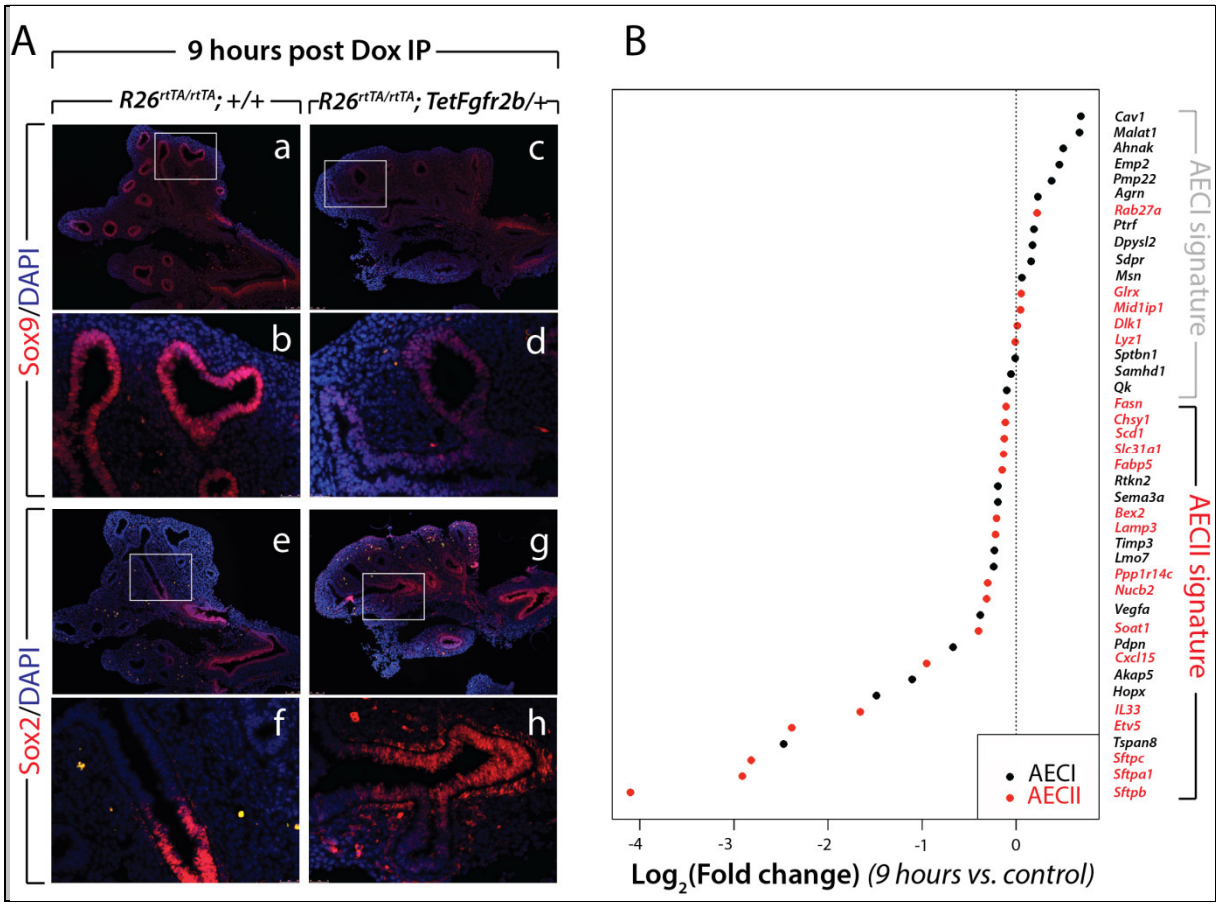

Figure 20: Role of Fgf10 signaling in the differentiation of multipotent epithelial progenitors. (A) Immunostaining for Sox9 in (a,b) controls and (c,d) experimental lungs. Immunostaining for Sox2 in (e,f) controls and (g,h) experimental lungs. Note the decrease in Sox9 expression distally. (B) Graph displaying Log2 (fold change) 9 hours post dox-IP experimental vs. control for the AECI (in black) and the AECII (in red) signatures. Note the decrease in the AECII signature upon FgfR2b signaling inhibition (p= 0.000004).

4.4 Gain of function (GoF): The use of the double transgenic approach *Rosa26$^{rtTA/rtTA}$;tg(tet(O)Fgf10)/+* to over express *Fgf10*. Validation of the system, impact on branching morphogenesis and gene array approach.

After analyzing the effect of the loss of function on early lung development, we analyzed the gain of function by using the double transgenic system *Rosa26$^{rtTA/rtTA}$;tg(tet(O)Fgf10)*, which allows the over-expression of *Fgf10* upon exposure to Doxycycline (dox) via food or intraperitoneal (IP) injection (Figure 21A). First, we validated the use of the double transgenic mice *Rosa26$^{rtTA/rtTA}$;tg(tet(O)Fgf10)*, by the administration of a single Dox IP to a pregnant female at E12.5. Then, lungs were harvested after 3, 6 and 9 hours (Figure 21B). After 3 and 6 hours no significant changes were observed (data not shown), while after 9 hours several changes start to occur: increase of the bud's number, the surface of the epithelium, the length of the main branches, as well as the distance between the distal epithelium and the mesothelium, a dilatation of the mesenchyme was also observed in the experimental compared to the control (Figure 21C). After validating the double transgenic system, and detecting the time point when abnormalities start to be seen (9 hours post Dox IP), we performed a gene array experiment at 9 hours post Dox IP to figure out which genes are up or down-regulated upon Fgf10 over- expression. To analyze the gene array, we created a heatmap for the first 100 genes based on their significance (p-values), compared to the control (Figure 21D). We noticed that the results are divided into 2 clusters, when the control is up-regulated, the experimental is down-regulated and vice versa, which means that *Fgf10* over-expression has an impact on the expression of the genes.

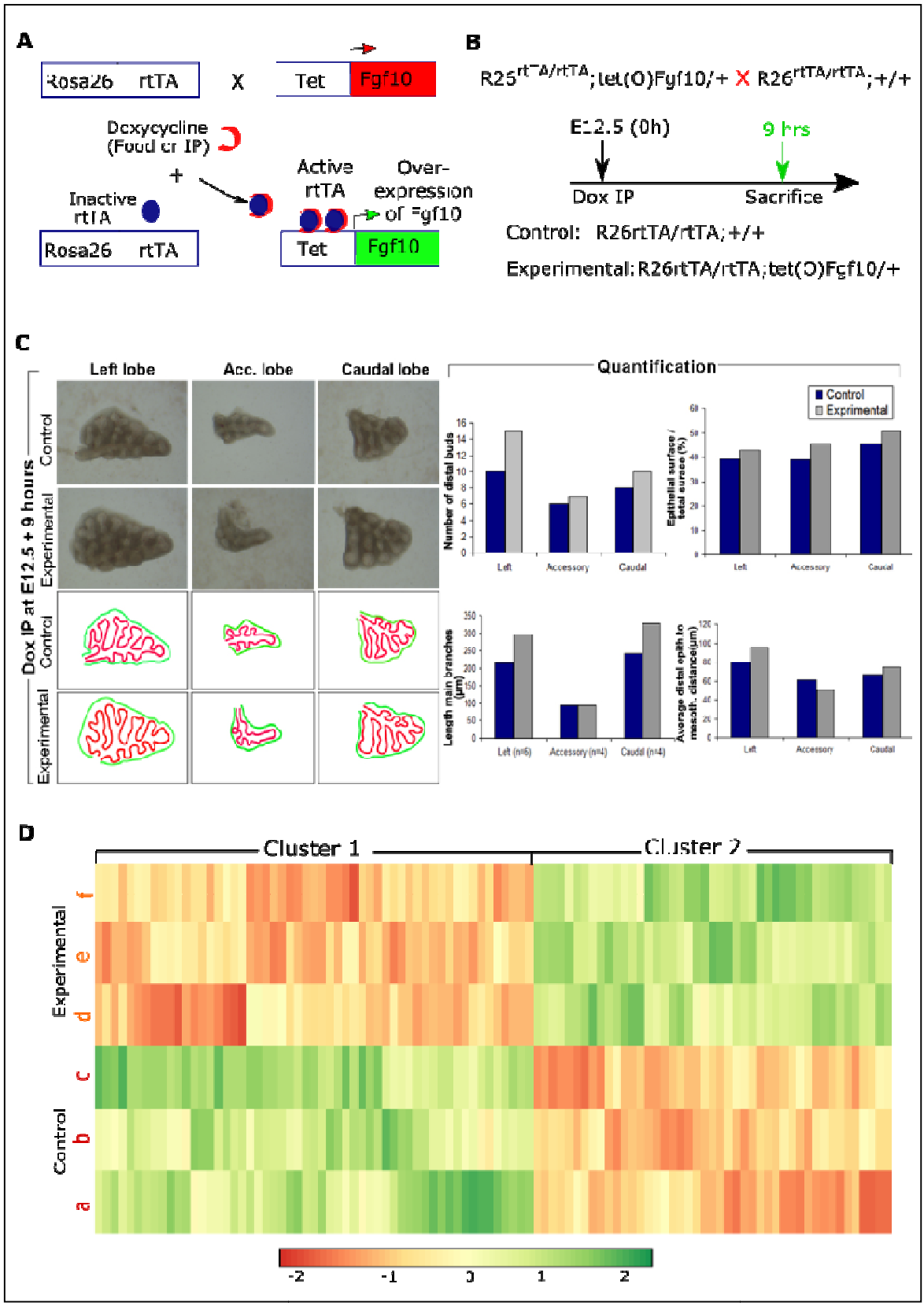

Figure 21: Gain of function using the double transgenic approach *Rosa26$^{rtTA/rtTA}$;tet(O)Fgf10/+* . (A) Double transgenic (DTG) system *Rosa26$^{rtTA/rtTA}$; tg(tet(O) Fgf10/+)* allowing upon dox exposure to induce the expression of *Fgf10*. (B) In vivo validation of the DTG system. Dox IP is administered to a pregnant female at E12.5, and then

lungs were harvested after 9 hours. (C) The corresponding control and experimental lungs are examined (left, accessory and caudal lobes), and then a quantification was done using ImageJ software for the number of distal buds, the epithelial surface, the length of the main branches and the distance between the distal epithelium and the mesothelium. (D) Heatmap of the first 100 genes for the experimental at 9 hrs post Dox IP compared to the control (based on p-values), two classes of genes were identified based on their expression pattern.

4.5 Comparison between LoF and GoF experiments 9 hours after Dox IP

To elucidate the impact of FGF signaling on E12.5 lungs, we compared the LoF experiments (attenuation of FGF10/FGFR2b signaling) and GoF experiments (over-expression of *Fgf10*) 9 hours post dox IP, as we already shown that at this time point abnormalities start to be seen. Figure 22A shows that compared to control, LoF inhibits the branching morphogenesis (reduced buds number and epithelial surface), in the opposite, GoF promote the branching morphogenesis (increased buds number and epithelial surface). In genomic scale, we performed a gene array analysis, for the LoF and GoF at E12.5+ 9 hours post dox IP compared to the control, we plotted the results into a heatmap for the first 100 genes based on their significance (p-values) with the GoF as reference time point, which revealed that the results are divided into 5 clusters (cluster 1-5) (Figure 22C) (for genes definition refer to supplementary data). In the cluster 1 the genes are down-regulated in LoF but not changed in GoF compared to control, in the cluster 2, the genes are slightly up-regulated in GoF, while in the cluster 3, the genes are not changed in the LoF compared to control but up-regulated in GoF. In the cluster 4, the genes are up-regulated in LoF but down-regulated in GoF. In the cluster 5, the genes are up-regulated in the LoF and not changed in the GoF compared to control (Figure 22D). The genes in the cluster 2 might be the one controlled by *Fgf10* as they are down-regulated upon *Fgf10* attenuation, and slightly up-regulated upon *Fgf10* over-expression. Among the genes, we can find genes involved in multicellular organism development and cell differentiation (*Ntng, Bmp7),* cell proliferation *(Phlda2)*; transcriptional regulation (*Lhx2, Cytl1*); signal transduction (*Chrm3, Sox9, Plch);* regulation of apoptotic process (*Nlrp1a);* protein secretion and transport *(Gnptab). Sox9* is also involved in cell fate specification and epithelial to mesenchymal transition. To have a good visibility on the comparison between GoF and LoF 9 hours post dox IP, we plotted the results into a Scatterplot, which shows that some genes are significantly up or down-regulated in the LoF but slightly up or down-regulated in the GoF such as *Cym* which has log fold change (LFC) in

the LoF (-2), and GoF (-0.2), *Sftpb* (LoF(-4.1), GoF(0.9)), *Sftpc*(-2.81, -0.58) and *Pthlh*(-3, 0.16) (Figure 22B). The genes in green are the one belonging to the cluster 2 which are down regulated in LoF and slightly up-regulated in GoF, Afp (LoF(-1.54), GoF(1.62)), Sox9 (-1.47, 0.96), Bex4 (-1.44, 0.17), Cytl1 (-2.65, 0.46). As we don´t have a clear up-regulation or down- regulation between control and GOF for the genes selected, we can conclude that the GoF is not very useful to validate the real targets for the FGF signaling.

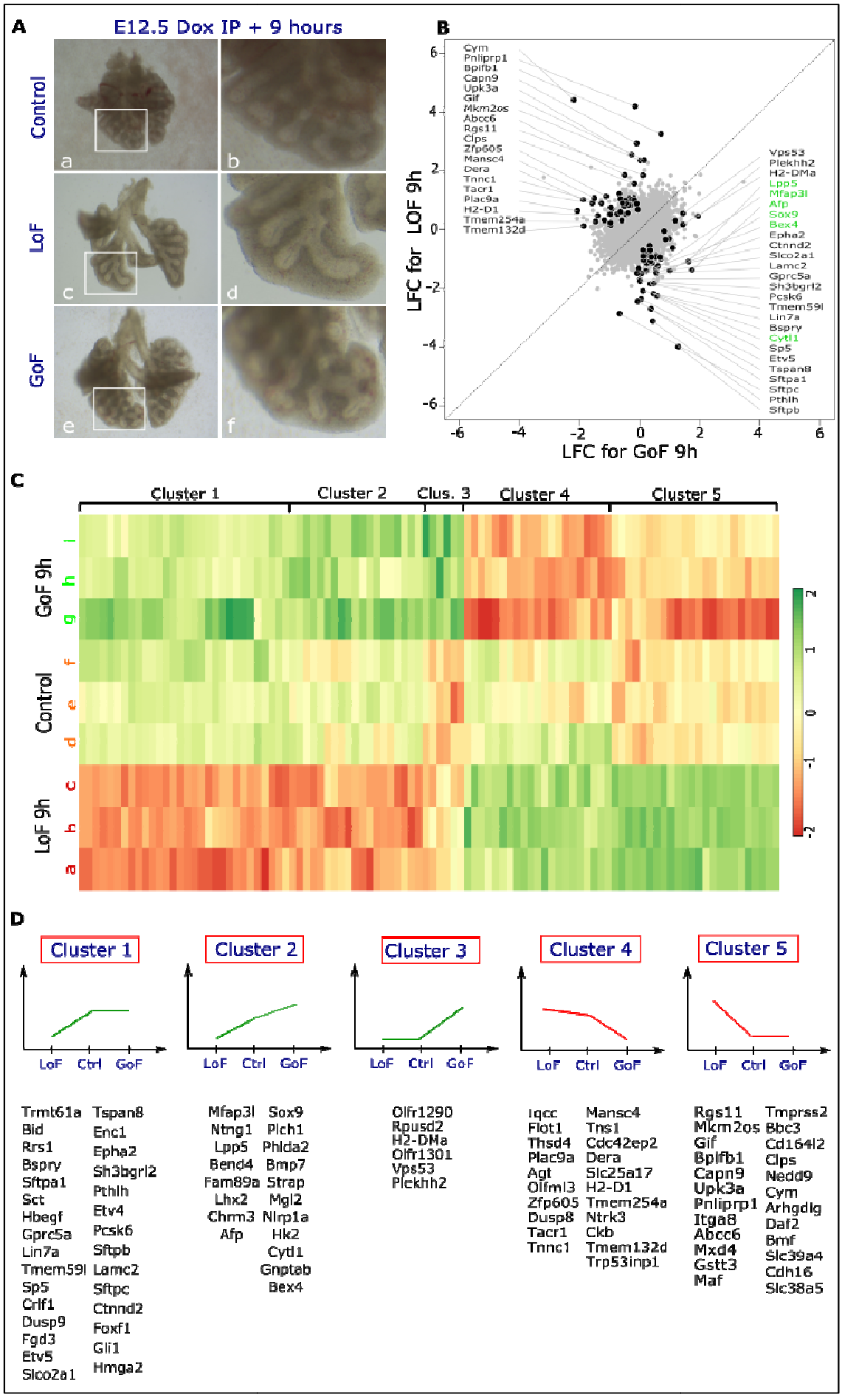
A
E12.5 Dox IP + 9 hours
Control
LoF
GoF
a
b
c
d
e
f
B
LFC for LOF 9h
LFC for GoF 9h
Cym
Pnliprp1
Bpifb1
Capn9
Upk3a
Gif
Mkm2os
Abcc6
Rgs11
Clps
Zfp605
Mansc4
Dera
Tnnc1
Tacr1
Plac9a
H2-D1
Tmem254a
Tmem132d
Vps53
Plekhh2
H2-DMa
Lpp5
Mfap3l
Afp
Sox9
Bex4
Epha2
Ctnnd2
Slco2a1
Lamc2
Gprc5a
Sh3bgrl2
Pcsk6
Tmem59l
Lin7a
Bspry
Cytl1
Sp5
Etv5
Tspan8
Sftpa1
Sftpc
Pthlh
Sftpb
C
Cluster 1
Cluster 2
Clus. 3
Cluster 4
Cluster 5
GoF 9h
Control
LoF 9h
i
h
g
f
e
d
c
b
a
2
1
0
-1
-2
D
Cluster 1
Cluster 2
Cluster 3
Cluster 4
Cluster 5
LoF Ctrl GoF
Trmt61a
Bid
Rrs1
Bspry
Sftpa1
Sct
Hbegf
Gprc5a
Lin7a
Tmem59l
Sp5
Crlf1
Dusp9
Fgd3
Etv5
Slco2a1
Tspan8
Enc1
Epha2
Sh3bgrl2
Pthlh
Etv4
Pcsk6
Sftpb
Lamc2
Sftpc
Ctnnd2
Foxf1
Gli1
Hmga2
Mfap3l
Ntng1
Lpp5
Bend4
Fam89a
Lhx2
Chrm3
Afp
Sox9
Plch1
Phlda2
Bmp7
Strap
Mgl2
Nlrp1a
Hk2
Cytl1
Gnptab
Bex4
Olfr1290
Rpusd2
H2-DMa
Olfr1301
Vps53
Plekhh2
Iqcc
Flot1
Thsd4
Plac9a
Agt
Olfml3
Zfp605
Dusp8
Tacr1
Tnnc1
Mansc4
Tns1
Cdc42ep2
Dera
Slc25a17
H2-D1
Tmem254a
Ntrk3
Ckb
Tmem132d
Trp53inp1
Rgs11
Mkm2os
Gif
Bpifb1
Capn9
Upk3a
Pnliprp1
Itga8
Abcc6
Mxd4
Gstt3
Maf
Tmprss2
Bbc3
Cd164l2
Clps
Nedd9
Cym
Arhgdig
Daf2
Bmf
Slc39a4
Cdh16
Slc38a5

Figure 22: Comparison between LoF and GoF experiments 9 hours after Dox IP. (A) (a,b) control lung at E12.5+9h compared to experimental lungs: (c,d) DTG lung ($Rosa26^{rtTA/rtTA}$; tet(O) *FGFR2b/+)* at E12.5+ 9h post dox IP, and (e,f) DTG lung ($Rosa26^{rtTA/rtTA}$; tet(O) *Fgf10/+)* at E12.5 + 9h post dox IP; note that FGFR2b signaling attenuation (LoF) leads to visible branching defects (reduced bud numbers, increased mesothelial-epithelial distance, branching inhibition), and *Fgf10* over-exression (GoF) leads to the opposite (increased bud numbers, increased of the epithelium surface, more branching). (B) Scatterplot showing the log fold change (LFC) for the loss of Fgfr2b signaling against the LFC for the gain of function of *Fgf10* which show the genes that are down or up-regulated both 9 hours post Dox IP. (C) Heatmap of the first 100 genes for the GoF and LoF at 9 hrs post Dox IP (based on p-values) compared to control, four classes of genes were identified based on their expression pattern (cluster 1-4)(refer to supplemetary data for more details on the list of the genes found in the clusters 1-4).

Then, we carried out a KEGG pathway analysis at 9 hours post Dox IP between control and experimental lungs (loss and gain of function) (Table 6) highlighting the cellular and environmental information processes, the analysis reveals some changes in cellular processes: transport and catabolism (lysosome and peroxisome), cell motility (Regulation of actin cytoskeleton) and cellular community (focal adhesion) in both loss and gain of function. In the environmental information processes, we observed significant changes in signaling molecules and interaction (cytokine-cytokine receptor interactions, cell adhesion molecules, ECM-receptor interaction, Neuroactive ligand-receptor interaction). Significant alterations are also observed in signal transduction (calcium signaling pathway) and membrane transport (ABC transporters) in both loss and gain of function.

KEGG analysis at E12.5 loss of function (Dox IP+9hours)

	KEGG name	nGenes InSet	nExpr. Genes	P value	Subgroup
Cellular process	Focal adhesion	201	155	1,40E-5	Cellular community
	Lysosome	123	105	0,00028	Transport and catabolism
	Endocytosis	217	169	0,00088	Transport and catabolism
	Peroxisome	80	63	0,00105	Transport and catabolism
	Cell cycle	124	110	0,023	Cell growth and death
	Phagosome	170	101	0,0256	Transport and catabolism
	Regulation of actin cytoskeleton	216	152	0,0438	Cell motility
Environment. Info. Process.	Calcium signaling pathway	179	88	1,174E-5	Signal transduction
	ECM-receptor interaction	87	59	2,0089E-5	Signaling molecules and interaction
	Cell adhesion molecules (CAMs)	146	71	5,61E-5	Signaling molecules and interaction
	Neuroactive ligand-receptor interaction	275	59	0,00107	Signaling molecules and interaction
	ABC transporters	170	101	0,0045	Membrane transport
	Cytokine-cytokine receptor interaction	238	100	0,0127	Signaling molecules and interaction
	Hedgehog signal. pathw.	55	38	0,0243	Signal transduction

KEGG analysis at E12.5 Gain of function (Dox IP+9hours)

	KEGG name	nGenes InSet	nExpr. Genes	P value	Subgroup
Cellular process	Lysosome	123	106	0,00118	Transport and catabolism
	Regulation of actin cytoskeleton	216	151	0,0025	Cell motility
	Tight junction	138	97	0,00815	Cellular community
	Phagosome	170	101	0,0095	Transport and catabolism
	Focal adhesion	201	151	0,0157	Cellular community
	Peroxisome	80	63	0,030	Transport and catabolism
Environment. Info. Process.	Cell adhesion molecules (CAMs)	146	71	1,104E-06	Signaling molecules and interaction
	ECM-receptor interaction	87	57	1,7715E-4	Signaling molecules and interaction
	Cytokine-cytokine receptor interaction	238	93	5,42E-4	Signaling molecules and interaction
	Neuroactive ligand-receptor interaction	275	57	0,00197	Signaling molecules and interaction
	Calcium signaling pathway	179	84	0,067	Signal transduction
	ABC transporters	45	28	0,0779	Membrane transport

Table 7: KEGG analysis for the loss and gain of function at E12.5 harvested 9 hours post Dox IP.

5. Discussion

5.1. Visualization of the FGF signaling domains of action.

During early lung development, *Etv4* and *Etv5* are expressed predominantly in the epithelium. At later developmental stages (E11-E15), *Etv5* is specifically expressed in the distal epithelium and *Etv4* is expressed in the distal epithelial and mesenchymal compartment (Chotteau-Le-lievre et al., 1997; Liu et al. 2002). *Etv4* and *Etv5* are downstream of FGF signaling from the mesenchyme and are involved in branching morphogenesis and epithelial cell differentiation (Mao et al., 2009; Liu et al., 2003; Herriges et al., 2012; Herriges et al., 2015). To determine the domains of action of FGF signaling during lung development, we used *Tg*(*Etv4*-GFP) a mouse reporter line for *Etv4*. Using fluorescence microscopy, we detected GFP signal in the organs responding to FGF signaling: head, tail, limb, and lung at different stages of mouse embryos. The reporter mouse line *Etv5* $^{\text{CreERT2–RFP}}$ was also used to determine the domains of action of FGF signaling by our group (Jones et al., 2019b). Both fluorescent reporters *Tg*(*Etv4*-GFP) and *Etv5* $^{\text{CreERT2–RFP}}$ responded to FGF10 inhibition in vitro. In conclusion, these two reporter lines appear to be promising tools to monitor FGF10/FGFR2b signaling in early lung development. These tools will have to be further validated at later stages and in other organs of interest.

Fibroblast growth factor 7 (Fgf7) is expressed in lung mesenchyme (Bellusci et al., 1997; Lebeche et al., 1999) and plays many roles in the lung: It participates in the specification and the proliferation of distal epithelial cell in the airway and alveoli (Ulich et al., 1994; Yano et al., 2000; Hyatt et al., 2002) and affects the morphology of the developing lung. The over-expression of *Fgf7* severely alters the lung development (Simonet et al., 1995). For the important roles that *Fgf7* plays in the lung, we have tested the effect of adding exogenous FGF7 and FGF10 on embryonic *Etv4*-GFP lungs, by incubating E12.5 lungs *in vitro* with human recombinant protein FGF7 or FGF10, the results show that exogenous FGF7 increases the width of the branches and form like a cyst, while exogenous FGF10 increases the number of buds; it has been shown by Liu and coworkers that FGF7 induces *Etv4/Etv5* expression more than FGF10 (Liu et al., 2003). FGF7 as well as FGF10 both amplify *Sox9* positive distal epithelial progenitors but not *Sox2* proximal epithelial progenitors (Figure S1), this amplification shows that over-expression of FGF10 at E12.5 prevent some distal epithelial progenitors to differentiate into *Sox2*-expressing airway epithelial cells, as it has been published by Volckaert group where they show that over-expression of Fgf10 from E11.5 onwards was able to prevent the differentiation of almost all distal *Sox9*-expressing epithelial

progenitors into *Sox2*-expressing airway epithelial cells, while Over-expression of Fgf10 from E12.5 onwards did not prevent the differentiation of all distal epithelial progenitors as some had already differentiated into Sox2-expressing airway epithelial cells by this time (Volckaert et al. 2013).

5.2 Validation of the double transgenic approach: *Rosa26$^{rtTA/rtTA}$;Tg(tet(O)sFgfr2b)/+* in other developmental models: limbs, mammary glands rodent incisors and lung.

The use of the double transgenic approach: *Rosa26$^{rtTA/rtTA}$;Tg(tet(O)sFgfr2b)/+* was validated in many developmental models: In the context of limbs (Danopoulos et al., 2013), mammary glands (Parsa et al., 2008), rodent incisors (Parsa et al., 2010), gut homeostasis (Al Alam et al., 2015). In addition, this line was also used to define the role of Fgfr2b ligands during early and late lung development (Hokuto et al., 2003). In the models cited above they used an rtTA transactivator/tetracycline promoter approach that allows inducible and reversible attenuation of FGFR2b signaling. Soluble Fgfr2b (sFgfr2b) molecules are generated by administration of doxycycline to mice via water, food or IP injection. During limb development, Fgfr2b-ligands signaling plays critical roles in maintaining the Apical Ectodermal Ridge (AER), which is formed by the action of *Fgf10* on *Fgfr2b* (Sekine et al.,1999; De Moerlooze et al., 2000). Indeed, Fgfr2b is the main receptor for Fgf10 during limb development as demonstrated by the absence of limbs in both *Fgf10* and *Fgfr2b* null embryos (Mariani et al., 2008; Mailleux et al., 2002; Ohuchi et al., 2000). To validate the double transgenic approach, the embryos were exposed to doxycycline-containing food; they failed to generate limbs (Danopoulos et al., 2013). In the context of mammary glands, attenuation of FGFR2b ligands in early lung development leads to impaired development of mammary buds: the mammary buds which normally are five pairs fail to develop, the mammary bud 4 is the only one detectable and it regressed due to decreased proliferation and increased apoptosis in the mammary gland epithelium (Mailleux et al., 2002). FGF signaling is also critical during postnatal mammary gland development, which upon attenuation the size of mammary glands is reduced by 40% compared to the wild type control (Parsa et al., 2008). In the context of rodent incisors, attenuation of FGFR2b signaling led to abnormal development of the labial cervical loop and differentiated cell types in both mandibular and maxillary incisors (Parsa et al., 2010). In early lung development, attenuation of FGF signaling caused severe fetal lung hypoplasia. At E14.5, expression of sFGFR2b decreased lung tubule formation before birth and caused severe emphysema at maturity. Activation of sFGFR2b postnatally did not alter

alveolarization, lung size, or histology. Although FGF signaling is mainly required for branching morphogenesis during early lung development, while alveolarization is not influenced Postnatally (Hokuto et al., 2003).

5.3 Validation and limitations of *in vivo* inhibition of Fgf10 signaling

One of the major limitations of our *in vivo* model to inhibit Fgf10 signaling during pseudoglandular lung development (E12.5) is that the production of the soluble FgfR2b is global. Furthermore, the soluble FgfR2b protein is secreted into the mesenchyme, and may inhibit mesenchyme-specific Fgf signaling, creating secondary effects. To validate that Fgf10 signaling acts on epithelial-specific targets, we attempted to verify the location of expression of Fgf10's primary targets by a gene array, comparing the expression of genes in the epithelium vs. mesenchyme of E12.5 wild type lungs (Figure 14), which reveals that most of the genes are enriched in the epithelium, this result was also verified by the online expression-profiling database 'genepaint.org' (Figure S2-S9). We are therefore confident that our global *in vivo* approach does indeed detect the impacts of Fgf signaling on epithelial-specific targets. Furthermore, we assessed the well-established Fgf10-Shh regulatory feedback loop during lung development as a means of validating our array (Figure 17). In our array, *Shh* is down-regulated within 6 hours of Fgf10 inhibition, as impacts Fgf10 is up- regulated after 9 hours. Additionally, our array supports the recently reported data showing that the inactivation of FGF signaling regulated *Etv4* and *Etv5* in the multipotent epithelial progenitor cells during lung development and leads to the loss of *Shh* expression (Herriges et al., 2015). We therefore propose that Fgf10 acts via Fgfr2b, positively regulating the expression of *Etv4/Etv5*, which in turn regulates *Shh* expression, and therefore the downstream genes involved in the Shh pathway.

5.4 LoF: Discussion on the genes, their biological activities and KEGG analysis

To identify FGF10 downstream target genes in early lung development, we have performed a gene array on E12.5 DTG lungs harvested after 6 hours and 9 hours post Dox IP; STG lungs were used as control. From our gene array data, we identified an 'FGF10 gene signature'. These genes, primarily enriched in the epithelium, decreased after FGF10 inhibition; therefore, these genes likely represent primary, direct targets of FGF10, and are potential key mediators of FGF10/FGFR2b signaling. Interestingly, in Fgf10 gene signature, we found that

Shh which is an epithelial gene encoding a secreted growth factor, is down-regulated concomitantly with *Etv4* and *Etv5*. The combined decrease of *Etv4* and *Etv5* was likely causative for the loss of *Shh* (Herriges et al., 2015). Following the decrease in *Shh* expression, the mesenchymal-specific Hedgehog signaling genes (*Foxl1, Foxf1, Gli1,* and *Ptch2)* all showed a delayed down-regulation. Furthermore, Shh is known to regulate Fgf10 transcription in the mesenchyme (Bellusci et al., 1997a; Lebeche et al., 1999). Taken together, this evidence functionally validates our gene array, and leads to the model proposed in Figure 17E.

5.4.1 Identification of lung-specific transcription factors controlled by FGF10

We have identified the transcription factors (TF) that are controlled by Fgf10. *Lef1, Etv4/5, Snai1, Sox9, Foxf1, Grhl2, Nkx2-1* and *Id2* are genes induced by Fgf10 as they are down-regulated upon Fgf10 attenuation; and *Sox2, Nkx1-2, Pitx2, Hoxa1, Lmo1, Ets1, Elf5* and *Tcf21* are repressed by Fgf10 as they are up-regulated upon Fgf10 attenuation. We also found that Fgf10 regulates many transcription factors previously identified to be lung specific (Herriges et al., 2012). Some of these transcription factors are established mediators of FGF10 signaling (e.g. *Etv4, Etv5, Sox9*), whereas little or nothing is known of the other transcription factors in the context of FGF10 signaling. Knock-out and over-expression studies on many of these transcription factors show impacts on lung branching and epithelial differentiation very similar to the effects seen in our study. For example, Metzger et al. (2008a; 2007) found that Elf5 (group TF6, Figure 17A) is regulated by FGF10 and FGF7 signaling via FGFR2b, and that over-expression of Elf5 leads to branching defects and delayed AEC2 differentiation. Quaggin et al. (1999) reported that Tcf21 (group TF6, Figure 17A) knock-out mice display reduced branching, smaller lungs, and a proximalization of lung epithelium at E14.5. Finally, Varma et al. (2012) studied the transcription factor *Grhl2* (group TF 3, Figure 17A) in the context of lung development, and found that *Grhl2* controls cell-cell interaction genes to regulate cell adhesion and migration, forms a positive feedback loop with *Nkx2-1* during branching morphogenesis, and is associated with proper AEC2 differentiation. We propose that the comprehensive set of target genes and transcription factors identified in our study is a valuable resource for future investigations on early lung branching morphogenesis and differentiation.

5.4.2 FGF10's regulation of tip cell differentiation and morphology

Sustained Sox9 expression in the tip epithelium of the developing lung has been associated with the capacity of epithelial stem cells to self-renew. The current model predicts that individual tip cells, under the influence of Fgf10, are prone to remain in the tip domain, and as these cells divide, some of the daughter cells acquire bronchial progenitor characteristics associated with the exit from the tip domain. The transcription factor Sox9 has been extensively studied in the context of early lung development (see (Chang et al., 2013; Perl et al., 2005; Rockich et al., 2013)). Chang et al. (2013) found that knocking out Sox9 before E12 leads to defects including fewer branches and dilated bud tips, an increase between the distal epithelium and mesothelium, and smaller lungs (even though proliferation appears unaffected). Furthermore, it was found that FGFR2b signaling regulates Sox9, and that Sox9 suppresses the initiation of alveolar differentiation. Concomitant with a loss of Sox9 is the expression of Sox2 in distal epithelial cells of experimental lungs, further suggesting these cells are losing their multipotency, and are adopting a proximal fate. This idea is additionally supported by the evidence, at this stage, of a loss of the AECII signature in the presumptive bipotent progenitors upon FGF10 inhibition. Taken together, our data show that the multipotent potential of distal epithelial cells of early lungs is tightly regulated by FGF10 signaling. Furthermore, the loss of Sox9, in particular, not only affects the multipotent potential of distal tip cells, but also their morphogenesis (Jones, Dilai et al., 2019a).

5.5 GoF: Validation and limitation

We validated the use of the double transgenic mice *Rosa26*$^{rtTA/rtTA}$*;Tg(tet(O)Fgf10)/*+, by the administration of a single Dox IP to a pregnant female at E12.5. Abnormalities start to be seen only after 9 hours of dox IP with more ramified lungs, increased epithelial surface as well as the length of the main branches, dilatation of the mesenchyme was also observed in the experimental lungs compared to control lungs. One of the major limitations of our in vivo model over-expressing FGF10 during pseudoglandular lung development (E12.5) is that the FGF10 expression is global, and the study was performed on the whole lung which make it difficult to identify targets that result primarily from Fgf10-Fgfr2b activation, because in the mesoderm, Fgf10 is present with several other endogenous signals such as Wnts, hepatocyte growth factor, or epidermal growth factor. To overcome this limitation, Lü and co-workers used mesenchyme-free lung epithelial explants at E11.5 cultured in serum-free medium containing recombinant human FGF10 as the sole growth factor in the medium, to eliminate other endogenous signaling. Then, they assessed gene expression in the lung epithelium

during the initial stages of bud formation *in vitro* without intervening signals from the mesenchyme. They identified genes associated with cell rearrangement, cell migration, inflammatory processes, lipid metabolism, and tumor invasion (Lü et al., 2005).

5.6 LoF vs. GoF: Discussion on the genes, their biological activities and KEGG analysis

We have shown that the LoF inhibits the branching morphogenesis (reduced buds number and epithelial surface); whereas, the GoF promote the branching morphogenesis (increased buds number and epithelial surface). In the genomic scale, the heat map for the first 100 genes based on their significance (p-values) revealed that the results are divided into 4 clusters (cluster 1-4). The genes in the cluster 1 and 2 are down-regulated in LoF but up-regulated in GoF, while in the cluster 3 and 4, the genes are up-regulated in LoF but down-regulated in GoF which means that the GoF and LoF have an opposite impact on the expression of the genes. The genes in the cluster 2 might be the one directly controlled by *Fgf10* as they are down-regulated upon *Fgf10* attenuation, and up-regulated upon *Fgf10* over-expression.

6. Summary

FGF10 signaling through FGFR2b is mandatory during early lung development as the deletion of either the ligand or the receptor leads to lung agenesis. In this dissertation, we report the role of FGF10/FGFR2b signaling on the early lung development (E12.5) by attenuating FGFR2b ligands primarily Fgf10 (loss of function), and by over-expressing *Fgf10* (gain of function). In the loss of function part, we used a dominant negative transgenic mouse model *(Rosa26rtTA; tg(tet(o)sFgfr2b)/+),* we conditionally inhibited FGF10 signaling *in vivo* at E12.5 embryonic lungs via doxycycline IP injection to pregnant females, and *in vitro* by culturing control and experimental lungs with doxycycline. Both *in vivo* and *in vitro* experiments inhibiting *Fgf10* resulted in arrested epithelial branching collapsed distal bud and dilatation of the mesenchyme; the impact on branching morphogenesis was also analyzed by morphometry, and electron microscopy (Jones, Dilai et al., 2019a). Gene arrays at 6 and 9 hours post dox IP was carried out and revealed the transcriptomic regulation of FGFR2b signaling with significant changes in cytokine-cytokine receptor interactions, calcium signaling, WNT signaling and Hedgehog signaling. By gene array analysis, we identified an FGF10 gene signature primarily composed of genes enriched in the epithelium and positively regulated by *Fgf10*. We also identified a set of lung specific transcription factors significantly regulated by *Fgf10*. The impact of blocking FGFR2b ligands signaling on the differentiation of multipotent epithelial progenitors was also identified, which demonstrate the loss of distal differentiation markers 9 hours after FGF10 inhibition and the proximalization of the tip epithelium which is enriched with differentiated genes encoding for AECII that are controlled by Fgf10. Furthermore, we assessed the well-established FGF10-SHH regulatory feedback loop during lung development as a means of validating our array (Figure 18E). Not only does our array detect the down-regulation of Shh within 6 hours of FGF10 inhibition, but also it picks up the expected delayed impacts on the downstream targets of Shh at 9 hours, including the up-regulation of Fgf10. Additionally, our array supports the reported data showing that the inactivation of FGF signaling regulated *Etv4* and *Etv5* in the multipotent epithelial progenitor cells during lung development and leads to the loss of Shh expression (Herriges et al., 2015). We therefore propose that FGF10 acts via FGFR2b, positively regulating the expression of Etv4/Etv5, which in turn transcriptionally regulates Shh expression, and therefore the downstream genes involved in the SHH pathway. In the gain of function part, over-expressing Fgf10 resulted in a lung more ramified compared to the control, increased epithelial surface, elongated branches, and dilated mesenchyme. Gene arrays analysis at 9 hours of Fgf10 over-expression revealed a regulation of FGFR2b signaling with significant alterations in cytokine-

cytokine receptor interactions, cell adhesion molecules and ECM-receptor interaction, these data support changes in the rearrangements of the epithelial changes linked to impaired cell-cell or cell-matrix interactions. By the Comparison of the LoF and The GoF, we found a cluster containing genes that are down-regulated upon *Fgf10* attenuation, and up-regulated upon *Fgf10* over-expression these genes might be the one controlled by *Fgf10*. In summary, we validated the reporter mouse line *Tg(Etv4/GFP)* which appear to be a promising tool to monitor FGF10/FGFR2b signaling in early lung development. We also carried out a comprehensive analysis of fibroblast growth factor receptor 2b signaling on multipotent epithelial progenitor cells during early mouse lung branching morphogenesis, where we defined the "FGF10 transcriptomic signature" which will be instrumental to design new mechanistic studies concerning the role of FGF10 in alveolar epithelium formation during development, as well as maintenance during homeostasis and repair after injury.

7. Supplementary Data

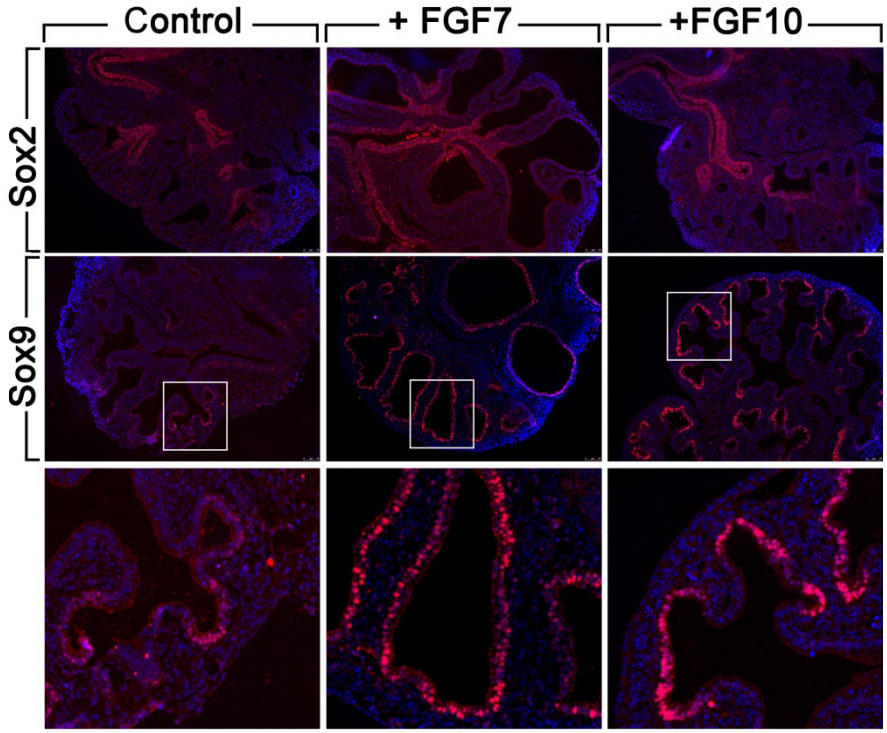

Figure S1: The effect of adding exogenous FGF7 and FGF10 on *Etv4-GFP* lungs. Sox2 (marker for proximal airway progenitor cells) and Sox9 (marker for distal airway progenitor cells) Immunostaining on E12.5 *Tg*(*Etv4*-GFP) lungs grown and incubated with human recombinant protein FGF7 (25 ng/ml) and FGF10 (250 ng/ml) *in vitro* for 40 hours.

7.1 Loss of function part

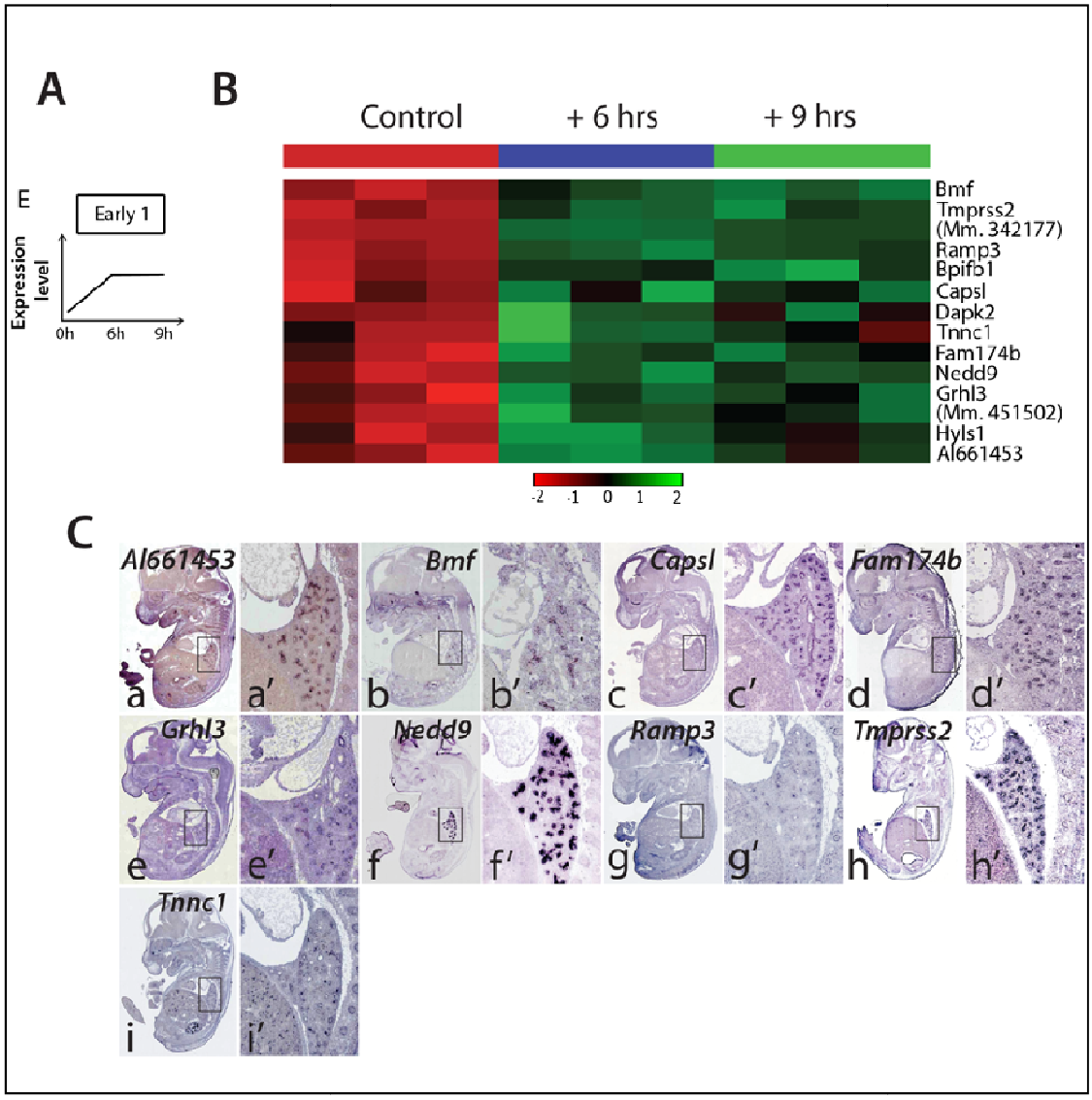

Figure S2: Gene expression level and gene expression pattern in Early 1. (A) Schematic representation of gene expression level in the Early 1 cluster between control, dox-IP+6 and dox-IP+9 conditions. The expressions of these genes are up-regulated between control and dox-IP+6 and not changed between dox-IP+6 and dox-IP+9 conditions. (B) Heat map for the main genes in the Early 1 cluster (selected through their p-value). (C) In situ hybridization from genepaint for lungs at E14.5 for (a, a') Al661453, (b, b') Bmf, (c, c') Capsl, (d, d') Fam174b, (e, e') Grhl3, (f, f') Nedd9, (g, g') Ramp3, (h, h') Tmprss2, (i, i') Tnnc1.

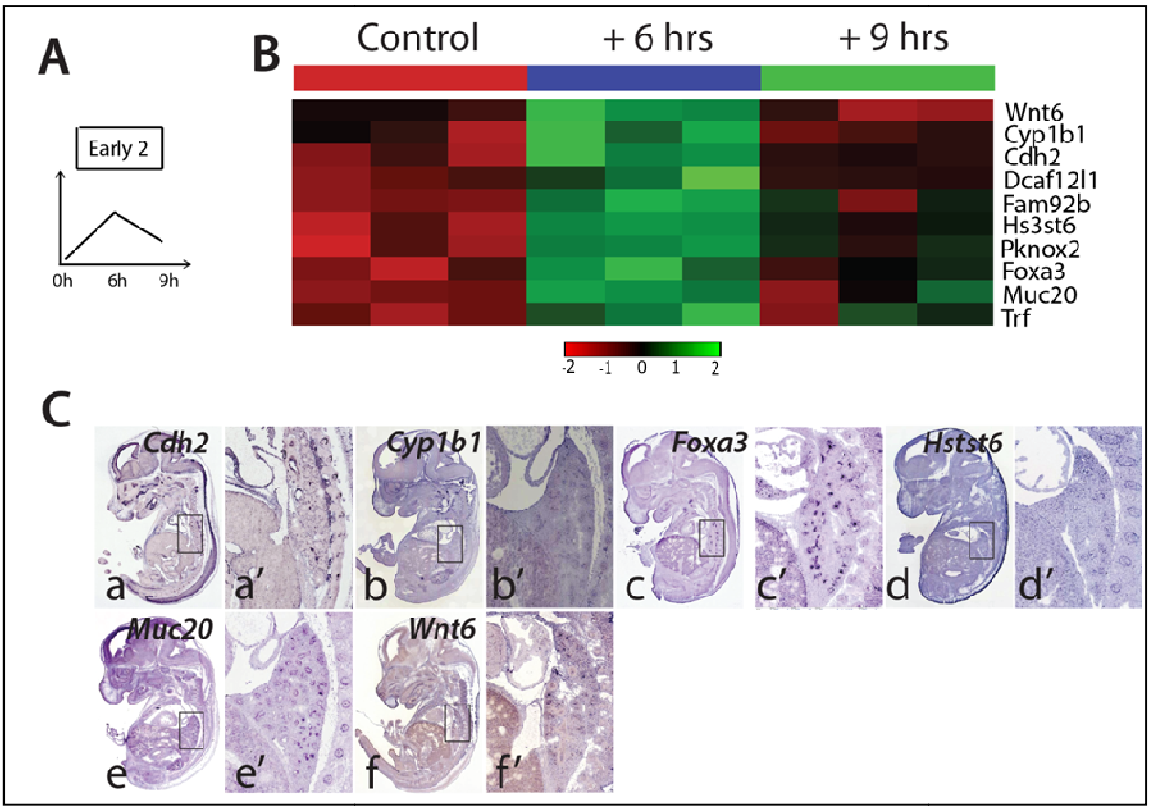

Figure S3: Gene expression level and gene expression pattern in Early 2. (A) Schematic representation of gene expression level in the Early 2 cluster for control, dox-IP+6 hours and dox-IP+9 hours conditions. These genes are up-regulated between control and dox-IP+6 hours and down-regulated between dox-IP+6 hours and dox-IP+9 hours conditions. (B) Heat map for the main genes in the Early 2 cluster (selected through their p-value). (C) In situ hybridization from genepaint for lungs at E14.5 for (a, a') Cdh2, (b, b') Cyp1b1, (c, c') Foxa3, (d, d') Hstst6, (e, e') Muc20, (f, f') Wnt6.

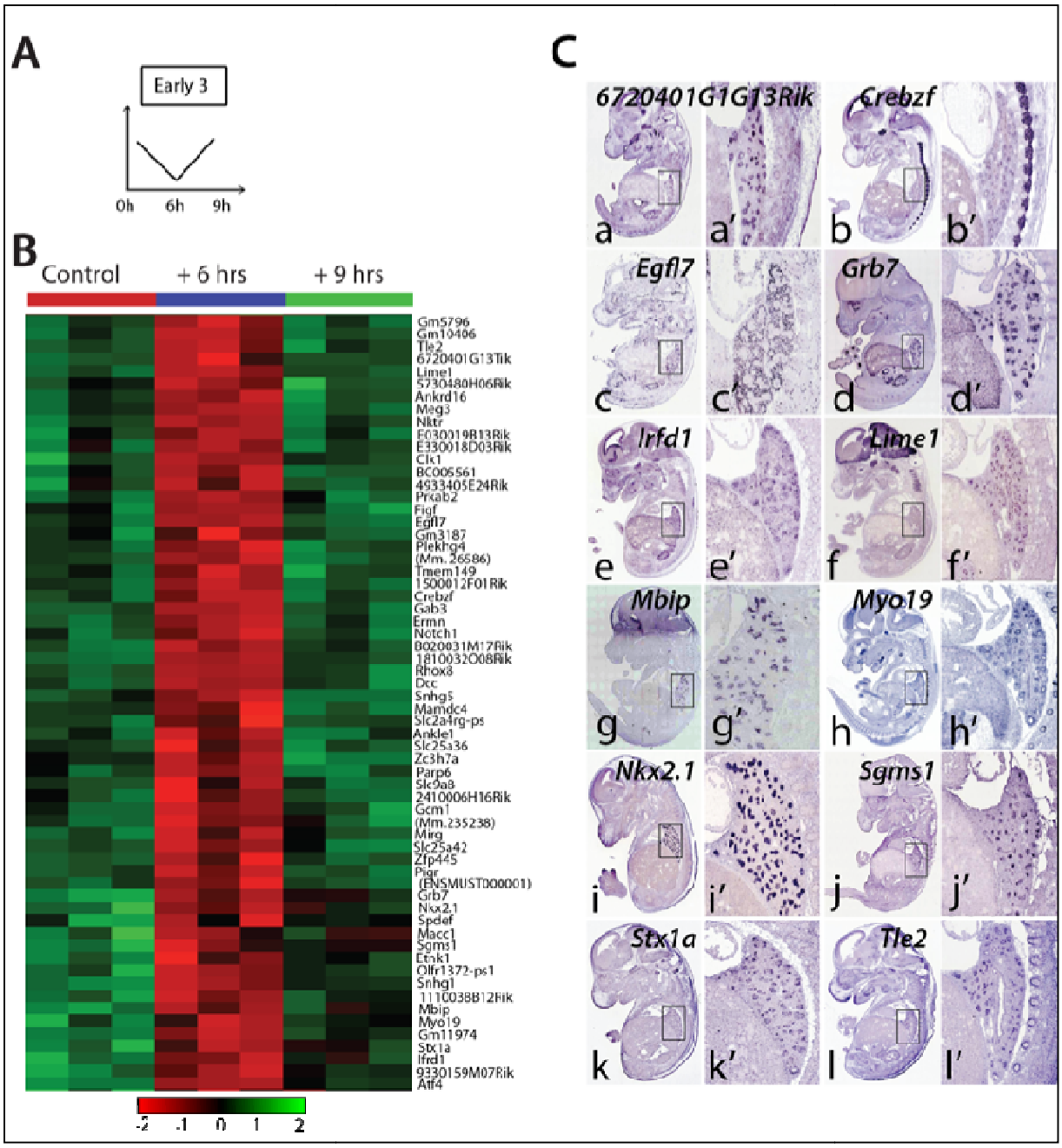

Figure S4: Gene expression level and gene expression pattern in Early 3. (A) Schematic representation of gene expression level in the Early 3 cluster for control, dox-IP+6 hours and dox-IP+9 hours conditions. These genes are down-regulated between dox-IP+6 hours and control and up-regulated between dox-IP+9 hours and dox-IP+6 hours conditions. (B) Heat map for the main genes in the Early 3 cluster (selected through their p-value). (C) In situ hybridization from genepaint website for lungs at E14.5 for (a, a') *6720401G13Rik*, (b, b') *Crebzf*, (c, c') *Egfl1*, (d, d') *Grb7*, (e, e') *Irfd1*, (f, f') *Lime1*, (g, g') *Mbip*, (h, h') *Myo19*, (i, i') *Nkx2.1*, (j, j') *Sgms1*, (k, k') *Stx1a,* (l ,l') *Tle2*.

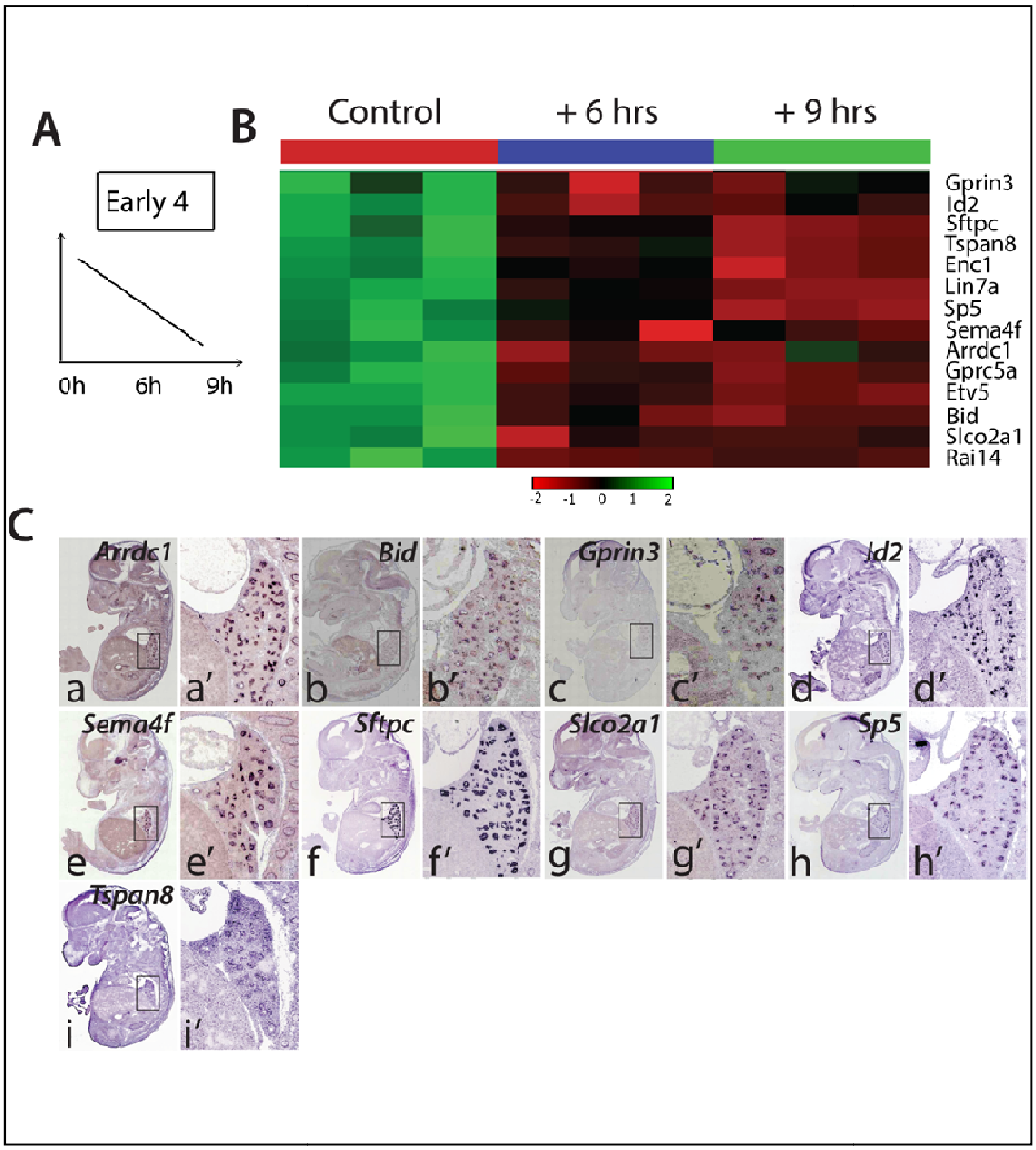

Figure S5: Gene expression level and gene expression pattern in Early 4. (A) Schematic representation of gene expression level in the Early 4 cluster for control, dox-IP+6 hours and dox-IP+9 hours conditions. These genes are down-regulated between dox-IP+6 hours and control and further down-regulated between dox-IP+9 hours and dox-IP+6 hours conditions. (B) Heat map for the main genes in the Early 4 cluster (selected through their p-value). (C) In situ hybridization from genepaint website for lungs at E14.5 for (a, a') *Arrdc1, (b, b') Bid, (c, c') Gprin3, (d, d') Id2, (e, e') Sema4f, (f, f') Sftpc, (g, g') Slco2a1, (h, h') Sp5, (i, i') Tspan8*, these genes are strongly expressed in the epithelium than the mesenchyme.

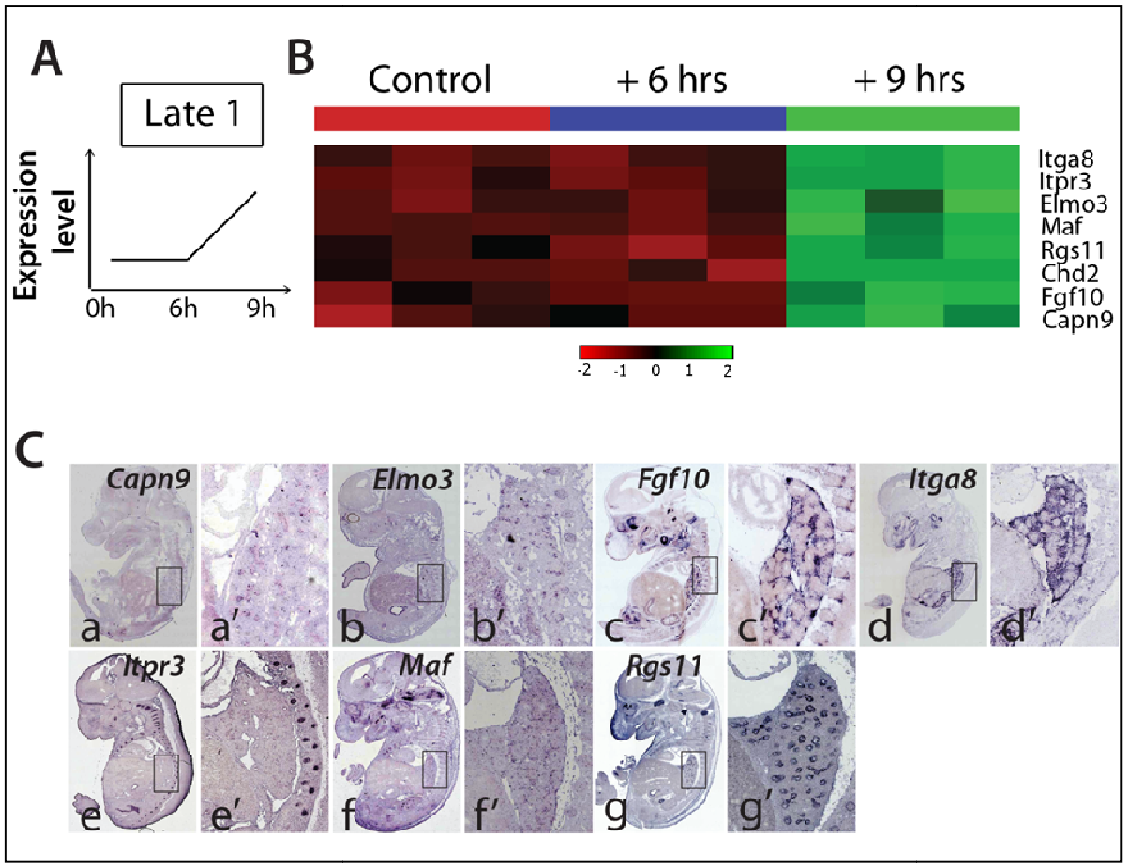

Figure S6: Gene expression level and gene expression pattern in Late 1. (A) Schematic representation of gene expression level in the Late 1 cluster for control, dox-IP+6 hours and dox-IP+9 hours conditions. The expressions of these genes are not changed between dox-IP+6 hours and control but up-regulated between dox-IP+9 hours and dox-IP+6 hours conditions. (B) Heat map for the more significant genes in the Late 1 cluster (selected through their p-value). (C) In situ hybridization from genepaint website for lungs at E14.5 for (a, a') *Capn9,* (b, b') *Elmo3*, (c, c') *Fgf10* (mesenchymal expression), (d, d') *Itga8* (mesenchymal expression), (e, e') *Itpr3*, (f, f') *Maf*, (g, g') *Rgs11*(epithelial expression).

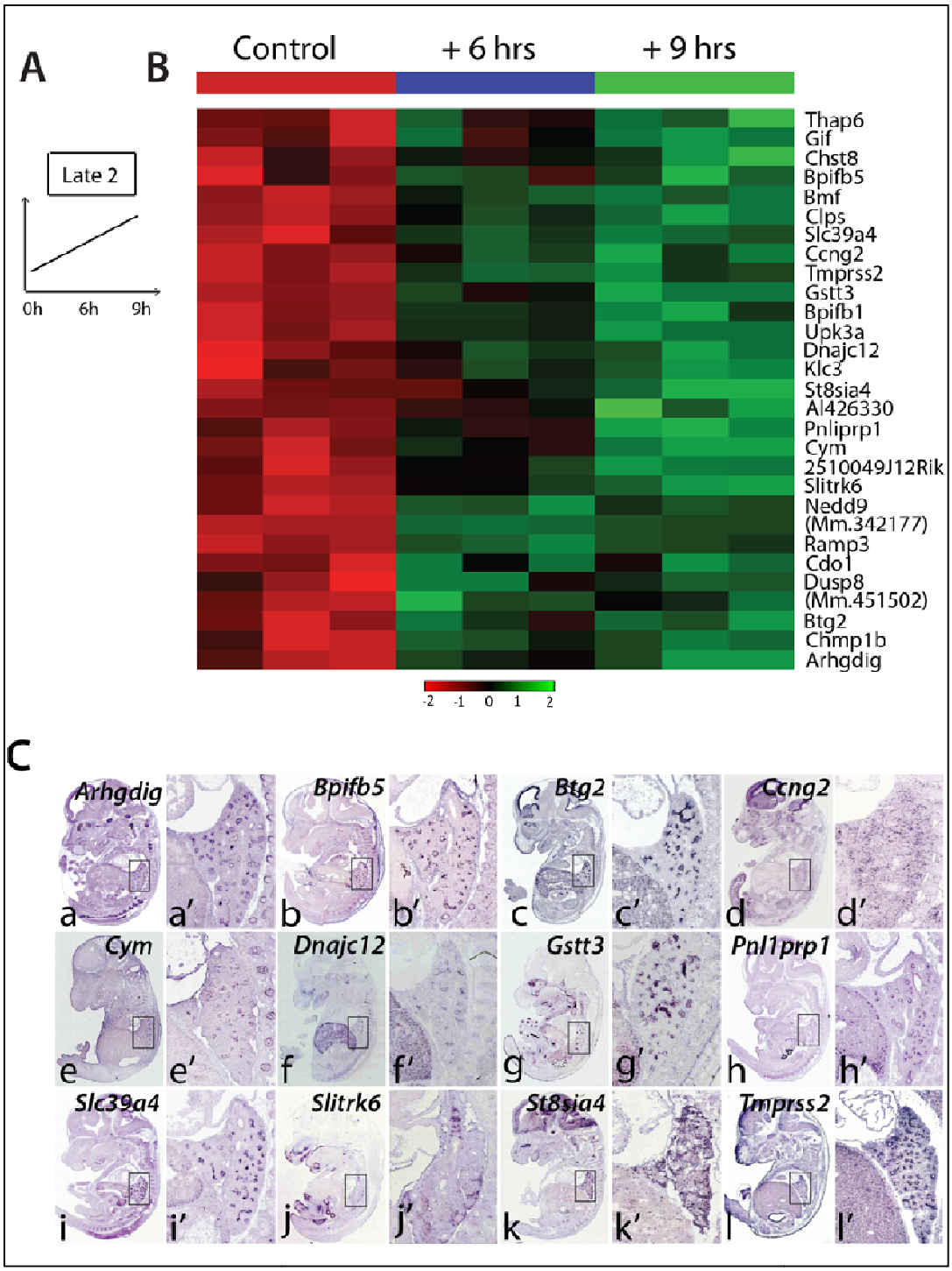

Figure S7: Gene expression level and gene expression pattern in Late 2. (A) Schematic representation of gene expression level in the Late 2 cluster for control, dox-IP+6 hours and dox-IP+9 hours conditions. These genes are up-regulated between dox-IP+6 hours and control and further up-regulated between dox-IP+9 hours and dox-IP+6 hours conditions. (B) Heat map for the more significant genes in the Late 2 cluster (selected through their p-value). (C) In situ hybridization from genepaint website for lungs at E14.5 for (a, a') *Arhgdig, (b, b') Bpifd5, (c, c') Btg2, (d, d') Ccng2, (e, e') Cym, (f, f') Dnajc12, (g, g') Gstt3, (h, h') Pnl1prp1, (i, i') Slc39a4, (j, j') Slitrk6, (k, k') St8sia4, (l, l') Tmprss2.*

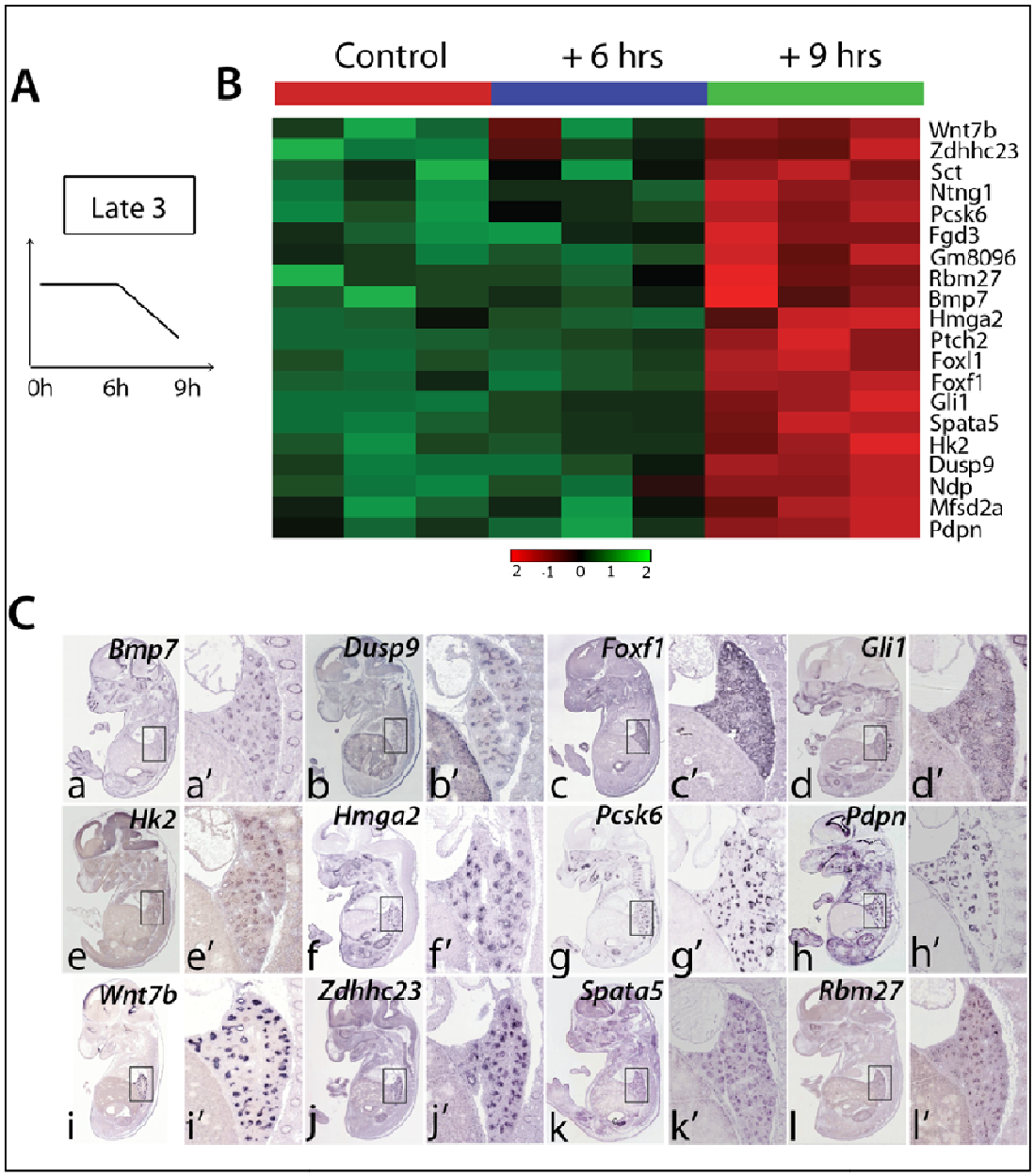

Figure S8: Gene expression level and gene expression pattern in Late 3. (A) Schematic representation of gene expression level in the Late 3 cluster between control, dox-IP+6 hours and dox-IP+9 hours conditions. The expression of these genes is not changed between dox-IP+6 hours and control but down-regulated between dox-IP+9 hours and dox-IP+6 hours conditions. (F)Heat map for the main genes in the Late 3 cluster (selected through their p-value). (C) In situ hybridization from genepaint website for lungs at E14.5 for (a, a') *Bmp7, (b, b') Dusp9, (c, c') Foxf1, (d, d') Gli1, (e, e') Hk2, (f, f') Hmga2, (g, g') Pcsk6, (h, h') Pdpn, (i, i') Wmt7b, (j, j') Zdhhc23, (k, k') Spata5, (l, l') Rbm27.*

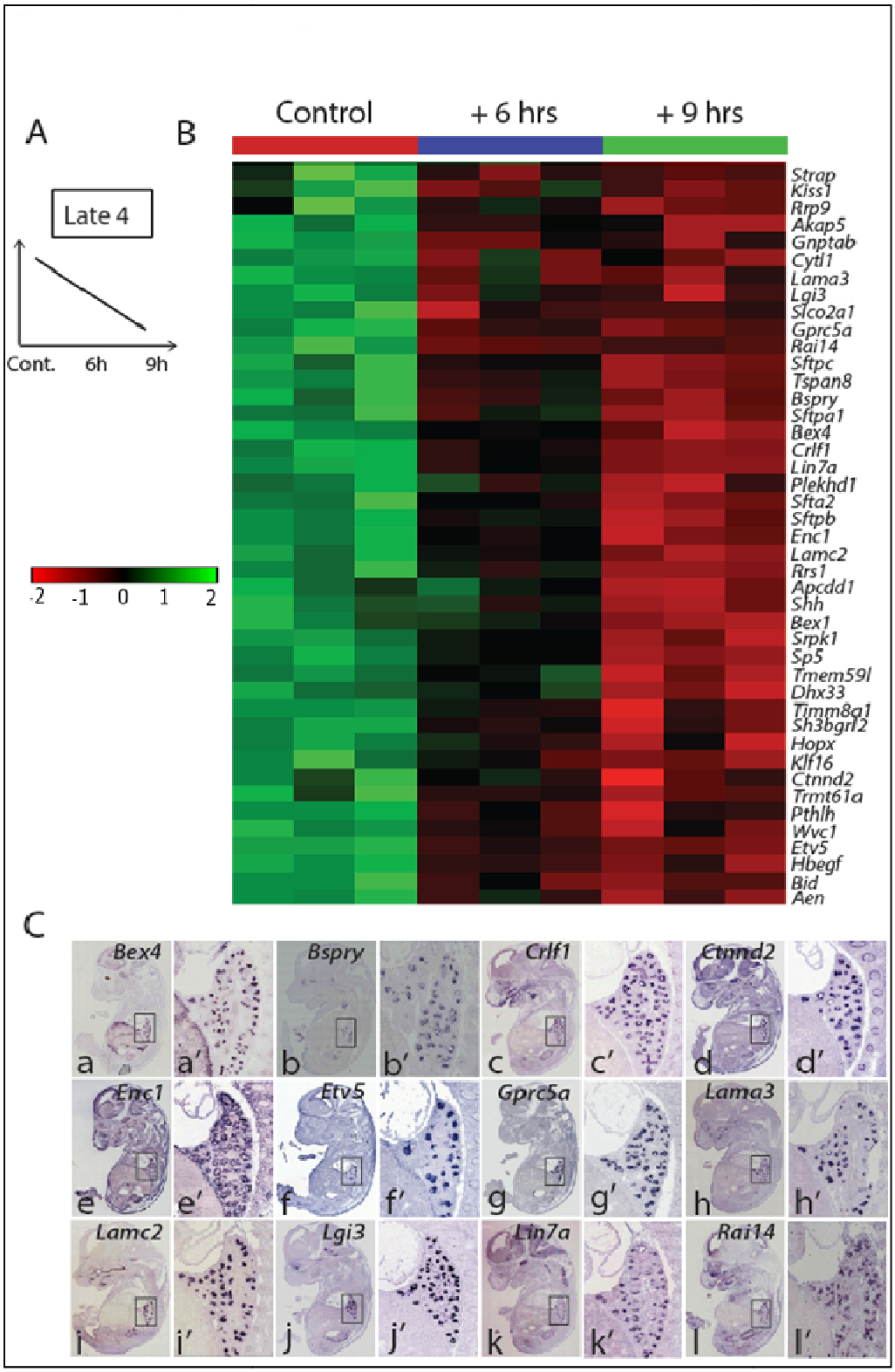

Figure S9: Gene expression level and gene expression pattern in Late 4. (A) Schematic representation of gene expression level in the Late 4 cluster between control, dox-IP+6 hours and dox-IP+9 hours conditions. The expression of these genes is down-regulated between dox-IP+6 hours and control and further down-regulated between dox-IP+9 hours and dox-IP+6 hours conditions. (B) Heat map for the main genes in the Late 4 cluster (selected

through their p-value). (C) In situ hybridization from genepaint website for lungs at E14.5 for (a, a') *Bex4, (b, b') Bspry, (c, c') Crlf1, (d, d') Ctnnd2, (e, e') Enc1, (f, f') Etv5, (g, g') Gprc5a, (h, h') Lama3, (i, i') Lamc2, (j, j') Lgi3, (k, k') Lin7a, (l, l') Rai14*, these genes are strongly expressed in the epithelium than the mesenchyme.

7.1.1 List 1: Definition of genes in Early4 group (LoF)

(The definition is done from GeneCards and DAVID bioinformatics tool)

Gprin3: G protein-regulated inducer of neurite outgrowth 3, the function of GRIN3 is still unclear, but it has been published that GRIN3 has two human homologs GRIN1, and GRIN2, and that GRIN1 is expressed specifically in brain, GRIN1 family may function as a downstream effector for G_o to regulate neurite growth (Naoyuki Iida et al. 2004)

Id2: inhibitor of DNA binding 2, is a member of the inhibitor of differentiation (Id) family, members of which are transcriptional regulators that contain a helix-loop-helix (HLH) domain, there are four Id transcription factor genes Id1, Id2, Id3 and Id4, and all of them are expressed in the lung: Id2 and Id4 are expressed in the epithelium, whereas Id1 and Id3 are expressed in the mesenchyme (Jen et al. 1996). Lineage tracing using Id2-creER^{T2} that allows following the fate of Id2 cells has shown that Id2-expressing cells contributes to both the proximal airway epithelial and the distal alveolar epithelial cell populations (Rawlins 2009). It was also shown by Dijke et al. that Id genes are specifically induced by Bone morphogenetic proteins (BMPs) in tissues of different origin (Ten Dijke et al. 2003).

Sftpc: Surfactant Protein C, is incorporated together with specific phospholipids and proteins into lamellar bodies in alveolar type 2 cells, then released via regulated exocytosis in the gas-liquid interface of the alveolus, playing a critical role in the modulation of lung mechanics (Salerno et al. 2016). Sftpc is used as differentiation marker for AECII.

Tspan8: Tetraspanin 8, play a role in the regulation of cell development, activation, growth and motility. This encoded protein is a cell surface glycoprotein that is known to complex with integrins. This gene is expressed in different carcinomas.

Enc1: Ectodermal-Neural Cortex 1, a member of the KELCH family, is widely expressed in the nervous system and plays an important role in nervous system development

Lin7a: Lin-7 Homolog A has a crucial role in the polarity abnormalities associated with breast carcinogenesis (Gruel et al. 2016); it has been shown that Lin7a is also associated with pulmonary aspergilloma disease.

Sp5: Trans-acting transcription Factor 5, it has been shown that Sp5 is gene-specific transcriptional coactivators in the Wnt/β-catenin pathway (Kennedy et al. 2016)

Sema4f: Semaphorin 4F has roles in embryologic axon guidance and is expressed in adults. S4F is involved in cancer-induced neurogenesis, it has also been shown that S4F is significantly involved in human prostate cancer progression (Ding et al. 2013).

Arrdc1: Arrestin Domain Containing 1, the corresponding protein is expressed in many organs including: stomach, liver, lung, mammary glands, kidney…, but not much is known about this gene.

Etv5: ETS Translocation Variant 5 was identified as being expressed in the distal lung epithelium. It has been shown to be positively regulated by FGF signaling, which could explain their expression within the distal epithelium, as Fgf10 is strongly expressed within the distal mesenchyme of the branching lung and signals to the adjacent epithelium (Liu et al. 2003). ETV5 belongs to the three-member Pea3 subgroup of ETS domain containing proteins ETV1 and ETV4, which has been shown to play a role in epithelial–mesenchymal interactions during lung organogenesis (Liu et al. 2003).

Bid: BH3 Interacting Domain Death Agonist, is a pro-apoptotic member of the Bcl-2 protein family that act as anti- or pro-apoptotic regulators that are involved in a wide variety of cellular activities such as regulation of cell death, establishment of protein localization, release of cytochrome c from mitochondria, protein targeting, intracellular protein transport and membrane organization.

Slco2a1: Solute Carrier Organic Anion Transporter Family Member 2A1, also known as the prostaglandin transporter (PGT). It may be involved in mediating the uptake and clearance of prostaglandins in numerous tissues. In the lung, it has been shown that SLCO2A1 plays a critical role in protecting it from bleomycin-induced fibrosis (Nakanishi et al., 2015)

Rai14: retinoic acid induced 14; it has been shown by Yuan and coworkers that Rai14 is a new potential biomarker for lung adenocarcinoma (Yuan et al., 2017).It plays a role in actin regulation at the ectoplasmic specialization, a type of cell junction specific to testis. It is also

important for establishment of sperm polarity and normal spermatid adhesion. It May also promote integrity of Sertoli cell tight junctions at the blood-testis barrier.

7.1.2 List 2: Definition of genes in Late 4 group (LoF)

Sftpa1: Surfactant proteins A (SP-A), play important roles in innate host defense by binding and clearing invading microbes from the lung, influence surfactant homeostasis, contributing to the physical structures of lipids in the alveoli and to the regulation of surfactant function and metabolism, SP-A bind to the surfaces of host defense cells, promoting or inhibiting immune cell activity through multiple cellular pathways. (Kingma P, 2006).

Kiss1: Kisspeptin or KiSS-1 metastasis-suppressor is a Protein Coding gene, The encoded protein in involved in different biological processes such as cell surface receptor linked signal transduction, G-protein coupled receptor protein signaling pathway, regulation of cell proliferation and regulation of cell migration. This gene is a metastasis suppressor gene that suppresses metastases of melanomas and breast carcinomas without affecting tumorigenicity.

Rrp9: Ribosomal RNA Processing 9, U3 Small Nucleolar RNA Binding Protein, is a Protein Coding gene. The encoded protein is involved in many biological processes such as RNA and rRNA processing, ribonucleoprotein complex biogenesis and ribosome biogenesis.

Akap5: A kinase (PRKA) anchor protein 5 is a protein coding gene, which has the function of binding to the enzyme, kinase and protein kinase.

Gnptab: N-acetylglucosamine-1-phosphate transferase, alpha and beta subunits, is a Protein Coding gene. The encoded protein is involved in many biological processes such as phosphate metabolic process, protein localization, protein secretion, protein transport, phosphorylation, secretion by cell, and establishment of protein localization.

Cytl1: cytokine-like 1, is a protein specifically expressed in bone marrow and cord blood mononuclear cells that bear the CD34 (MIM 142230) surface marker (Liu et al., 2000). It is involved in many biological processes such as skeletal system development, regulation of transcription, positive regulation of gene expression, positive regulation of cellular biosynthetic process, positive regulation of DNA binding, regulation of transcription factor activity, cartilage development and regulation of RNA metabolic process

Lama3: laminin alpha 3, the protein encoded by this gene belongs to the laminin family of secreted molecules. Laminins are essential for formation and function of the basement

membrane and have additional functions in regulating cell migration and mechanical signal transduction. Lama3 is also in involved in many biological activities such as cell adhesion, biological adhesion, regulation of cell adhesion, regulation of embryonic development and regulation of cell motion. Diseases associated with LAMA3 include Laryngoonychocutaneous Syndrome which is a disorder that leads to abnormalities of the voicebox (laryngo-), finger-, toenails (onycho-), and skin (cutaneous), LAMA3 is also associated with Epidermolysis Bullosa, Junctional, Herlitz Type disease, which is an autosomal recessive skin disorder in which blisters occur at the level of the lamina lucida in the skin basement membrane.

Lgi3: leucine-rich repeat LGI family, member 3, is a protein coding gene, the encoded protein is involved in many biological processes such as vesicle-mediated transport, regulation of exocytosis, regulation of secretion and regulation of cellular localization.

Gprc5a: G protein-coupled receptor, family C, group 5, member A; is a Protein Coding gene, the encoded protein is involved in cell surface receptor linked signal transduction, and G-protein coupled receptor protein signaling pathway. This gene may play a role in embryonic development and epithelial cell differentiation. Diseases associated with GPRC5A include Lung Cancer.

Bspry: B-box and SPRY domain containing, is a protein coding gene, it may regulate epithelial calcium transport by inhibiting TRPV5 activity, it is involved in many biological activities such as ion transport, cation transport, calcium ion transport, di-, tri-valent inorganic cation transport, and metal ion transport

Bex4: Brain Expressed X-Linked 4 is a protein coding gene; it is a member of the brain expressed X-linked gene family. The proteins encoded act as transcription elongation factors which allow RNA polymerase II to escape pausing during elongation.

Crlf1: Cytokine receptor-like factor, this gene encodes a member of the cytokine type I receptor family. The protein forms a secreted complex with cardiotrophin-like cytokine factor 1 and acts on cells expressing ciliary neurotrophic factor receptors. The complex can promote survival of neuronal cells. Diseases associated with CRLF1 include Cold-Induced Sweating Syndrome which is an autosomal dominant disease characterized by problems with regulating body temperature and other abnormalities affecting many parts of the body

Sfta2: Surfactant associated 2, is a protein coding gene, the encoded protein is involved in respiratory gaseous exchange.

Sftpb: Surfactant associated protein B is a protein coding gene, Sftpb is an amphipathic surfactant protein essential for lung function and homeostasis after birth, it is involved in respiratory gaseous exchange, membrane lipid metabolic process and sphingolipid metabolic process. Sftpb is used as a differentiation marker for alveolar epithelial cells type 2 (AECII). Diseases associated with SFTPB include pulmonary surfactant metabolism dysfunction type 1 and respiratory failure.

Lamc2: Laminin Subunit Gamma 2 is a protein coding gene; it belongs to laminins family which is a family of extracellular matrix glycoproteins, that are the major noncollagenous constituent of basement membranes. They have been implicated in a wide variety of biological processes including cell adhesion, differentiation, migration, signaling, neurite outgrowth and metastasis. Lamc2 is involved in cell adhesion and biological adhesion. Diseases associated with LAMC2 include Epidermolysis Bullosa, Junctional, Herlitz and Non-Herlitz Type, which is a blistering skin diseases characterized by tissue separation which occurs within the dermo-epidermal basement.

Rrs1: RRS1 ribosome biogenesis regulator homolog (S. cerevisiae) is a protein coding gene. The encoded protein is involved in ribonucleoprotein complex biogenesis and ribosome biogenesis. Diseases associated with RRS1 include Robinow Syndrome.

Apcdd1: Adenomatosis polyposis coli down-regulated 1, Negative regulator of the Wnt signaling pathway. Apcdd1 inhibits Wnt signaling in a cell-autonomous manner and functions upstream of beta-catenin, it may act via its interaction with Wnt and LRP proteins and may play a role in colorectal tumorigenesis.

Shh: Sonic hedgehog is one of three proteins in the mammalian signaling pathway family called hedgehog. It plays a key role in many cellular processes like cell growth, survival, differentiation, migration, and tissue polarity. In the adult, it controls cell division of adult stem cells and has been implicated in the development of some cancers. Among the three HH proteins, Sonic Hedgehog plays an essential role during lung development, any defects of this secreted protein lead to lung hypoplasia.

Bex1: Brain expressed gene 1, is a protein coding gene, it is involved in many biological activities such as cell cycle progression and neuronal differentiation, cell surface receptor linked signal transduction, enzyme linked receptor protein signaling pathway, transmembrane receptor protein tyrosine kinase signaling pathway, regulation of cell proliferation, regulation of neurogenesis and regulation of cell development

Srpk1: Serine/Arginine-Rich Protein-Specific Kinase 1, is a protein coding gene, it is thought to play a role in regulation of both constitutive and alternative splicing by regulating intracellular localization of splicing factors.

Dhx33: DEAH-Box Helicase 33, is a Protein Coding gene, some members of this DEAD box protein family are believed to be involved in embryogenesis, spermatogenesis, and cellular growth and division. Alternative splicing results in multiple transcripts variants.

Timm8a1: Translocase of inner mitochondrial membrane 8 homolog a1 (yeast); the encoded protein is involved in many biological processes such as protein targeting, protein import and transport, membrane organization, cellular protein localization, transmembrane transport, mitochondrion organization and mitochondrial transport.

Sh3bgrl2: SH3 domain binding glutamic acid-rich protein like 2 is a protein coding gene. The encoded protein is involved in SH3 domain binding and protein domain specific binding. Not much is known about this gene.

Hopx: HOP Homeobox is a protein coding gene; the corresponding protein is involved in many biological activities such as transcription, heart development, embryonic development, negative regulation of gene expression, lung development, lung alveolus development, respiratory system development, regulation of cell differentiation, regulation of developmental growth and regulation of muscle cell differentiation. Hopx transcription factor was previously reported to regulate alveolar maturation by suppressing surfactant protein production in AECII cells (Yin et al., 2006); Diseases associated with HOPX include Choriocarcinoma and Oral Squamous Cell Carcinoma.

Klf16: Kruppel-like factor 16, is a Protein Coding gene, it belongs to KLF family which is a family of transcription factors that regulate various cellular functions, such as proliferation, differentiation, and apoptosis, as well as the development and homeostasis of several types of tissue. Klf16 encoded protein is involved in different biological activities such as regulation of transcription, cell surface receptor linked signal transduction, G-protein coupled receptor protein signaling pathway and regulation of RNA metabolic process.

Ctnnd2: Catenin (cadherin associated protein), delta 2 is a protein coding gene, it is implicated in brain, eye development and cancer formation, ctnnd2 is also involved in many biological processes such as morphogenesis of a branching structure transcription, cell adhesion, behavior, learning or memory, regulation of neurological system process, regulation

of synaptic transmission and regulation of transmission of nerve impulse. Diseases associated with CTNND2 include Benign Adult Familial Myoclonic Epilepsy and Cri-Du-Chat Syndrome.

Trmt61a: TRNA Methyltransferase 61A is a protein coding gene, among its related pathways are Gene Expression and tRNA processing.

Pthlh: Parathyroid hormone-like peptide is a protein coding gene; it is a member of the parathyroid hormone family. This hormone, via its receptor, PTHR1, regulates endochondral bone development and epithelial-mesenchymal interactions during the formation of the mammary glands and teeth, it is also involved in many biological processes such as respiratory system development, lung development, lung alveolus development, mammary gland development, nipple development, lactation, epithelium development, protein processing, regulation of cell proliferation, intracellular signaling cascade, regulation of transcription and regulation of DNA binding. Diseases associated with PTHLH include Brachydactyly, type E1 and type E2 which is an inherited disease characterized by shortness of the fingers and toes.

Hbegf: Heparin-Binding Epidermal Growth Factor is a protein coding gene. The encoded protein is involved in many biological activities such as angiogenesis, blastocyst development, vasculature development, cell motion, signal transduction, transmembrane receptor protein tyrosine kinase signaling pathway, epidermal growth factor receptor signaling pathway, regulation of heart contraction, positive regulation of cell proliferation, embryonic development, cell migration, wound healing, regulation of cell proliferation and regulation of smooth muscle cell proliferation. Diseases associated with HBEGF include Diphtheria which is an infection caused by the bacterium Corynebacterium diphtheriae. It can lead to difficulty breathing, heart failure, paralysis, and even death; and Bladder disease which is an urinary system disease that is located in the bladder.

Aen: apoptosis enhancing nuclease is a protein coding gene; the corresponding protein is involved in many biological processes such as apoptosis, induction of apoptosis, intracellular signaling cascade, DNA damage response, regulation of cell death and signal transduction by p53 class mediator resulting in induction of apoptosis.

7.2 Gain of function part

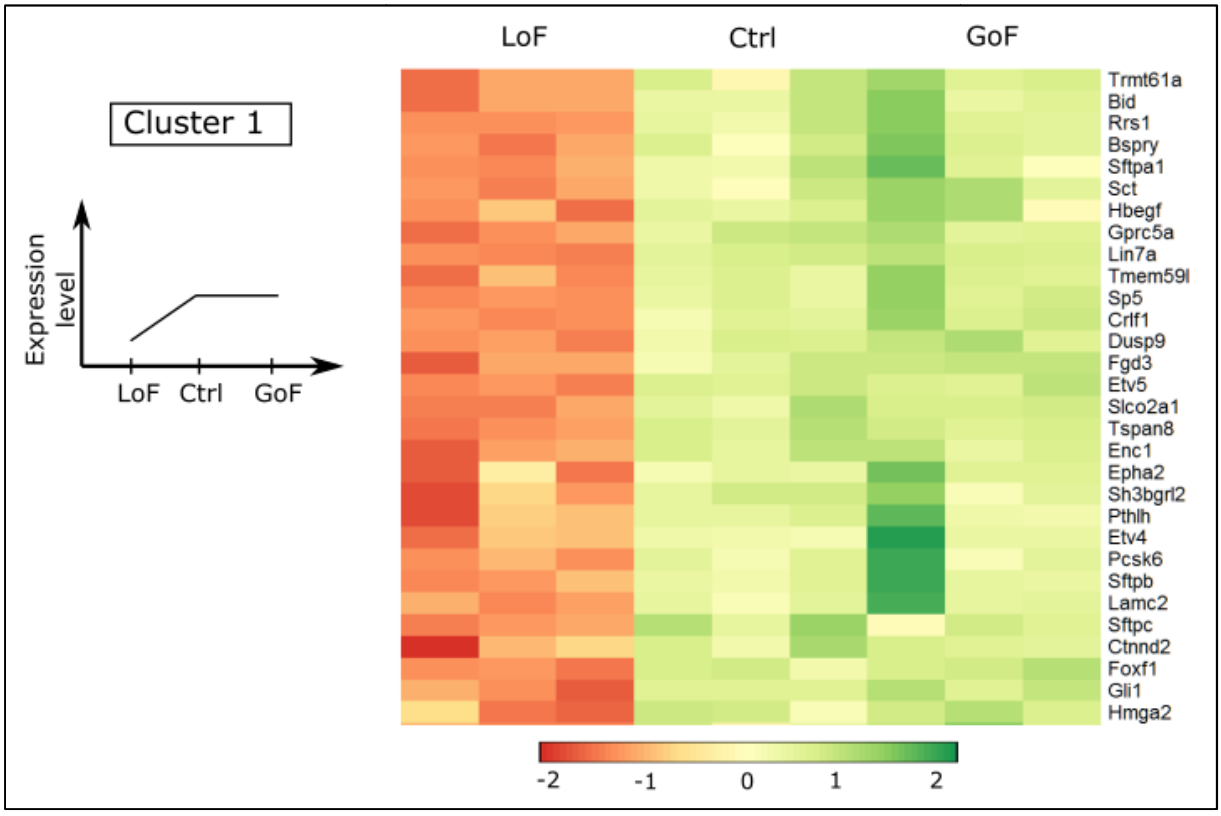

Figure S10: Gene expression level in the Cluster 1. (A) Schematic representation of gene expression level in the cluster 1 between control, loss of function (LoF) dox-IP+9 hours and gain of function (GoF) dox-IP+9 hours conditions. The expression of these genes is down-regulated in LoF and not changed in GoF compared to control. (B) Heat map for the main genes in the cluster 1 (selected through their p-value). The definition of the genes are listed in the list 3 in supplementary data.

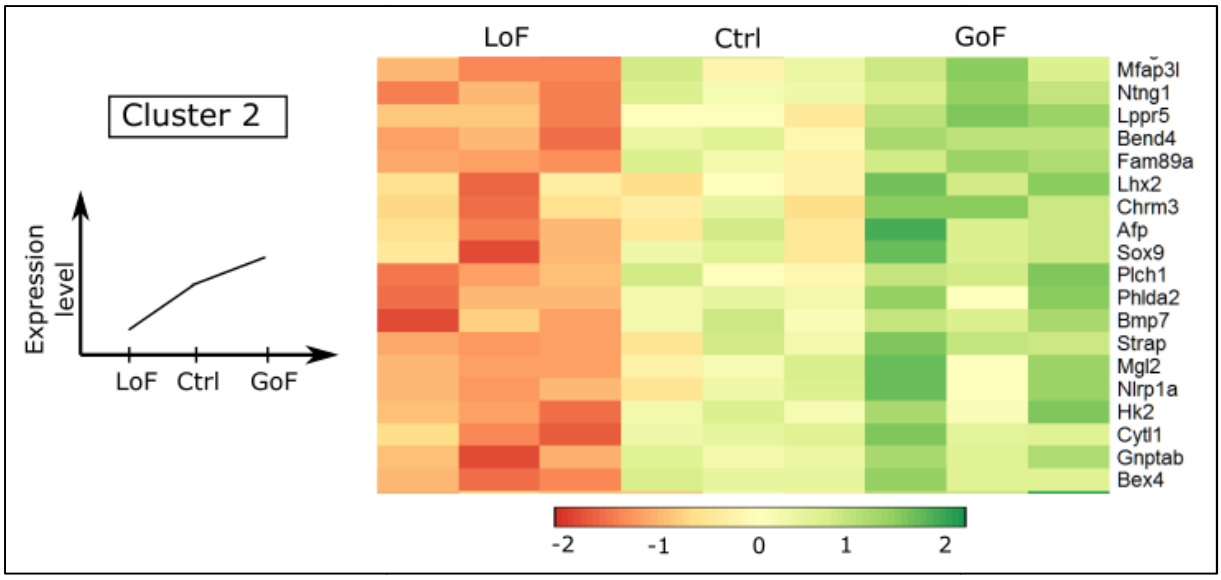

Figure S11: Gene expression level in the Cluster 2. (A) Schematic representation of gene expression level in the cluster 2 between control, loss of function (LoF) dox-IP+9 hours and gain of function (GoF) dox-IP+9 hours conditions. The expression of these genes is down-regulated in LoF and slightly up-regulated in GoF compared to control. (B) Heat map for the main genes in the cluster 2 (selected through their p-value). The definition of the genes are listed in the list 4 in supplementary data.

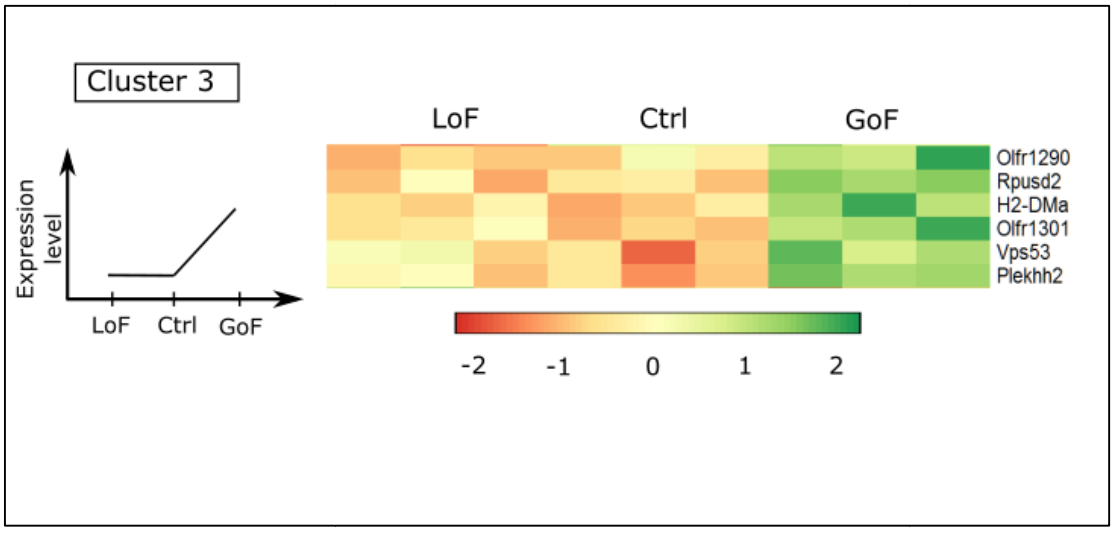

Figure S12: Gene expression level in the Cluster 3. (A) Schematic representation of gene expression level in the cluster 3 between control, loss of function (LoF) dox-IP+9 hours and gain of function (GoF) dox-IP+9 hours conditions. The expression of these genes is not changed between LoF and control but up-regulated in GoF. (B) Heat map for the main genes in the cluster 3 (selected through their p-value). The definition of the genes are listed in the list 5 in supplementary data.

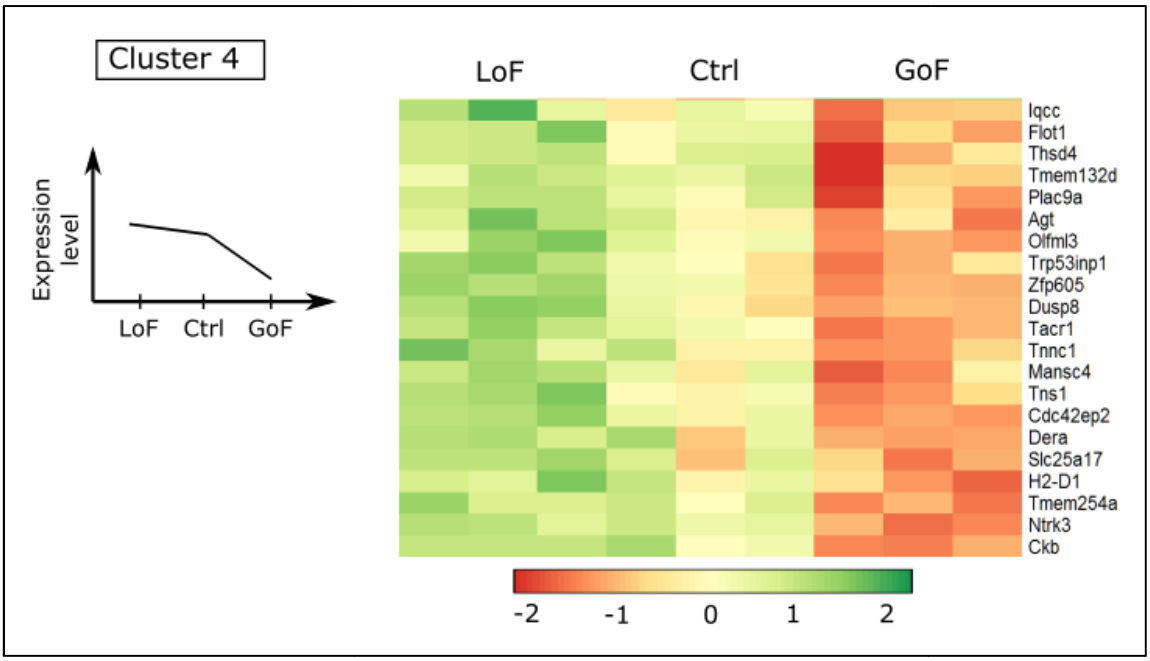

Figure S13: Gene expression level in the Cluster 4. (A) Schematic representation of gene expression level in the cluster 3 between control, loss of function (LoF) dox-IP+9 hours and gain of function (GoF) dox-IP+9 hours conditions. The expression of these genes is up-regulated in LoF but down-regulated in GoF compared to control. (B) Heat map for the main genes in the cluster 4 (selected through their p-value). The definition of the genes are listed in the list 6 in supplementary data.

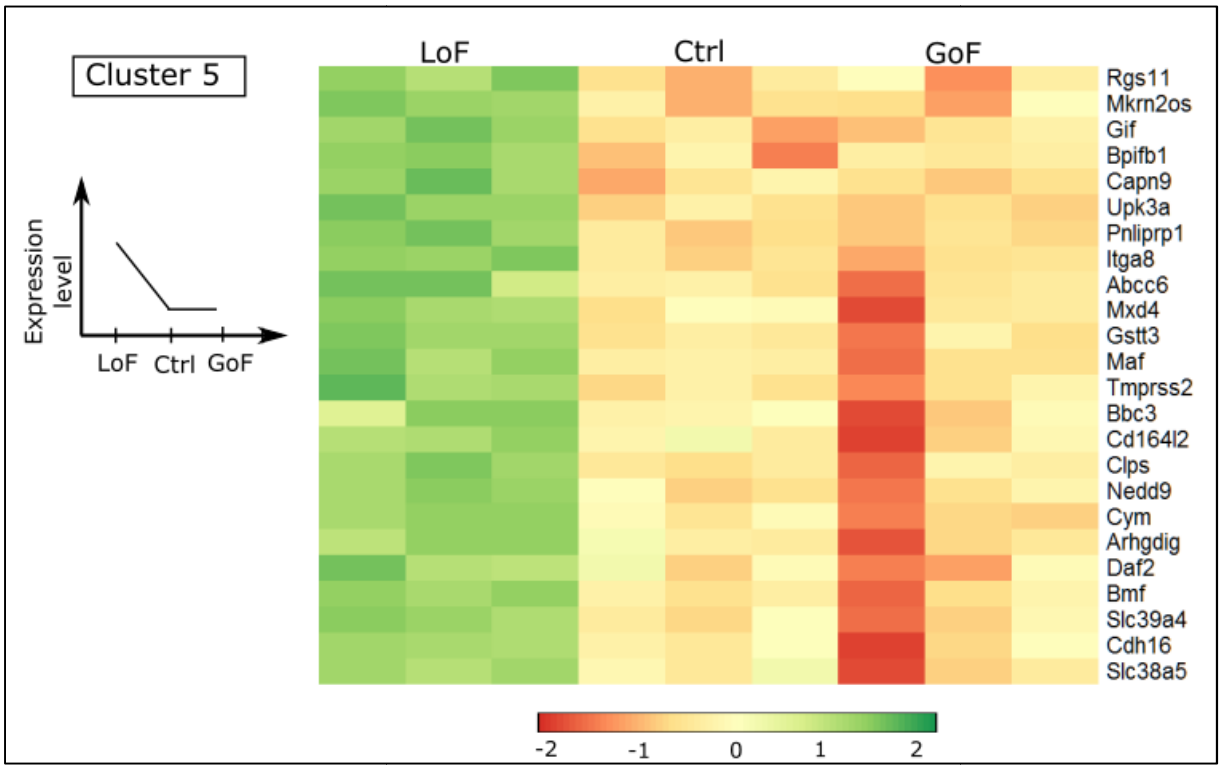

Figure S14: Gene expression level in the Cluster 5. (A) Schematic representation of gene expression level in the cluster 4 between control, loss of function (LoF) dox-IP+9 hours and gain of function (GoF) dox-IP+9 hours conditions. The expression of these genes is up-regulated in LoF and not changed in GoF compared to control. (B) Heat map for the main genes in the cluster 5 (selected through their p-value).

7.2.1 List 3: Definition of genes in the cluster 1 (GoF)

(The definition is done using GeneCards and DAVID bioinformatics tool)

Trmt61a: See List 2 from supplementary data.

Bid: See List 1 from supplementary data.

Rrs1: See List 2 from supplementary data.

Bspry: See List 2 from supplementary data.

Sftpa1: See List 2 from supplementary data.

Sct: Secretin is a Protein Coding gene; this gene encodes a member of the glucagon family of peptides. The encoded preproprotein is secreted by endocrine S cells in the proximal small intestinal mucosa as a prohormone, and then proteolytically processed to generate the mature peptide hormone. The release of this active peptide hormone is stimulated by either fatty acids or acidic pH in the duodenum. This hormone stimulates the secretion of bile and bicarbonate in the duodenum, pancreatic and biliary ducts. It is also involved in many biological processes such as brain development, visual learning, dentate gyrus development, negative regulation of neuron apoptotic process, embryonic digestive tract development, positive regulation of pancreatic juice secretion, positive regulation of somatostatin secretion, neuronal stem cell population maintenance, and negative regulation of gastrin-induced gastric acid secretion

Hbegf: See List 2 from supplementary data.

Gprc5a: See List 1 from supplementary data.

Lin7a: See List 1 from supplementary data.

Tmem59l: Transmembrane protein 59-like is a Protein Coding gene, The encoded protein may play a role in functioning of the central nervous system.

Sp5: See List 1 from supplementary data.

Crlf1: See List 2 from supplementary data.

Dusp9: Dual specificity phosphatase 9 is is a Protein Coding gene, The protein encoded by this gene is a member of the dual specificity protein phosphatase subfamily. These phosphatases inactivate their target kinases by dephosphorylating both the phosphoserine/threonine and phosphotyrosine residues. They negatively regulate members of the mitogen-activated protein (MAP) kinase superfamily (MAPK/ERK, SAPK/JNK, p38), which is associated with cellular proliferation and differentiation. Aberrant expression of this gene is associated with type 2 diabetes and cancer progression in several cell types.

Fgd3: FYVE, RhoGEF and PH domain containing 3, is a Protein Coding gene. Among its related pathways are RET signaling and p75 NTR receptor-mediated signaling, it promotes the formation of filopodia, and regulates Rho protein signal transduction, and plays a role in regulating the actin cytoskeleton and cell shape (By similarity).

Etv5: See List 1 from supplementary data.

Slco2a1: See List 2 from supplementary data.

Tspan8: See List 1 from supplementary data.

Enc1: See List 2 from supplementary data.

Epha2: Eph receptor A2(Epha2), is a Protein Coding gene, this gene belongs to the ephrin receptor subfamily of the protein-tyrosine kinase family. The encoded protein is involved in many biological activities such as skeletal system development, angiogenesis, blood vessel development, vasculogenesis, osteoblast differentiation, negative regulation of cytokine production, blood vessel endothelial cell proliferation involved in sprouting angiogenesis, protein phosphorylation, apoptotic process, inflammatory response, cell adhesion, transmembrane receptor protein tyrosine kinase signaling pathway, intrinsic apoptotic signaling pathway in response to DNA damage, regulation of ERK1 and ERK2 cascade and response to growth factor. Mutations in this gene are the cause of certain genetically-related cataract disorders.

Sh3bgrl2: See List 2 from supplementary data.

Pthlh: See List 2 from supplementary data.

Etv4: Ets variant 4**,** is a protein coding gene. The encoded protein is involved in many biological activities such as transcription, DNA-templated, regulation of transcription, DNA-templated, motor neuron axon guidance, positive regulation of gene expression, negative regulation of mammary gland epithelial cell proliferation, positive regulation of transcription, DNA-templated, positive regulation of transcription from RNA polymerase II promoter, stem cell differentiation, branching involved in mammary gland duct morphogenesis and regulation of branching involved in mammary gland duct morphogenesis.

Pcsk6: Proprotein convertase subtilisin/kexin type 6 is a Protein Coding gene. This gene encodes a member of the subtilisin-like proprotein convertase family, which includes proteases that process protein and peptide precursors trafficking through regulated or constitutive branches of the secretory pathway. The encoded protease is constitutively secreted into the extracellular matrix and expressed in many tissues, including neuroendocrine, liver, gut, and brain. This gene encodes one of the seven basic amino acid-specific members which cleave their substrates at single or paired basic residues. This gene is thought to play a role in tumor progression and left-right patterning.

Sftpb: See List 2 from supplementary data.

Lamc2: See List 2 from supplementary data.

Sftpc: See List 1 from supplementary data.

Ctnnd2: See List 2 from supplementary data.

Foxf1: Forkhead box F1 is a protein coding gene. This gene belongs to the forkhead family of transcription factors which is characterized by a distinct forkhead domain. The encoded protein may be involved in many biological processes such as negative regulation of transcription from RNA polymerase II promoter, blood vessel development, vasculogenesis, in utero embryonic development, somitogenesis, morphogenesis of a branching structure, positive regulation of mesenchymal cell proliferation, , transcription, DNA-templated, regulation of transcription, DNA-templated, smoothened signaling pathway, heart development, organ morphogenesis, detection of wounding, extracellular matrix organization, respiratory tube development, lung development, positive regulation of cell migration, lung alveolus development, regulation of smooth muscle cell differentiation, lung morphogenesis, lung vasculature development, trachea development and epithelial tube branching involved in lung morphogenesis

Gli1: GLI-Kruppel family member GLI1 is a Protein Coding gene. This gene encodes a member of the Kruppel family of zinc finger proteins. The encoded transcription factor is activated by the sonic hedgehog signal transduction cascade and regulates stem cell proliferation. It is also involved in many biological processes such as osteoblast differentiation, transcription, DNA-templated, regulation of transcription, DNA-templated, signal transduction, smoothened signaling pathway, multicellular organism development, spermatogenesis, ventral midline development, positive regulation of cell proliferation, response to wounding, epidermal cell differentiation, dorsal/ventral pattern formation, proximal/distal pattern formation, cerebellar cortex morphogenesis pituitary gland development, cell differentiation and lung development.

Hmga2: High mobility group AT-hook 2 is protein coding gene, the encoded protein is involved in biological activities such as cell proliferation, positive regulation of cell proliferation, regulation of cell cycle process, positive regulation of gene expression, cell proliferation in forebrain, pituitary gland development, negative regulation of Wnt signaling pathway, chromosome condensation, endodermal cell differentiation, chondrocyte proliferation, regulation of growth, positive regulation of multicellular organism growth, DNA damage response, detection of DNA damage, positive regulation of apoptotic process, negative regulation of apoptotic process, negative regulation of DNA binding, negative regulation by host of viral transcription, fat cell differentiation, negative regulation of single stranded viral RNA replication via double stranded DNA intermediate, negative regulation of transcription, DNA-templated, positive regulation of transcription from RNA polymerase II promoter, negative regulation of JAK-STAT cascade, mesodermal cell differentiation, mesenchymal cell differentiation, positive regulation of sequence-specific DNA binding transcription factor activity, cell division, meiotic cell cycle, regulation of growth hormone secretion, lung epithelium development, epithelial tube branching involved in lung morphogenesis, and positive regulation of epithelial cell proliferation.

7.2.2 List 4: Definition of genes in the cluster 2 (GoF)

Mfap3l: Microfibrillar-associated protein 3-like is a Protein coding gene. It may participate in the nuclear signaling of EGFR and MAPK1/ERK2 and may a have a role in metastasis.

Ntng1: Netrin G1 is a Protein Coding gene. This gene encodes a preproprotein that is processed into a secreted protein containing eukaroytic growth factor (EGF)-like domains. The encoded protein is involved in many biological activities such as multicellular organism

development, nervous system development, axonogenesis and cell differentiation. Diseases associated with NTNG1 include Rett Syndrome and Schizophrenia**.**

Bend4: BEN domain containing 4 is a protein coding gene, not much is known about this gene.

Fam89a: Family with sequence similarity 89, member A, is a protein coding gene, not much is known about this gene.

Lhx2: LIM homeobox protein 2, is a protein coding gene, it acts as a transcriptional activator, the encoded protein is involved in many biological activities such as regulation of transcription, nervous system development, brain development, mesoderm development, dorsal/ventral pattern formation, cerebral cortex development, neurogenesis, maintenance of epithelial cell apical/basal polarity, positive regulation of transcription from RNA polymerase II promoter, anatomical structure formation involved in morphogenesis and hair follicle development. Diseases associated with LHX2 include Schizencephaly which is an extremely rare congenital disorder characterized by a full-thickness cleft within the cerebral hemispheres.

Chrm3: Cholinergic receptor, muscarinic 3. The muscarinic cholinergic receptors belong to a larger family of G protein-coupled receptors. The encoded protein is involved in many biological activities such as regulation of vascular smooth muscle contraction, signal transduction, G-protein coupled receptor signaling pathway, adenylate cyclase-inhibiting G-protein coupled acetylcholine receptor signaling pathway, phospholipase C-activating G-protein coupled acetylcholine receptor signaling pathway, G-protein coupled acetylcholine receptor signaling pathway, synaptic transmission, cholinergic, digestion, regulation of vasoconstriction, positive regulation of smooth muscle contraction, saliva secretion, regulation of insulin secretion. Diseases associated with CHRM3 include Prune Belly Syndrome and Cholinergic Urticaria**.**

Afp: Alpha fetoprotein, a major plasma protein produced by the yolk sac and the liver during fetal life. The encoded protein is involved in many biological activities such as ovulation from ovarian follicle, transport, sexual reproduction, progesterone metabolic process, SMAD protein signal transduction.

Sox9: SRY (sex determining region Y)-box 9, is a protein coding gene the encoded protein is involved in many biological activities such as negative regulation of transcription from RNA

polymerase II promoter, skeletal system development, ossification, cell fate specification, epithelial to mesenchymal transition, tissue homeostasis, positive regulation of protein phosphorylation, positive regulation of mesenchymal cell proliferation, chondrocyte development and differentiation, transcription, DNA-templated, protein complex assembly, cytoskeleton organization, signal transduction, epidermal growth factor receptor signaling pathway, Notch signaling pathway, heart development, positive and negative regulation of cell proliferation, regulation of cell cycle process, regulation of gene expression, positive regulation of epithelial cell migration, cell differentiation, regulation of cell adhesion, extracellular matrix organization, male sex determination, positive regulation of mesenchymal stem cell differentiation, regulation of epithelial cell proliferation involved in lung morphogenesis, negative regulation of mesenchymal cell apoptotic process. Deficiencies lead to the skeletal malformation syndrome campomelic dysplasia, frequently with sex reversal.

Plch1: Phospholipase C, eta 1 is a protein coding gene; it is a member of the PLC-eta family of the phosphoinositide-specific phospholipase C (PLC) superfamily of enzymes. The encoded protein is involved in many biological activities such as lipid metabolic process, signal transduction, lipid catabolic process, intracellular signal transduction and phosphatidylinositol-mediated signaling.

Phlda2: pleckstrin homology like domain, family A, member 2 is a protein coding gene, the encoded protein is involved in many biological activities such as placenta development, organ morphogenesis, regulation of gene expression, regulation of cell migration, regulation of embryonic development, regulation of spongiotrophoblast cell proliferation, regulation of glycogen metabolic process and regulation of growth hormone activity.

Bmp7: bone morphogenetic protein 7, this gene encodes a secreted ligand of the TGF-beta (transforming growth factor-beta) superfamily of proteins. the encoded protein is involved in many biological activities such as ossification, eye development, ureteric bud development, mesoderm formation, kidney development, endocardial cushion formation, pericardium morphogenesis, multicellular organism development, pattern specification process, salivary gland morphogenesis, negative regulation of cell proliferation, embryonic pattern specification, organ morphogenesis, positive regulation of pathway-restricted SMAD protein phosphorylation, positive regulation of cell death, cell differentiation, embryonic limb morphogenesis, positive regulation of bone mineralization, BMP signaling pathway, epithelial cell differentiation, regulation of phosphorylation, positive regulation of apoptotic process, regulation of MAPK cascade, response to peptide hormone, positive regulation of cell

differentiation, regulation of neuron differentiation, negative regulation of Notch signaling pathway, negative regulation of cell cycle, negative regulation of mitotic nuclear division, negative regulation of transcription, DNA-templated, positive regulation of transcription, positive regulation of transcription from RNA polymerase II promoter, cell development, cardiac muscle tissue development, branching morphogenesis of an epithelial tube, mesenchymal cell differentiation, regulation of pathway-restricted SMAD protein phosphorylation, SMAD protein signal transduction. Diseases associated with BMP7 include Spondylolisthesis and Renal Fibrosis.

Strap: Serine/Threonine kinase receptor associated protein is a protein coding gene, the encoded protein is involved in many biological activities such as negative regulation of transcription from RNA polymerase II promoter, spliceosomal snRNP assembly, mRNA processing, RNA splicing, negative regulation of epithelial cell migration, negative regulation of epithelial to mesenchymal transition, maintenance of gastrointestinal epithelium, negative regulation of transforming growth factor beta receptor signaling pathway, negative regulation of epithelial cell proliferation and negative regulation of pathway-restricted SMAD protein phosphorylation.

Mgl2: macrophage galactose N-acetyl-galactosamine specific lectin 2, Not much is known about this gene.

Nlrp1a: NLR family, pyrin domain containing 1A, the encoded protein is involved in many biological activities such as activation of cysteine-type endopeptidase activity involved in apoptotic process, inflammatory response, response to muramyl dipeptide, defense response to bacterium, regulation of apoptotic process, innate immune response, positive regulation of interleukin-1 beta secretion, neuron apoptotic process and programmed necrotic cell death.

Hk2: Hexokinase 2 is a protein coding gene, hexokinases phosphorylate glucose to produce glucose-6-phosphate, the first step in most glucose metabolism pathways. The encoded protein is involved in many biological activities such as cellular glucose homeostasis, response to ischemia, carbohydrate metabolic process, glucose metabolic process, glycolytic process, lactation, apoptotic mitochondrial changes, phosphorylation, regulation of glucose import and carbohydrate phosphorylation. Diseases associated with HK2 include Pediatric Osteosarcoma and Chondroblastoma.

Cytl1: See List 2 from supplementary data.

Gnptab: See List 2 from supplementary data.

Bex4: See List 2 from supplementary data.

7.2.3 List 5: Definition of genes in the cluster 3 (GoF)

Olfr1290; Olfr1301: Olfactory receptor 1290; Olfactory receptor 1301, the encoded protein is involved in many biological activities such as G-protein coupled receptor signaling pathway, sensory perception of smell and detection of chemical stimulus involved in sensory perception.

Rpusd2: RNA pseudouridylate synthase domain containing 2 is a protein coding gene; the encoded protein is involved in many biological activities such as pseudouridine synthesis, RNA modification, tRNA pseudouridine synthesis. Diseases associated with VPS53 include Pontocerebellar Hypoplasia, Type 2E and Cerebral Atrophy**.**

H2-DMa: Histocompatibility 2, class II, locus DMa; is a Protein Coding gene. The encoded protein is involved in many biological activities such as the immune system process, peptide antigen assembly with MHC class II protein complex, antigen processing and presentation of peptide or polysaccharide antigen via MHC class II, positive regulation of germinal center formation, positive regulation of humoral immune response, protein complex assembly, immune response, protein transport, immunoglobulin mediated immune response, antigen processing and presentation, antigen processing and presentation of exogenous peptide antigen via MHC class II, positive thymic T cell selection, positive regulation of T cell differentiation, inner ear development, positive regulation of immune response, chaperone mediated protein folding requiring cofactor**.** Diseases associated with HLA-DMA include Rheumatoid Arthritis and Diabetes Mellitus**.**

Vps53: Vacuolar Protein Sorting-Associated Protein 53 Homolog, is a protein coding gene, it acts as component of the GARP complex that is involved in retrograde transport from early and late endosomes to the trans-Golgi network (TGN), the encoded protein is involved in many biological activities such as transport, lysosomal transport, protein transport, endocytic recycling, retrograde transport, endosome to Golgi.

Plekhh2: Pleckstrin homology domain containing, family H (with MyTH4 domain) member 2 is a protein coding gene; it is involved in the regulation of actin filament depolymerization.

Diseases associated with PLEKHH2 include Focal Segmental Glomerulosclerosis which is a type of kidney disorder.

7.2.4 List 6: Definition of genes in the cluster 4 (GoF)

Iqcc: IQ motif containing C is a protein coding gene. Not much is known about this gene. Diseases associated with IQCC include Bardet-Biedl Syndrome which is an inherited condition that affects many parts of the body.

Flot1: Flotillin 1 is a protein coding gene, the encoded protein is involved in many biological activities such as membrane raft assembly, positive regulation of cytokine production, positive regulation of protein phosphorylation, regulation of receptor internalization, endocytosis, axonogenesis, axon guidance, extracellular matrix disassembly, positive regulation of protein binding, positive regulation of synaptic transmission, dopaminergic, positive regulation of interferon-beta production, dsRNA transport, positive regulation of heterotypic cell-cell adhesion, positive regulation of toll-like receptor 3 signaling pathway, response to endoplasmic reticulum stress, regulation of Rho protein signal transduction, plasma membrane raft assembly, positive regulation of endocytosis, positive regulation of skeletal muscle tissue development, protein homooligomerization, positive regulation of cell adhesion molecule production, protein kinase C signaling, cellular response to exogenous dsRNA, protein localization to plasma membrane, establishment of protein localization to plasma membrane, positive regulation of myoblast fusion, positive regulation of cell junction assembly, protein localization to membrane raft and positive regulation of cell-cell adhesion mediated by cadherin.

Thsd4: Thrombospondin, type I, domain containing 4 is a protein coding gene. The encoded protein is involved in the assembly of elastic fiber and it may attenuate TGFB signaling.

Tmem132d: Transmembrane protein 132D is a protein coding gene. The encoded protein is involved in the regulation of phosphatase activity and may serve as a cell-surface marker for oligodendrocyte differentiation.

Plac9a: Placenta specific 9a is a protein coding gene, not much is known about this gene.

Agt: angiotensinogen (serpin peptidase inhibitor, clade A, member 8), is a protein coding gene, the protein encoded by this gene pre-angiotensinogen, is expressed in the liver and is cleaved by the enzyme renin in response to lowered blood pressure. It is involved in many

biological processes such as blood vessel development, branching involved in ureteric bud morphogenesis, kidney development, regulation of systemic arterial blood pressure by circulatory renin-angiotensin, angiotensin mediated vasoconstriction involved in regulation of systemic arterial blood pressure, renal response to blood flow involved in circulatory renin-angiotensin regulation of systemic arterial blood pressure, renin-angiotensin regulation of aldosterone production, regulation of renal output by angiotensin, regulation of heart rate, brain renin-angiotensin system, renal system process, angiotensin-mediated drinking behavior, regulation of systemic arterial blood pressure by renin-angiotensin, positive regulation of extracellular matrix constituent secretion, cellular sodium ion homeostasis, cell-matrix adhesion, cell surface receptor signaling pathway, G-protein coupled receptor signaling pathway, fibroblast proliferation, positive regulation of fibroblast proliferation, regulation of long-term neuronal synaptic plasticity, smooth muscle cell proliferation , positive regulation of MAPK cascade, smooth muscle cell differentiation, positive regulation of multicellular organism growth, vasoconstriction, and vasodilation. Diseases associated with AGT include Renal Tubular Dysgenesis and Hypertension, Essential**.**

Olfml3: Olfactomedin-like 3 is a protein coding gene, the encoded protein is a secreted extracellular matrix glycoprotein with a C-terminal olfactomedin domain that facilitates protein-protein interactions, cell adhesion, and intercellular interactions and is involved in multicellular organism development.

Trp53inp1: Transformation related protein 53 inducible nuclear protein 1 is a protein coding gene. The encoded protein is involved in many biological activities such as autophagosome assembly, transcription, DNA-templated, regulation of transcription, DNA-templated, autophagy, apoptotic process, cell cycle arrest, negative regulation of cell proliferation, response to heat, regulation of autophagy, positive regulation of autophagy, positive regulation of gene expression, negative regulation of gene expression, negative regulation of cell migration, cellular response to UV, positive regulation of apoptotic process, positive regulation of transcription, DNA-templated, autophagic cell death, negative regulation of fibroblast proliferation, cellular response to ethanol, cellular response to hydroperoxide, cellular response to methyl methanesulfonate, negative regulation of myofibroblast differentiation and positive regulation of apoptotic signaling pathway.

Zfp605: Zinc finger protein 605 is a protein coding gene. The encoded protein is involved in the regulation of transcription and DNA-templated.

Dusp8: Dual specificity phosphatase 8 is a protein coding gene. The encoded protein is involved in many biological activities such as the regulation of MAP Kinase Pathways through dual specificity phosphatases, inactivation of MAPK activity and protein dephosphorylation.

Tacr1: Tachykinin receptor 1 is a protein coding gene. The encoded protein is involved in many biological activities such as the positive regulation of leukocyte migration, angiotensin-mediated drinking behavior, signal transduction, cell surface receptor signaling pathway, G-protein coupled receptor signaling pathway, positive regulation of cytosolic calcium ion concentration, tachykinin receptor signaling pathway, chemical synaptic transmission, learning or memory, long-term memory, regulation of blood pressure, associative learning, response to heat, response to hormone, response to ozone, positive regulation of epithelial cell migration, response to auditory stimulus, response to organic cyclic compound, regulation of smooth muscle cell migration, sensory perception of pain, positive regulation of synaptic transmission, cholinergic, response to nicotine, positive regulation of vasoconstriction, positive regulation of smooth muscle contraction, positive regulation of saliva secretion, positive regulation of hormone secretion, response to pain, behavioral response to pain, regulation of smooth muscle cell proliferation, positive regulation of lymphocyte proliferation, positive regulation of epithelial cell proliferation, positive regulation of stress fiber assembly, smooth muscle contraction involved in micturition, regulation of uterine smooth muscle contraction and positive regulation of uterine smooth muscle contraction.

Tnnc1: Troponin C1, Slow Skeletal And Cardiac Type is a protein coding gene; Troponin is a central regulatory protein of striated muscle contraction, and together with tropomyosin, is located on the actin filament. The encoded protein is involved in many biological activities such as diaphragm contraction, skeletal muscle contraction, cardiac ventricle development, regulation of muscle contraction, response to metal ion, transition between fast and slow fiber, regulation of muscle filament sliding speed, regulation of ATPase activity, ventricular cardiac muscle tissue morphogenesis, cardiac muscle contraction**.** Diseases associated with TNNC1 include Cardiomyopathy, Familial Hypertrophic, 13 and Cardiomyopathy, Dilated, 1Z.

Mansc4: MANSC domain containing 4, is a protein coding gene, not much is known about this gene.

Tns1: Tensin 1 is a protein coding gene. The encoded protein is involved in many biological activities such as integrin signaling pathway, cell-substrate junction assembly, fibroblast migration, intracellular signal transduction**.**

Cdc42ep2: CDC42 effector protein (Rho GTPase binding) 2, a small Rho GTPase, regulates the formation of F-actin-containing structures through its interaction with the downstream effector proteins, the encoded protein is involved in many biological activities such as Rho protein signal transduction, regulation of cell shape, actin cytoskeleton organization, positive regulation of actin filament polymerization, positive regulation of pseudopodium assembly.

Dera: Deoxyribose-phosphate aldolase, is a protein coding gene. The encoded protein is involved in many biological activities such as deoxyribonucleotide catabolic process, carbohydrate catabolic process, deoxyribonucleoside catabolic process and deoxyribose phosphate catabolic process.

Slc25a17: Solute carrier family 25 (mitochondrial carrier, peroxisomal membrane protein), member 17, is a protein coding gene. This gene is expressed in the liver and encodes a peroxisomal membrane protein that belongs to the family of mitochondrial solute carriers. The encoded protein is also involved in many biological activities such as translation, fatty acid beta-oxidation, transport, ADP transport, ATP transport, fatty acid transport, coenzyme A transmembrane transport, FAD transmembrane transport, NAD transport, transmembrane transport, and AMP transport.

H2-D1: Histocompatibility 2, D region locus 1, the encoded protein is involved in many biological activities such as CTL mediated immune response against target cells, Ras-Independent pathway in NK cell-mediated cytotoxicity, positive regulation of T cell mediated cytotoxicity, immune system process, antigen processing and presentation of peptide antigen via MHC class I, antigen processing and presentation of exogenous peptide antigen via MHC class I, TAP-dependent, antigen processing and presentation of endogenous peptide antigen via MHC class I via ER pathway, TAP-dependent, defense response, immune response, negative regulation of neuron projection development, antigen processing and presentation.

Tmem254a: Transmembrane protein 254a is a protein coding gene, not much is known about this gene.

Ntrk3: Neurotrophic tyrosine kinase, receptor, type 3 is a protein coding gene; this gene encodes a member of the neurotrophic tyrosine receptor kinase (NTRK) family. This kinase is

a membrane-bound receptor that, upon neurotrophin binding, phosphorylates itself and members of the MAPK pathway. Signalling through this kinase leads to cell differentiation. The encoded protein is involved in many biological activities such as activation of MAPK activity, neuron migration, negative regulation of protein phosphorylation, protein phosphorylation, transmembrane receptor protein tyrosine kinase signaling pathway, multicellular organism development, nervous system development, heart development, circadian rhythm, positive regulation of cell proliferation, positive regulation of gene expression, phosphorylation, modulation by virus of host transcription, cell differentiation, positive regulation of cell migration, activation of protein kinase B activity, positive regulation of positive chemotaxis, negative regulation of cell death, activation of GTPase activity and positive regulation of actin cytoskeleton reorganization

Ckb: creatine kinase, brain is a protein coding gene. The encoded protein is involved in many biological processes such as phosphorylation, substantia nigra development, and cellular chloride ion homeostasis. Diseases associated with CKB include Prostate Rhabdomyosarcoma and Dressler's Syndrome which is a pericarditis characterized by inflammation, occurring after injury, located in pericardium.

8. References

1. Abolhassani A., Riazi G.H., Azizi E., Amanpour S., Muhammadnejad S., Haddadi M., et al., FGF10: type III epithelial mesenchymal transition and invasion in breast cancer cell lines, J. Cancer 5 (2014) 537–547.

2. Al Alam D, Danopoulos S, Schall K, Sala FG, Almohazey D, Fernandez GE, Frey MR, Ford HR, Grikscheit T. Fibroblast growth factor 10 alters the balance between goblet cells and Paneth cells in the adult mouse small intestine. Am J Physiol Gastrointest Liver Physiol 308: G678–G690, 2015.

3. Alarid ET, Rubin JS, Young P, Chedid M, Ron D, Aaronson SA, Cunha GR. Keratinocyte growth factor functions in epithelial induction during seminal vesicle development. Proc Natl Acad Sci U S A. 1994 Feb 1; 91(3):1074-8.

4. Arman, E., Haffner-Krausz, R., Gorivodsky, M., and Lonai, P. (1999) Proc. Natl. Acad. Sci. U. S. A. 96, 11895–11899.

5. Barbara Treutlein, Doug G. Brownfield, Angela R. Wu, Norma F. Neff, Gary L. Mantalas, F. Hernan Espinoza, Tushar J. Desai, Mark A. Krasnow, and Stephen R. Quake; Reconstructing lineage hierarchies of the distal lung epithelium using single cell RNA-seq. Nature. 2014 May 15; 509(7500): 371–375. doi:10.1038/nature13173.

6. Bartel, F.O., Higuchi, T., Spyropoulos, D.D., 2000. Mouse models in the study of the Ets family of transcription factors. Oncogene 19, 6443–6454.

7. Bellusci, S., Furuta, Y., Rush, M. G., Henderson, R., Winnier, G., and Hogan, B.L. (1997a). Involvement of Sonic hedgehog (Shh) in mouse embryonic lung growth and morphogenesis. Development 124, 53–63.

8. Bellusci S, Grindley J, Emoto H, Itoh N, Hogan BL. Fibroblast growth factor 10 (FGF10) and branching morphogenesis in the embryonic mouse lung. Development (1997b); 124: 4867-78.

9. Belteki G, et al. Conditional and inducible transgene expression in mice through the combinatorial use of Cre-mediated recombination and tetracycline induction. Nucleic Acids Res. 2005;33(5):e51. doi: 10.1093/nar/gni051.

10. Browne ML, Carter TC, Kay DM, Kuehn D, Brody LC, Romitti PA, Liu A, Caggana M, Druschel CM, Mills JL. 2012. Evaluation of genes involved in limb development, angiogenesis, and coagulation as risk factors for congenital limb deficiencies. Am J Med Genet Part A 158A: 2463–2472.

11. Cardoso WV, Lu J. Regulation of early lung morphogenesis: questions, facts and controversies. Development 2006; 133:1611 e 24.

12. Carlton M. Bates, 2007, Role of fibroblast growth factor receptor signaling in kidney development, Pediatric Nephrology 10.1007/s00467-006-0239-7.

13. Chang, D.R., Martinez Alanis, D., Miller, R.K., Ji, H., Akiyama, H., McCrea, P.D., Chen, J., 2013. Lung epithelial branching program antagonizes alveolar differentiation. Proc Natl Acad Sci U S A 110, 18042-18051.

14. Chao C.M., Yahya F., Moiseenko A.et al., Fgf10 deficiency is causative for lethality in a mouse model of bronchopulmonary dysplasia. J Pathol. 2017 Jan;241(1):91-103.

15. Chen F, Cao Y, Qian J, Shao F, Niederreither K, Cardoso WV. A retinoic acid-dependent network in the foregut controls formation of the mouse lung primordium. J Clin Invest 2010; 120:2040 e 8.)

16. David M Ornitz and Nobuyuki Itoh, Fibroblast growth factors Genome Biol. 2001; 2(3): reviews3005.1–reviews3005.12.

17. David Warburton, Ahmed El-Hashash, Gianni Carraro, et al. Lung Organogenesis, Curr Top Dev Biol. 2010 ; 90: 73–158. doi:10.1016/S0070-2153(10)90003-3.

18. De Langhe, S. P., Carraro, G., Warburton, D., Hajihosseini, M. K. and Bellusci, S. (2006). Levels of mesenchymal FGFR2 signaling modulate smooth muscle progenitor cell commitment in the lung. Developmental biology 299, 52–62.

19. Del Moral, P.-M., De Langhe, S. P., Sala, F. G., Veltmaat, J. M., Tefft, D., Wang, K., Warburton, D. and Bellusci, S. (2006). Differential role of FGF9 on epithelium and mesenchyme in mouse embryonic lung. Developmental biology 293, 77–89.

20. De Moerlooze L, Spencer-Dene B, Revest JM, Hajihosseini M, Rosewell I, Dickson C. An important role for the IIIb isoform of fibroblast growth factor receptor 2 (FGFR2)

in mesenchymal-epithelial signalling during mouse organogenesis. Development. 2000 Feb; 127(3):483-92.

21. Desai, T. J., Brownfield, D. G. & Krasnow, M. A. Alveolar progenitor and stem cells in lung development, renewal and cancer. Nature 507, 190–194 (2014).

22. Ding Y1, He D, Florentin D et al. Semaphorin 4F as a critical regulator of neuroepithelial interactions and a biomarker of aggressive prostate cancer. Clin Cancer Res. 2013 Nov 15; 19(22):6101-11. doi: 10.1158/1078-0432.CCR-12-3669. Epub 2013 Oct 4.

23. El Agha, E. and S. Bellusci (2014). "Walking along the Fibroblast Growth Factor 10 Route: A Key Pathway to Understand the Control and Regulation of Epithelial and Mesenchymal Cell-Lineage Formation during Lung Development and Repair after Injury." Scientifica (Cairo) 2014: 538379.

24. Entesarian M. , Dahlqvist J. , Shashi V., Stanley C.S. , Falahat B., Reardon W., Et al., FGF10 Missense Mutations In Aplasia Of Lacrimal And Salivary Glands (ALSG), Eur. J. Hum. Genet. 15 (2007) 379–382.

25. Gentleman R.C., Carey, V.J., Bates, D.M., Bolstad, B., Dettling, M., Dudoit, S., Ellis, B., Gautier, L., Ge, Y., Gentry, J., Hornik, K., Hothorn, T., Huber, W., Iacus, S., Irizarry, R., Leisch, F., Li, C., Maechler, M., Rossini, A.J., Sawitzki, G., Smith, C., Smyth, G., Tierney, L., Yang, J.Y., Zhang, J. (2004) Bioconductor: open software development for computational biology and bioinformatics. *Genome Biol*. 5:R80, URL http://genomebiology.com/2004/5/10/R80.

26. Gkatzis K, Taghizadeh S, Huh D, Stainier DYR, Bellusci S. Use of three-dimensional organoids and lung-on-a-chip methods to study lung development, regeneration and disease. Eur Respir J. 2018 Nov 29;52(5). pii: 1800876. doi: 10.1183/13993003.00876-2018. Print 2018 Nov. Review. PubMed PMID: 30262579

27. Goss, A. M., Tian, Y., Cheng, L., Yang, J., Zhou, D., Cohen, E. D. and Morrisey, E. E. (2011). Wnt2 signaling is necessary and sufficient to activate the airway smooth muscle program in the lung by regulating myocardin/Mrtf-B and Fgf10 expression. Developmental biology 356, 541–52.

28. Gospodarowicz D, Purification of a fibroblast growth factor from bovine pituitary. J Biol Chem. 1975 Apr 10; 250 (7):2515-20.

29. Gros J., Tabin C.J., Vertebrate limb bud formation is initiated by localized epithelial-to-mesenchymal transition, Science 343 (2014) 1253–1256.

30. Gruel N, Fuhrmann L, Lodillinsky C, et al. LIN7A is a major determinant of cell-polarity defects in breast carcinomas. Breast Cancer Research : BCR. 2016; 18:23. doi:10.1186/s13058-016-0680-x.

31. Guo L, Degenstein L, Fuchs E. Keratinocyte growth factor is required for hair development but not for wound healing. Genes Dev. 1996 Jan 15;10(2):165-75. PubMed PMID: 8566750.

32. Hashimoto, S., Chen, H., Que, J., Brockway, B. L., Drake, J. A., Snyder, J. C.,Randell, S. H. and Stripp, B. R. (2012). β-Catenin-SOX2 signaling regulates the fate of developing airway epithelium. J. Cell Sci. 125, 932-942.

33. Herriges JC, et al. (2015) FGF-Regulated ETV Transcription Factors Control FGF-SHH Feedback Loop in Lung Branching. Dev Cell 35(3):322–332.

34. Herriges JC, et al. (2012) Genome-scale study of transcription factor expression in the branching mouse lung. Dev Dyn 241(9):1432–1453.

35. His E, Chen KC, Chang WS et al., a functional polymorphism at the FGF10 gene is associated with extreme myopia, Invest. Ophthalmol. Vis. Sci. 54 (2013) 265–271.

36. Hisayo Emoto, Shuzo Tagashira, Marie-Geneviève Mattei, Masahiro Yamasaki, Gakuji Hashimoto, Takashi Katsumata, Takaharu Negoro, Masashi Nakatsuka, Daniel Birnbaum, François Coulier and Nobuyuki Itoh, Structure and Expression of Human Fibroblast Growth Factor-10, 10.1074/jbc.272.37.23191 September 12, 1997, *The Journal of Biological Chemistry,* 272, 23191-23194.

37. Hokuto, I., Perl, A.-K. T. and Whitsett, J. A. (2003). Prenatal, but not postnatal, inhibition of fibroblast growth factor receptor signaling causes emphysema. The Journal of biological chemistry 278, 415–21.

38. Hyatt, B.A., Shangguan, X., Shannon, J.M., 2002. BMP4 modulates fibroblast growth factor-mediated induction of proximal and distal lung differentiation in mouse embryonic tracheal epithelium in mesenchyme-free culture. Dev. Dyn. 225, 153–165.

39. Igarashi M. , P.W. Finch, S.A. Aaronson, Characterization of recombinant human fibroblast growth factor (Fgf-10) reveals functional similarities with keratinocyte growth factor (Fgf-7), J. Biol. Chem. 273 (1998) 13230–13235.

40. Itoh N, Ornitz DM. Functional evolutionary history of the mouse Fgf gene family. Dev Dyn. 2008;237(1):18□27. doi:10.1002/dvdy.21388.

41. Itoh Nobuyuki, FGF10: A multifunctional mesenchymal–epithelial signaling growth factor in development, health, and Disease Cytokine & Growth Factor Reviews 28 (2016) 63–69.

42. John T. Benjamin , Rebekah J. Smith , Brian A. Halloran et al. FGF-10 is decreased in bronchopulmonary dysplasia and suppressed by Toll-like receptor activationAmerican Journal of Physiology - Lung Cellular and Molecular PhysiologyPublished 1 February 2007Vol. 292no. 2, L550-L558DOI: 10.1152/ajplung.00329.2006.

43. Jones MR, Dilai S, Lingampally A, Chao CM, Danopoulos S, Carraro G, Mukhametshina R, Wilhelm J, Baumgart-Vogt E, Al Alam D, Chen C, Minoo P, Zhang JS, Bellusci S (2019 a). A Comprehensive Analysis of Fibroblast Growth Factor Receptor 2b Signaling on Epithelial Tip Progenitor Cells During Early Mouse Lung Branching Morphogenesis. Front Genet. 2019 Jan 23; 9:746. doi: 10.3389/fgene.2018.00746. eCollection 2018. PubMed PMID: 30728831; PubMed Central PMCID: PMC6351499.

44. Jones MR, Lingampally A, Dilai S, Shrestha A, Stripp B, Helmbacher F, Chen C, Chao C-M and Bellusci S (2019 b) Characterization of *Tg(Etv4-GFP)* and *Etv5* ^{RFP} Reporter Lines in the Context of Fibroblast Growth Factor 10 Signaling During Mouse Embryonic Lung Development. Front. Genet. 10:178. doi: 10.3389/fgene.2019.00178

45. Kato S1, Sekine K. FGF-FGFR signaling in vertebrate organogenesis. Cell Mol Biol (Noisy-le-grand). 1999 Jul; 45(5):631-8.

46. Kennedy MW, Chalamalasetty RB, et al. Sp5 and Sp8 recruit β-catenin and Tcf1-Lef1 to select enhancers to activate Wnt target gene transcription. Proc Natl Acad Sci U S A. 2016 Mar 29; 113(13):3545-50. doi: 10.1073/pnas.1519994113. Epub 2016 Mar 11.

47. Lamballe F, Genestine M, Caruso N, Arce V, Richelme S, Helmbacher F, et al. Pool-specific regulation of motor neuron survival by neurotrophic support. J Neurosci. 2011 Aug 3; 31(31):11144-58.

48. Lebeche, D., Malpel, S. and Cardoso, W. V (1999). Fibroblast growth factor interactions in the developing lung. Mechanisms of development 86, 125–36.

49. Liu, Y., Hogan, B.L., 2002. Differential gene expression in the distal tip endoderm of the embryonic mouse lung. Gene Expr. Patterns 2, 229–233.

50. Liu Yuru, Jiang Haiyan, C. Crawford Howard, and L.M. Hogan Brigid, Role for ETS domain transcription factors Pea3/Erm in mouse lung development, Developmental Biology 261 (2003) 10–24.

51. Lü J, Izvolsky KI, Qian J, Cardoso WV. Identification of FGF10 targets in the embryonic lung epithelium during bud morphogenesis. J Biol Chem. 2005 Feb 11; 280(6):4834-41. Epub 2004 Nov 19. PubMed PMID: 15556938.

52. Mailleux, A. A., Tefft, D., Ndiaye, D., Itoh, N., Thiery, J. P., Warburton, D., et al. (2001). Evidence that SPROUTY2 functions as an inhibitor of mouse embryonic lung growth and morphogenesis. Mech. Dev. 102, 81–94. doi: 10.1016/S0925-4773(01)00286-6.

53. Mailleux AA, Spencer-Dene B, Dillon C, Ndiaye D, Savona-Baron C, Itoh N, et al. Role of FGF10/FGFR2b signaling during mammary gland development in the mouse embryo. Development. 2002 Jan; 129(1):53-60.

54. Makarenkova HP, Ito M, Govindarajan V, Faber SC, Sun L, McMahon G, Overbeek PA, Lang RA. FGF10 is an inducer and Pax6 a competence factor for lacrimal gland development. Development 2000; 127: 2563 e 72.

55. Mao Junhao, Edwina McGlinn, Peng Huang, Clifford J. Tabin, and Andrew P. McMahon, Fgf-Dependent Etv4/5 Activity Is Required for Posterior Restriction of

Sonic hedgehog and Promoting Outgrowth of the Vertebrate Limb. DOI 10.1016/j.devcel.2009.02.005.

56. Mariani FV, Ahn CP, Martin GR. (2008) Genetic evidence that FGFs have an instructive role in limb proximal–distal patterning. Nature 453: 401–405.

57. Maroulakou, I.G., Bowe, D.B., 2000. Expression and function of Ets transcription factors in mammalian development: a regulatory network. Oncogene 19, 6432–6442.

58. Metzger, D.E., Stahlman, M.T., Shannon, J.M., 2008a. Misexpression of ELF5 disrupts lung branching and inhibits epithelial differentiation. Dev Biol 320, 149-160.

59. Metzger, D.E., Xu, Y., Shannon, J.M., 2007. Elf5 is an epithelium-specific, fibroblast growth factor-sensitive transcription factor in the embryonic lung. Dev Dyn 236, 1175-1192.

60. Metzger, R.J., Klein, O.D., Martin, G.R., Krasnow, M.A., 2008b. The branching programme of mouse lung development. Nature 453, 745-750.

61. Miki T., T.P.Fleming, D.P. Bottaro, J.S. Rubin, D. Ron, S.A. Aaronson, Expression cDNA cloning of the KGF Receptor by creation of a transforming autocrine loop, Science (1991)72–75.

62. Miller DL, Ortega S, Bashayan O, Basch R, Basilico C. Compensation by fibroblast growth factor 1 (FGF1) does not account for the mild phenotypic defects observed in FGF2 null mice. Mol Cell Biol. 2000 Mar; 20(6):2260-8. Erratum in: Mol Cell Biol 2000 May; 20(10):3752. PubMed PMID: 10688672; PubMed Central PMCID: PMC110842.

63. Milunsky JM, Zhao G, Maher TA, Colby R, Everman DB et al., (2006) LADD syndrome is caused by FGF10 mutations. Clin Genet; 69(4):349-54. Mol Cell Biol. 1993 Aug; 13(8):4513-22.

64. Min Hosung, Dimitry M. Danilenko, Sheila A. Scully, Brad Bolon, Brian D. Ring, John E. Tarpley, Margaret DeRose, and W. Scott Simonet. Fgf-10 is required for both limband lung development and exhibits striking functional similarity to Drosophila branchless. Genes Dev. 1998 Oct 15; 12(20): 3156–3161.

65. Minowada, G., L. A. Jarvis, C. L. Chi, A. Neubuser, X. Sun, N. Hacohen, M. A. Krasnow and G. R. Martin (1999). "Vertebrate Sprouty genes are induced by FGF signaling and can cause chondrodysplasia when overexpressed." Development 126(20): 4465-4475.

66. Molfino NA. Genetics of COPD. Chest 2004; 125:1929 e 40.

67. Moosa Mohammadi , Shaun K. Olsen, Omar A. Ibrahimi. Structural basis for fibroblast growth factor receptor activation. Cytokine & Growth Factor Reviews 16 (2005) 107–137

68. Nakanishi T, Hasegawa Y, Mimura R, Wakayama T, Uetoko Y, Komori H, Akanuma S, Hosoya K, Tamai I. Prostaglandin Transporter (PGT/SLCO2A1) Protects the Lung from Bleomycin-Induced Fibrosis. PLoS One. 2015 Apr 29;10(4):e0123895. doi: 10.1371/journal.pone.0123895. eCollection 2015.

69. Naoyuki Iida, Tohru Kozasa, Identification and Biochemical Analysis of GRIN1 and GRIN2, Methods in Enzymology Volume 390, 2004, Pages 475–483 Regulators of G-Protein Signaling, Part B.

70. Nomura S., Yoshitomi H., Takano S., Shida T., Kobayashi S., Ohtsuka M., Kimura F., Shimizu H., Yoshidome H., Kato A. & Miyazaki M.; FGF10/FGFR2 signal induces cell migration and invasion in pancreatic cancer. British Journal of Cancer (2008) 99, 305 – 313.

71. Nyeng, P., Norgaard, G. A., Kobberup, S. and Jensen, J. (2008). FGF10 maintains distal lung bud epithelium and excessive signaling leads to progenitor state arrest, distalization, and goblet cell metaplasia. BMC Dev. Biol. 8, 2.

72. Ohuchi H, Hori Y, Yamasaki M, Harada H, Sekine K, Kato S, and Itoh, N. , FGF10 acts as a major ligand for FGF receptor 2 IIIb in mouse multi-organ development. Biochem Biophys Res Commun. 2000 Nov 2; 277(3):643-649.

73. Ornitz DM, Itoh N. Fibroblast growth factors. Genome Biol. 2001; 2(3):REVIEWS3005.De Moerlooze L, Spencer-Dene B, Revest JM, Hajihosseini M, Rosewell I, Dickson C. An important role for the IIIb isoform of fibroblast growth factor receptor 2 (FGFR2) in mesenchymal-epithelial signalling during mouse organogenesis. Development. 2000 Feb;127(3):483-92.

74. Ornitz DM, Yayon A, Flanagan JG, Svahn CM, Levi E, Leder P. Heparin is required for cell-free binding of basic fibroblast growth factor to a soluble receptor and for mitogenesis in whole cells. Mol Cell Biol. 1992 Jan; 12(1):240-7.

75. Ornitz, D. M., Xu, J., Colvin, J. S., McEwen, D. G., MacArthur, C. A., Coulier, F., Gao, G. and Goldfarb, M. (1996). Receptor specificity of the fibroblast growth factor family.J. Biol. Chem. 271, 15292-15297.

76. Park W. Y., Miranda B., Lebeche D., Hashimoto G., and Cardoso W. V. FGF-10 Is a Chemotactic Factor for Distal Epithelial Buds during Lung Development. Developmental biology 201,125–134 (1998) Article No. DB988994

77. Paul S Kingma and Jeffrey A Whitsett, In defense of the lung: surfactant protein A and surfactant protein D, Current Opinion in Pharmacology 2006, 6:277–283, DOI 10.1016/j.coph.2006.02.003.

78. Perl, A.K., Kist, R., Shan, Z., Scherer, G., Whitsett, J.A., 2005. Normal lung development and function after Sox9 inactivation in the respiratory epithelium. Genesis 41, 23-32.

79. Peter ten Dijke, Olexander Korchynskyi, Gudrun Valdimarsdottir, Marie-José Goumans. Controlling cell fate by bone morphogenetic protein receptors, Molecular and Cellular Endocrinology Volume 211, Issues 1–2, 15 December 2003, Pages 105–113.

80. Quaggin, S.E., Schwartz, L., Cui, S., Igarashi, P., Deimling, J., Post, M., Rossant, J., 1999. The basic-helix-loop-helix protein pod1 is critically important for kidney and lung organogenesis. Development 126, 5771-5783.

81. Que, J., Okubo, T., Goldenring, J. R., Nam, K. T., Kurotani, R., Morrisey, E. E.,Taranova, O., Pevny, L. H. and Hogan, B. L. (2007). Multiple dose-dependent roles for Sox2 in the patterning and differentiation of anterior foregut endoderm. Development 134, 2521-2531.

82. R Development Core Team (2007). R: A language and environment for statistical computing. R Foundation for Statistical Computing, Vienna, Austria. ISBN 3-900051-07-0, URL http://www.R-project.org.

83. Ramasamy, S. K., Mailleux, A. a, Gupte, V. V, Mata, F., Sala, F. G., Veltmaat, J. M., Del Moral, P. M., De Langhe, S., Parsa, S., Kelly, L. K., et al. (2007). Fgf10 dosage is critical for the amplification of epithelial cell progenitors and for the formation of multiple mesenchymal lineages during lung development. Developmental biology 307, 237–47.

84. Rawlins Emma L., Clark Cheryl P., [...], and Hogan Brigid L. M.; The Id2+ distal tip lung epithelium contains individual multipotent embryonic progenitor cells, Development (Cambridge, England) 136.22 (2009): 3741–3745.

85. Rawlins, E.L., 2008. Lung epithelial progenitor cells: lessons from development. Proc Am Thorac Soc 5, 675-681.

86. Ritchie, M.E., Phipson, B., Wu, D., Hu, Y., Law, C.W., Shi, W., and Smyth, G.K. (2015). limma powers differential expression analyses for RNA-sequencing and microarray studies. Nucleic Acids Research 43(7), e47.

87. Riley BM, Mansilla MA, Ma J, et al., Impaired FGF signaling contributes to cleft lip and palate. PNAS March 13, 2007. 104 (11) 4512-4517.

88. Rockich, B.E., Hrycaj, S.M., Shih, H.P., Nagy, M.S., Ferguson, M.A., Kopp, J.L., Sander, M., Wellik, D.M., Spence, J.R., 2013. Sox9 plays multiple roles in the lung epithelium during branching morphogenesis. Proc Natl Acad Sci U S A 110, E4456-4464.

89. Salerno T, Peca D, Menchini L, et al. Surfactant Protein C-associated interstitial lung disease; three different phenotypes of the same *SFTPC* mutation. *Italian Journal of Pediatrics*. 2016; 42:23. doi:10.1186/s13052-016-0235-x.

90. Sara Parsa, Suresh K. Ramasamy, Stijn De Langhe, Varsha V. Gupte, Jody J. Haigh, Daniel Medina, Savério Bellusci. Terminal end bud maintenance in mammary gland is dependent upon FGFR2b signaling. Developmental Biology 317 (2008) 121 – 131.

91. Sara Parsa, Koh-ichi Kuremoto, Kerstin Seidel, Reza Tabatabai, BreAnne MacKenzie, Takayoshi Yamaza, Kentaro Akiyama, Jonathan Branch, Chester J. Koh, Denise Al Alam, Ophir D. Klein and Saverio Bellusci. Signaling by FGFR2b controls the regenerative capacity of adult mouse incisors. Development 137, 3743-3752 (2010) doi:10.1242/dev.051672.

92. Schwertfeger KL, 2009, Fibroblast growth factors in development and cancer: insights from the mammary and prostate glands. Curr Drug Targets; 10(7):632-44.

93. Sekine K, Ohuchi H, Fujiwara M, Yamasaki M, Yoshizawa T, et al. (1999). Fgf10 is essential for limb and lung formation. Nat Genet. 21: 138–41.

94. Sharrocks, A.D., 2001. The ETS-domain transcription factor family. Nat. Rev. Mol. Cell. Biol. 2, 827–827.

95. Silver, JD, Ritchie, ME, and Smyth, GK (2009). Microarray background correction: maximum likelihood estimation for the normal-exponential convolution. *Biostatistics* 10, 352-363, URL http://biostatistics.oxfordjournals.org/content/10/2/352.

96. Simonet WS, DeRose ML, Bucay N, Nguyen HQ, Wert SE, Zhou L, et al. Pulmonary malformation in transgenic mice expressing human keratinocyte growth factor in the lung. Proc Natl Acad Sci U S A. 1995;92:12461–5.

97. Shu, W., Guttentag, S., Wang, Z., Andl, T., Ballard, P., Lu, M. M., Piccolo, S.,Birchmeier, W., Whitsett, J. A., Millar, S. E. et al. (2005). Wnt/beta-catenin signaling acts upstream of N-myc, BMP4, and FGF signaling to regulate proximal-distal patterning in the lung. Dev. Biol. 283, 226-239.

98. Szebenyi G, Fallon JF. Fibroblast growth factors as multifunctional signaling factors. Int Rev Cytol. 1999; 185():45-106.

99. Taylor KR, Rudisill JA, Gallo RL. Structural and sequence motifs in dermatan sulfate for promoting fibroblast growth factor-2 (FGF-2) and FGF-7 activity. J Biol Chem. 2005 Feb 18; 280(7):5300-6.

100. Theodorou V., Boer M., Weigelt B. et al., Fgf10 is an oncogene activated by MMTV insertional mutagenesis in mouse mammary tumors and overexpressed in a subset of human breast carcinomas. Oncogene (2004) 23, 6047–6055.

101. Thiery J.P., Acloque H., Huang R.Y., Nieto M.A., Epithelial–mesenchymal transitions in development and disease, Cell 139 (2009) 871–890.

102. Ulich TR, Yi ES, Longmuir K, Yin S, Biltz R, Morris CF, et al. Keratinocyte growth factor is a growth factor for type II pneumocytes in vivo. J Clin Invest. 1994;93:1298–306.

103. Varma, S., Cao, Y., Tagne, J.B., Lakshminarayanan, M., Li, J., Friedman, T.B., Morell, R.J., Warburton, D., Kotton, D.N., Ramirez, M.I., 2012. The transcription factors Grainyhead-like 2 and NK2-homeobox 1 form a regulatory loop that coordinates lung epithelial cell morphogenesis and differentiation. J Biol Chem 287, 37282-37295.

104. Volckaert T, Dill E, Campbell A, Tiozzo C, Majka S, Bellusci S, De Langhe SP. Parabronchial smooth muscle constitutes an airway epithelial stem cell niche in the mouse lung after injury. J Clin Invest. 2011 Nov;121(11):4409-19. doi: 10.1172/JCI58097. Epub 2011 Oct 10. PubMed PMID: 21985786; PubMed Central PMCID: PMC3204843.

105. Volckaert Thomas, Campbell Alice , Dill Erik , Li Changgong , Minoo Parviz and De Langhe Stijn, Localized Fgf10 expression is not required for lung branching morphogenesis but prevents differentiation of epithelial progenitors. Development 140, 3731-3742 (2013) doi:10.1242/dev.096560 2013.

106. Warburton David, Bellusci Saverio, Del Moral Pierre-Marie, Kaartinen Vesa, Lee Matt, Tefft Denise and Shi Wei. Growth factor signaling in lung morphogenetic centers: automaticity, stereotypy and symmetry. Respiratory Research 2003 4:5 https://doi.org/10.1186/1465-9921-4-5.

107. Warburton, D., Perin, L., Defilippo, R., Bellusci, S., Shi, W., Driscoll, B., 2008. Stem/progenitor cells in lung development, injury repair, and regeneration. Proc Am Thorac Soc 5, 703-706.

108. Warburton, D., El-Hashash, A., Carraro, G., Tiozzo, C., Sala, F., Rogers, O., Langhe, S.D., Kemp, P.J., Riccardi, D., Torday, J., Bellusci, S., Shi, W., Lubkin, S.R., Jesudason, E., 2010. Lung Organogenesis, Organogenesis in Development, pp. 73-158.

109. Weaver, M., Dunn, N. R. and Hogan, B. L. (2000). Bmp4 and Fgf10 play opposing roles during lung bud morphogenesis. Development (Cambridge, England) 127, 2695–704.

110. Yale Jen, Katia Manova, and Robert Benezra, Expression Patterns of I&, Id2, and Id3 Are Highly Related But Distinct From That of Id4 During Mouse Embryogenesis, Cell

Biology Program, Memorial Sloan Kettering Cancer Center, New York, New York 10021, Developmental Dynamics 207235-252 (1996).

111. Yan G, Fukabori Y, McBride G, Nikolaropolous S, McKeehan WL. Exon switching and activation of stromal and embryonic fibroblast growth factor (FGF)-FGF receptor genes in prostate epithelial cells accompany stromal independence and malignancy.

112. Yano T, Mason RJ, Pan T, Deterding RR, Nielsen LD, Shannon JM. KGF regulates pulmonary epithelial proliferation and surfactant protein gene expression in adult rat lung. Am J Physiol Lung Cell Mol Physiol. 2000; 279: L1146–58.

113. Yin, Z. et al. Hop functions downstream of Nkx2.1 and GATA6 to mediate HDAC-dependent negative regulation of pulmonary gene expression. Am. J. Physiol. Lung Cell. Mol. Physiol. 291, L191–L199 (2006).

114. Yuan C., Hu H., Kuang M., Chen Z., Tao X., Fang S., Sun Y., Zhang Y. and Chen H. (2017). Super enhancer associated RAI14 is a new potential biomarker in lung adenocarcinoma. Oncotarget. 2017 Oct 27; 8(62):105251-105261. doi: 10.18632/oncotarget.22165.

115. Zhang, X., Ibrahimi, O. A., Olsen, S. K., Umemori, H., Mohammadi, M. and Ornitz, D. M. (2006). Receptor specificity of the fibroblast growth factor family. The complete mammalian FGF family. The Journal of biological chemistry 281, 15694–700.

9. Acknowledgments

I would like to thank all the people who helped me through and made the completion of my doctoral study possible. First of all, I would like to express my deep gratitude to Prof. Dr.

Saverio Bellusci for believing in me, as I came from a different field, he gave me the basis knowledge that I needed in my PhD. His passion for his work has certainly inspired me throughout my doctoral studies. I want to thank him for providing me with all the resources as well as mentorship that I needed.

I would like to thank Kerstin and Heike for their help in administrative tasks and the friendly atmosphere, to Jana for managing and genotyping the mice used for experiments. Many thanks also to Matthew for his support and his help in the redaction of the papers. I would also like to acknowledge the Bellusci lab members: Elie, Amit, Aleona, Cho,Vahid and Negah , my MBML friends: Karla, Gayatri, Lina and Dijana. I wish them all the best in their future career. I thank also Dr. Jochen Wilhelm for the statistical interpretation of the generated data.

To my husband Tahar, the person who believed in me the most and offered me unconditional support, I express my thanks and my gratitude. Thank you for your presence beside me throughout my journey. This work would not have been possible without your support and encouragement. To my children Ilias and Jasmin, thank you for your love. You are making my life prettier!

Finally, I would like to express my deep love and gratitude to my parents in Morocco, Anissa and Ali, for their love, support and encouragement. I owe them everything that I am. I would also like to thank my brother Mohamed and his wife Zineb, my sister Zineb and her husband Mohamed Bennani, my sister Imane, my niece Sara and my nephews Youssef and Mehdi, thank you for your presence in my life, I wish you all Success and Happiness. To my parents in law Houria and Abderrahmane and to all the Azzam Jai Family thank you for your encouragement. I would also like to thank my aunts, uncles and cousins, especially my grandfather Mohamed, my uncle Mehdi and my aunty Bouchra, thank you for your encouragement, support and unconditional love until the end of your life, I know you would have been very proud of what I have accomplished until now, I miss you so much! My dear friend Oum keltoum, thank you for your support and for being there when I needed your advice. And finally to all the families Dilai, Mikou and Azzam Jai and to all my friends, thank you for being in my life you are the best!